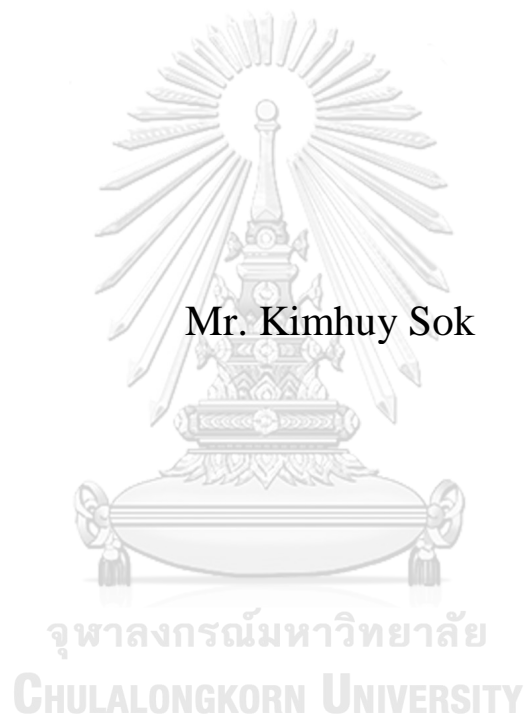


**DROUGHT ASSESSMENT FOR THE GREATER
BARIBO BASIN IN CAMBODIA**



A Thesis Submitted in Partial Fulfillment of the Requirements
for the Degree of Master of Engineering in Water Resources Engineering
Department of Water Resources Engineering
Faculty of Engineering
Chulalongkorn University
Academic Year 2018
Copyright of Chulalongkorn University

การประเมินความเสี่ยงภัยแล้งในลุ่มน้ำบริโบใหญ่ ประเทศกัมพูชา



วิทยานิพนธ์นี้เป็นส่วนหนึ่งของการศึกษาตามหลักสูตรปริญญาวิศวกรรมศาสตรมหาบัณฑิต
สาขาวิชาวิศวกรรมแหล่งน้ำ ภาควิชาวิศวกรรมแหล่งน้ำ
คณะวิศวกรรมศาสตร์ จุฬาลงกรณ์มหาวิทยาลัย
ปีการศึกษา 2561
ลิขสิทธิ์ของจุฬาลงกรณ์มหาวิทยาลัย

Thesis Title DROUGHT ASSESSMENT FOR THE GREATER
BARIBO BASIN IN CAMBODIA
By Mr. Kimhuy Sok
Field of Study Water Resources Engineering
Thesis Advisor Supattra Visessri, Ph.D.
Thesis Co Advisor Sokchhay Heng, Ph.D.

Accepted by the Faculty of Engineering, Chulalongkorn University in Partial
Fulfillment of the Requirement for the Master of Engineering

..... Dean of the Faculty of Engineering
(Associate Professor Supot Teachavorasinskun, D.Eng.)

THESIS COMMITTEE

..... Chairman
(Assistant Professor Anurak Sriariyawat, Ph.D.)
..... Thesis Advisor
(Supattra Visessri, Ph.D.)
..... Thesis Co-Advisor
(Sokchhay Heng, Ph.D.)
..... Examiner
(Piyatida Ruangrassamee, Ph.D.)
..... External Examiner
(Associate Professor Chaiyuth Sukhsri)



จุฬาลงกรณ์มหาวิทยาลัย
CHULALONGKORN UNIVERSITY

กิมสุข ชก : การประเมินความเสี่ยงภัยแล้งในลุ่มน้ำบาริโบใหญ่ ประเทศกัมพูชา. (

DROUGHT ASSESSMENT FOR THE GREATER BARIBO BASIN IN CAMBODIA) อ.ที่ปรึกษาหลัก : ดร.สุภัทรา วิเศษศรี, อ.ที่ปรึกษาร่วม : ดร.ชกเชษฐ์ เสง

กัมพูชาเป็นประเทศกำลังพัฒนา ซึ่งการพัฒนาและเศรษฐกิจของประเทศพึ่งพาการผลิตจากภาคการเกษตรเป็นหลัก ประเทศกัมพูชาเป็นผู้ส่งออกข้าวรายใหญ่ของโลก โดยมีลุ่มน้ำโคนเลสาบซึ่งมีพื้นที่ครอบคลุมประมาณร้อยละ 44 ของประเทศเป็นตัวขับเคลื่อนหลักในการพัฒนาเศรษฐกิจและสังคมแห่งชาติ ความผันผวนทางธรรมชาติและและการเปลี่ยนแปลงภูมิอากาศมีส่วนก่อให้เกิดภัยพิบัติทางธรรมชาติในหลากหลายรูปแบบ เช่น พายุฝน น้ำท่วม และภัยแล้ง ในลุ่มน้ำโคนเลสาบ ในช่วงหลายทศวรรษที่ผ่านมา ปัญหาภัยแล้งเป็นปัญหาที่ได้รับความสนใจเพิ่มขึ้นเนื่องจากปริมาณฝนมีแนวโน้มลดลง รัฐบาลกัมพูชาจึงได้กำหนดนโยบายในการแก้ไขปัญหาภัยแล้งโดยเพิ่มประสิทธิภาพการจัดการด้านการเกษตรและการปรับตัวต่อภัยแล้ง ลุ่มน้ำโคนเลสาบประกอบด้วย 11 ลุ่มน้ำย่อย ซึ่งลุ่มน้ำบาริโบใหญ่เป็นหนึ่งในลุ่มน้ำย่อยของลุ่มน้ำโคนเลสาบและเป็นพื้นที่ปลูกข้าวที่มีความสำคัญของประเทศกัมพูชา นอกจากนี้ลุ่มน้ำบาริโบใหญ่ยังเป็นหนึ่งในพื้นที่ที่ได้รับผลกระทบจากการลดลงของปริมาณฝน ดังนั้น ลุ่มน้ำบาริโบใหญ่จึงถูกเลือกให้เป็นกรณีศึกษาในงานวิจัยนี้ ซึ่งดำเนินการศึกษาโดยใช้ข้อมูลตั้งแต่ปี พ.ศ. 2528-2551

เนื่องจากภัยแล้งเป็นภัยธรรมชาติแบบไม่ลับพลับและมีกระบวนการพัฒนาอย่างซ้ำๆ ดังนั้น การบรรเทาผลกระทบจากภัยแล้งจึงสามารถกระทำโดยการประเมินและติดตามคุณลักษณะของภัยแล้งผ่านดัชนีภัยแล้ง (Drought index) ซึ่งเป็นตัวเลขสรุปข้อมูลที่คำนวณได้จากตัวแปรซึ่งภัยแล้งตั้งแต่หนึ่งตัวขึ้นไป ซึ่งนำไปใช้งานได้สะดวกมากกว่าการใช้ข้อมูลดิบจากตัวแปรซึ่งภัยแล้งแต่ละตัว ในการศึกษาการประเมินภัยแล้ง 3 ประเภท ได้แก่ ภัยแล้งเชิงอุตุนิยมวิทยา (Meteorological drought) ภัยแล้งเชิงเกษตรกรรม (Agricultural drought) และภัยแล้งเชิงอุทกวิทยา (Hydrological drought) โดยใช้ดัชนีภัยแล้ง 3 ตัว ได้แก่ ดัชนีน้ำฝนมาตรฐาน (Standardize Precipitation Index: SPI), ดัชนีพืชพรรณมาตรฐาน (Standardized Vegetation Index: SVI) และดัชนีน้ำท่ามาตรฐาน (Streamflow Drought Index: SDI) ตามลำดับ ในการประเมินภัยแล้งแต่ละประเภท โดยดัชนีภัยแล้งทั้ง 3 ตัวนี้ ถูกนำมาใช้ศึกษาคุณลักษณะต่างๆ ของภัยแล้ง ได้แก่ ความถี่ (Frequency) ระดับความรุนแรง (Severity) ช่วงเวลา (Duration) อัตราความรุนแรงต่อช่วงเวลา (Intensity) และการกระจายตัวของพื้นที่ประสบภัยแล้งในลุ่มน้ำบาริโบใหญ่ ทั้งนี้ เนื่องจากลุ่มน้ำบาริโบใหญ่เป็นลุ่มน้ำที่ไม่มีสถานีตรวจวัดน้ำท่าจำนวนน้อย จึงต้องอาศัยเทคนิคการพยากรณ์น้ำท่าสำหรับลุ่มน้ำที่ไม่มีสถานีตรวจวัด (Prediction in Ungauged Basin: PUB) ในการประมาณปริมาณน้ำท่าเพื่อวิเคราะห์ดัชนีภัยแล้งเชิงอุทกวิทยาในลุ่มน้ำบาริโบใหญ่

จากผลการศึกษาพบว่า สมการถดถอยเชิงเส้น (regressive equations) ที่พัฒนาจากความสัมพันธ์ระหว่างพารามิเตอร์ของแบบจำลองน้ำฝน-น้ำท่าและคุณลักษณะของลุ่มน้ำโดยใช้เทคนิคการพยากรณ์น้ำท่าสำหรับลุ่มน้ำที่ไม่มีสถานีตรวจวัดสามารถใช้ประมาณปริมาณน้ำท่าเพื่อประเมินภัยแล้งเชิงอุทกวิทยาได้ ผลการวิเคราะห์จากดัชนีทั้ง 3 ตัว (ดัชนีน้ำฝนมาตรฐาน ดัชนีพืชพรรณมาตรฐาน และดัชนีน้ำท่ามาตรฐาน) ชี้ว่า ภาคการเกษตรในลุ่มน้ำบาริโบใหญ่ได้รับผลกระทบจากภัยแล้งเป็นอย่างมากในปี พ.ศ.2536 และ 2537 ซึ่งระหว่างปี พ.ศ.2544-2549 เป็นช่วงการเกิดภัยแล้งที่ยาวที่สุดและรุนแรงที่สุด โดยภัยแล้งที่เกิดในช่วงเดือนพฤศจิกายนจะเป็นช่วงที่ส่งผลให้เกิดความเสียหายต่อผลผลิตทางการเกษตรอย่างมาก แต่จากผลการวิเคราะห์พบว่า ในช่วงระหว่างปี

สาขาวิชา วิศวกรรมแหล่งน้ำ

ปีการศึกษา 2561

ลายมือชื่อ นิสิต

ลายมือชื่อ อ.ที่ปรึกษาหลัก

ลายมือชื่อ อ.ที่ปรึกษาร่วม

5970382421 : MAJOR WATER RESOURCES ENGINEERING

KEYWORD: Tonle Sap basin Baribo basin SPI SVI and SDI

Kimhuy Sok : DROUGHT ASSESSMENT FOR THE GREATER
BARIBO BASIN IN CAMBODIA. Advisor: Supattra Visessri, Ph.D. Co-advisor:
Sokchhay Heng, Ph.D.

Cambodia is a developing country. The development and economic of the country rely mainly on agricultural production. Cambodia is a major exporter in the world rice market. The Tonle Sap basin covers about 44% of country. Rice production in the Tonle Sap basin is a main driver for national economic and social development. Due to natural variability and climate change, many forms of the natural disaster such as heavy storm, flood, and drought have occurred in the Tonle Sap basin. Over the recent decades, increased attention has been drawn to drought due to the tendency of rainfall decline. The Royal Government of Cambodia (RGC), has implemented the “Rectangular Strategies” policy to support and enhance the agricultural management and adaptation. The Greater Baribo basin, one of the Tonle Sap’s 11 basins and major rice production area, was selected as a study site. The period of the study was from 1985 to 2008.

Since drought is a slowly evolving natural disaster, its negative impacts can be mitigated through monitoring and characterizing drought levels by assimilating data from one or several indicators into a single numerical index. The single numerical index is more readily usable than raw indicator data. Standardize Precipitation Index (SPI), Standardized Vegetation Index (SVI) and Streamflow Drought Index (SDI) are employed for assessing the three types of drought namely a meteorological, agricultural, and hydrological drought, respectively. These indices were used to explore the drought frequency, severity, duration, intensity, and spatial distribution over the Greater Baribo basin. However, the Greater Baribo is considered an ungauged basin lacking of the streamflow data. Therefore, the Prediction in Ungauged Basin (PUB) technique was applied to generate streamflow in the Greater Baribo basin.

The result indicated that the regressive equations between the rainfall-runoff model parameters and basin properties from PUB technique were able to generate the streamflow for assessing the hydrological drought. The SPI, SVI, and SDI suggested that the agriculture was heavily impacted by drought in 1993 and 1994. The longest duration and the most severe drought occurred between 2001 and 2006. The drought occurring in November led to severe damage on the annual rice production. However, agriculture sector was found to be slightly affected by the longest and most severe drought in 2001-2006.

Field of Study: Water Resources
Engineering

Academic Year: 2018

Student's Signature

Advisor's Signature

Co-advisor's Signature

ACKNOWLEDGEMENTS

I would like to first express my deepest appreciation and gratitude to Dr. Supattra Visessri, my advisor and the deputy head of Department of Water Resources Engineering, Faculty of Engineering, Chulalongkorn University (Thailand), for her enthusiastic effort, invaluable guidance, moral support, and constructive comments from the inception to the completion of this research up to the final work of the thesis. Without her encouragement, insight, and guidance, the completion of this work would have been impossible.

I am highly indebted to Dr. Sokchhay Heng, my co-advisor and a lecturer in Faculty of Hydrology and Water Resources Engineering in Institute of Technology of Cambodia (ITC), for his encouragement, indispensable advice, provision of reference materials, and meticulous guidance. Moreover, he introduced me to the truly diverse and fascinating topic of drought assessment.

Financial support from ASEAN University Network Southeast Asia Engineering Education Development Network Program (AUN/SEED-Net) of Japan International Cooperation Agency (JICA) is also highly acknowledged.

I am also very grateful to my helpful friends Ms. Cheat Morakot and Mr. Chhorn Sopheaktra who guided me to develop the code with MATLAB program

I wish to thank Ms. Pinnara Ket (researcher and lecturer in Department of Water Resources and Rural Infrastructures Engineering in ITC), Mr. Sok Phun (Head Agriculture Machinery Office), Mr. Douk Bunthun (Head Department of Water Resources and Meteorological in Kompong Chhnang Province) and farmers in the Kompong Chhnang province such as Ms. Sarit, Mr. Khout Not, Ms. Chan Sareun, and Mr. Sat Song for facilitating the site visit and sharing information of drought in the study area.

Last but not least, I would also like to say a heartfelt thank you to my wife and parents, for always believing in me, encouraging and helping me in whatever way they could during my academic life.

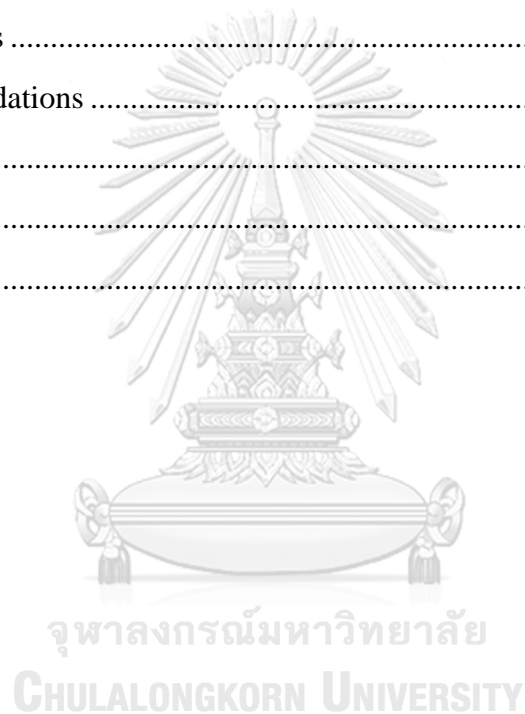
Kimhuy Sok

TABLE OF CONTENTS

	Page
ABSTRACT (THAI)	iii
ABSTRACT (ENGLISH)	iv
ACKNOWLEDGEMENTS	v
TABLE OF CONTENTS	vi
LIST OF TABLES	ix
LIST OF FIGURES	xi
LIST OF ABBREVIATIONS	xiv
CHAPTER 1 INTRODUCTION	1
1.1 Background	1
1.2 Objectives	2
1.3 Scope of the Study	2
1.4 Overall Research Framework	3
1.5 Thesis Outline	4
1.6 Expected Outputs and Outcomes	4
1.6.1 Outputs	4
1.6.2 Outcomes	4
CHAPTER 2 LITERATURE REVIEW	5
2.1 Definitions of Drought	5
2.2 Types of Drought	6
2.3 Assessment of Drought	8
2.4 Drought Indices	11
2.5 Previous Studies of Drought	16
CHAPTER 3 STUDY CATCHMENT	19
3.1 General Catchment Characteristics	19
3.2 Geographical Characteristics	20

3.2.1 Land Use.....	20
3.2.2 Soil Types.....	22
3.3 Rainfall Data in the Greater Baribo Basin.....	23
3.3.1 Rainfall Consistency Test.....	23
3.3.2 Rainfall Characteristic.....	25
3.3.3 Mean Annual Rainfall Distribution.....	31
3.4 Satellite Images Data.....	32
3.5 Hydrological Characteristic of Gauged Basins.....	34
3.5.1 Rainfall Characteristic.....	35
3.5.2 Temperature Characteristic.....	37
3.5.3 Streamflow Characteristic.....	39
CHAPTER 4 METHODOLOGY.....	42
4.1 Data Preparation.....	42
4.1.1 Data Collection.....	42
4.1.2 Data Quality Checking and Cleaning.....	42
4.1.3 Data Pre-processing.....	44
4.2 Drought Indices.....	44
4.2.1 Selection of Drought Index.....	44
4.2.2 Meteorological Drought Index.....	51
4.2.3 Agricultural Drought Index.....	55
4.2.4 Hydrological Drought Index.....	57
4.2.5 Theory of Runs (ToR).....	60
CHAPTER 5 RESULTS AND DISCUSSION.....	62
5.1 Meteorological Drought.....	62
5.1.1 Analysis of Meteorological Drought.....	62
5.1.2 Theory of Runs for SPI.....	65
5.2 Agricultural Drought Index.....	69
5.2.1 Analysis of Agricultural Drought.....	69
5.2.2 Theory of Runs for SVI.....	73

5.3 Hydrological Drought.....	76
5.3.1 Prediction in Ungauged Basin (PUB)	76
5.3.2 Analysis of Hydrological Drought	81
5.3.3 Theory of Runs for SDI.....	85
5.4 Impact of Drought on Cropping Pattern	88
5.5 Spatial Distribution of Drought	101
5.6 Discussion.....	110
CHAPTER 6 CONCLUSIONS AND RECOMMENDATIONS.....	112
6.1 Conclusions	112
6.2 Recommendations	114
REFERENCES	116
APPENDICES	120
VITA.....	127



LIST OF TABLES

	Page
Table 2.1. Level of Vulnerability (LV) based on score value (MoE, 2005).....	9
Table 2.2. Drought classification based on the SPI value (Guo et al., 2017)	10
Table 3.1. Description of the land use in the Greater Baribo basin.	21
Table 3.2. Description of major soil types in the Greater Baribo basin.....	22
Table 3.3. Description of rainfall stations in the Greater Baribo basin	29
Table 4.1. Description of the data collection	43
Table 4.2. Converting data to the time-scale of 3-, 6-, 12-, 24-, and 48-month	44
Table 4.3. Brief process and main features of widely used drought indices	45
Table 4.4. Classification of vegetation condition based on SVI value	57
Table 4.5. Drought classification based on the SDI value.....	60
Table 5.1. Characteristics of the drought event in the three sub-basins for SPI3	67
Table 5.2. Characteristics of the drought event in the three sub-basins for SPI6	68
Table 5.3. Characteristics of the drought event in the three sub-basins for SPI12	68
Table 5.4. Characteristics of the drought event in the three sub-basins for SPI24	69
Table 5.5. Characteristics of the drought event in the three sub-basins for SPI48	69
Table 5.6. Characteristic of the vegetation in the three sub-basins for SVI3	74
Table 5.8. Characteristic of the vegetation in the three sub-basins for SVI12	75
Table 5.9. Characteristic of the vegetation in the three sub-basins for SVI24	75
Table 5.10. Characteristic of the vegetation in the three sub-basins for SVI48	75
Table 5.11. Performance of the model calibration and validation.....	78
Table 5.12. Six model parameters of six gauged basins from the calibration	78
Table 5.13. Correlation between the model and basin properties parameters	80
Table 5.14. Six model parameters of six gauged basins from the regression.....	80
Table 5.15. Performance of model calibration and validation of the model parameters from the regression	81

Table 5.16. Six model parameters of nine ungauged basins of the Greater Baribo basin	81
Table 5.17. Characteristics of the drought event in the three sub-basins for SDI3	86
Table 5.18. Characteristics of the drought event in the three sub-basins for SDI6	87
Table 5.19. Characteristics of the drought event in the three sub-basins for SDI12 ...	87
Table 5.20. Characteristics of the drought event in the three sub-basins for SDI24 ...	88
Table 5.21. Characteristics of the drought event in the three sub-basins for SDI48 ...	88
Table 5.22. SPI3 for early duration rice.....	92
Table 5.23. SPI3 for medium duration rice.....	93
Table 5.24. SPI6 for long duration rice.....	94
Table 5.25. SVI3 for early duration rice.....	95
Table 5.26. SVI3 for medium duration rice.....	96
Table 5.27. SVI6 for long duration rice.....	97
Table 5.28. SDI3 for early duration rice.....	98
Table 5.29. SDI3 for medium duration rice.....	99
Table 5.30. SDI6 for long duration rice.....	100

LIST OF FIGURES

	Page
Figure 1.1 Framework of research procedure	3
Figure 2.1. Four main terms of the water deficit (Vlachos and James, 1983).....	6
Figure 2.2. General sequence for the occurrence of different types of drought	8
Figure 3.1. Tonle Sap and Greater Baribo basins with sub-basins, main river, and elevation.....	20
Figure 3.2. Land use map of the Greater Baribo basin	21
Figure 3.3. Soil types map of the Greater Baribo basin.....	22
Figure 3.4. Consistency test by double mass curve of the 12 rainfall stations	24
Figure 3.5. DMC of rainfall data of the inconsistent station after adjusted.....	24
Figure 3.6. Daily rainfall of stations in the Bamnak sub-basin	25
Figure 3.7. Daily rainfall of stations in the Baribo sub-basin from	25
Figure 3.8. Daily rainfall of stations in the Kraing Ponley sub-basin.....	26
Figure 3.9. Monthly rainfall of stations in the Bamnak sub-basin.....	26
Figure 3.10. Monthly rainfall of stations in the Baribo sub-basin.....	27
Figure 3.11. Monthly rainfall of stations in the Kraing Ponley sub-basin.....	27
Figure 3.12. Annual rainfall of stations in the Bamnak sub-basin.....	28
Figure 3.13. Annual rainfall of stations in the Baribo sub-basin.....	28
Figure 3.14. Annual rainfall of stations in the Kraing Ponley sub-basin.....	28
Figure 3.15. Monthly average rainfall of stations in the Kraing Ponley sub-basin	29
Figure 3.16. Monthly average rainfall of stations in the Bamnak sub-basin	30
Figure 3.17. Monthly average rainfall of stations in the Kraing Ponley sub-basin	30
Figure 3.18. Annual rainfall distribution of the Greater Baribo basin.....	32
Figure 3.19. Monthly average of Infrared Radiation (IR)	33
Figure 3.20. Monthly average of Near-Infrared Radiation (NIR)	33
Figure 3.21. Pictorial description of IR, NIR and NDVI calculation.	34
Figure 3.22. Monthly average of NDVI.....	34

Figure 3.23. Daily rainfall data of gauged basins in the Tonle Sap basin	35
Figure 3.24. Monthly rainfall data of gauged basins in the Tonle Sap basin	36
Figure 3.25. Annual rainfall data of gauged basins in the Tonle Sap basin	36
Figure 3.26. Daily temperature of gauged basins in the Tonle Sap basin	37
Figure 3.27. Monthly average temperature of gauged basins in the Tonle Sap basin ..	38
Figure 3.28. Annual average temperature of gauged basins in the Tonle Sap basin ...	38
Figure 3.29. Yield of daily streamflow of gauged basins in the Tonle Sap basin	39
Figure 3.30. Yield of monthly streamflow of gauged basins in the Tonle Sap basin ..	40
Figure 3.31. Yield of annual streamflow of gauged basins in the Tonle Sap basin.....	41
Figure 4.1. Framework for computing SPI	52
Figure 4.2. Fitting gamma distribution of each month in 110405	53
Figure 4.3. Example of equiprobability transformation from fitted gamma distribution to the standard normal distribution in June at 110405	54
Figure 4.4. Framework for calculating SVI	55
Figure 4.5. Example of PDF and CDF of normal distribution of NDVI value for three sub-basins in June	56
Figure 4.6. Framework for PUB technique.....	57
Figure 4.7. Map of the gauged and ungauged basins.....	58
Figure 4.8. General structure of IHACRES model.....	59
Figure 4.9. Fitting Gamma distribution of each month in sub-basin 1	59
Figure 4.10. Properties of the ToR.....	61
Figure 5.1. SPI3 between 1985 and 2008 of the three sub-basins	63
Figure 5.2. SPI6 between 1985 and 2008 of the three sub-basins	63
Figure 5.3. SPI12 between 1985 and 2008 of the three sub-basins	64
Figure 5.4. SPI24 between 1985 and 2008 of the three sub-basins	64
Figure 5.5. SPI48 between 1985 and 2008 of the three sub-basins	65
Figure 5.6. SVI3 between 1985 and 2008 of the three sub-basins	70
Figure 5.7. SVI6 between 1985 and 2008 of the three sub-basins	71
Figure 5.8. SVI12 between 1985 and 2008 of the three sub-basins	71
Figure 5.9. SVI24 between 1985 and 2008 of the three sub-basins	72

Figure 5.10. SVI48 between 1985 and 2008 of the three sub-basins	72
Figure 5.11. Scatter plot of observed and simulated streamflow for calibration	77
Figure 5.12. Scatter plot of observed and simulated streamflow for validation	78
Figure 5.13. SDI6 between 1985 and 2008 of the three sub-basins	82
Figure 5.14. SDI3 between 1985 and 2008 of the three sub-basins	83
Figure 5.15. SDI12 between 1985 and 2008 of the three sub-basins	83
Figure 5.16. SDI24 between 1985 and 2008 of the three sub-basins	84
Figure 5.17. SDI48 between 1985 and 2008 of the three sub-basins	84
Figure 5.18. Rice development phases for long, medium, and early rice varieties	89
Figure 5.19. Drought map of SPI.....	104
Figure 5.20. Vegetation condition map of SVI.....	105
Figure 5.21. Drought map of SDI	106
Figure 5.22. Drought map of the three indices in July 1987.....	107
Figure 5.23. Drought map of the three indices in October 1990.	107
Figure 5.24. Drought map of the three indices in November 1993	108
Figure 5.25. Drought map of the three indices in April 1994.....	108
Figure 5.26. Drought map of the three indices in August 2000.....	109
Figure 5.27. Drought map of the three indices in March 2005.....	109

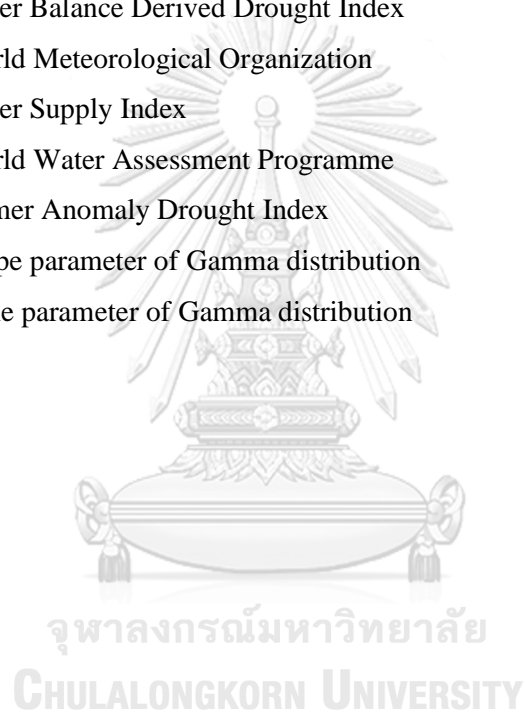
LIST OF ABBREVIATIONS

A	Agriculture
a_1	DMC slope before changing
a_2	DMC slope after changing
AAM	Asian-Australian Monsoon
AI	Aridity Index
AMSR-E	Advanced Microwave Scanning Radiometer-Earth Observing System
AusAID	Australian Agency for International Development
AVHRR	Advanced Very High-Resolution Radiometer
AWC	Available Water Content
BMDI	Bhalme Mooley Drought Index
c	Volumetric storage coefficient
CDF	Cumulative Distribution Function
CDR	Climate Data Record
CHIRPS	Climate Hazards Group InfraRed Precipitation with Station
CMi	Crop Moisture Index
CSDI	Crop Specific Drought Index
CWSI	Crop Water Stress Index
CWSI	Crop Water Stress Index
DD	Drought Duration
DE	Drought Event
DI	Drought Intensity
DM index	Dry Condition and Excessive Moisture Index
DMC	Double Mass Curve
DS	Drought Severity
DSI	Drought Severity Index
ED	Early Duration rice
EDI	Effective Drought Index
ETDI	Evapotranspiration Deficit Index
EVI	Enhanced Vegetation Index
f	Temperature modulation of the drying rate
FAO	Food and Agriculture Organization

GDP	Gross Domestic Product
GWP	Global Water Partnership
H	Hydrological
IDW	Inverse Distance Weighting
IHACRES	Identification of unit Hydrographs And Component flows from Rainfall, Evaporation and Streamflow
IPCC	Intergovernmental Panel on Climate Change
IR	Infrared Radiation
ITCZ	Inter-Tropical Convergence Zone
KBDI	Keetch-Byram Drought Index
LD	Long Duration rice
LMB	Lower Mekong Basin
LST	Land Surface Temperature
LV	Level of Vulnerability
LWDD	Land and Water Development Division
M	Meteorological
m	Numbers of zeros in the rainfall time series
MD	Medium Duration rice
MODIS	Moderate Resolution Imaging Spectroradiometer
MoE	Ministry of Environment
MOWRAM	Ministry of Water Resources and Meteorology
MPDI	Modified Perpendicular Drought Index
MRC	Mekong River Commission
n	Total number time series of the rainfall
NAPA	Nation Adaptation Program of Action to climate change
NDII	Normalized Difference Infrared Index
NDVI	Normalized Difference Vegetation Index
NESDB	National Economic and Social Development Board
NIR	Near-Infrared Radiation
NOAA	National Oceanic and Atmospheric Administration's
NRI	National Rainfall Index
NSE	Nash Sutcliffe Efficiency
°C	Degree Celsius
P	Precipitation

P_a	adjusted annual rainfall
PDF	Probability Density Function
PDI	Perpendicular Drought Index
PDSI	Palmer Drought Severity Index
PHDI	Palmer Hydrological Drought Index
PMDI	Palmer Modified Drought Index
PNP	Percent of Normal Precipitation
P_o	Observed annual rainfall
PUB	Prediction of Ungauged Basin
q	Probability of the rainfall of the zero value
R^2	Coefficient of determine
RAI	Rainfall Anomaly Index
RDI	Reconnaissance Drought Index
RDI	Reclamation Drought Index
RGCC	Royal Government of Cambodia
RS	Remote Sensing
RSDI	Regional Streamflow Deficiency Index
RSDRI	Remote Sensing Drought Risk Index
RSM	Relative Soil Moisture
SAI	Standardized Anomaly Index
SAVI	Soil Adjusted Vegetation Index
SD	Standard Deviation
SDI	Streamflow Drought Index
SF	Streamflow
SMA	Soil Moisture Anomaly
SMDI	Soil Moisture Drought Index
SPEI	Standardized Precipitation Evapotranspiration Index
SPI	Standardized Precipitation Index
SVI	Standard Vegetation Index
SWIR	Short Wave Infrared
T	Temperature
TCI	Temperature Condition Index
ToR	Theory of Runs
t_q	Time constant for the quick flow

TRMM	Tropical Rainfall Measuring Mission
t_s	Time constant for the slow flow
TRVDI	Temperature Vegetation Dryness Index
t_w	Drying rate of catchment
VCADI	Vegetation Condition Albedo Drought Index
VCI	Vegetation Condition Index
VIT	Vegetation Index/Temperature
VITT	Vegetation Index/Temperature Trapezoid
v_q	Relative volume of the quick flow response
WBDDI	Water Balance Derived Drought Index
WMO	World Meteorological Organization
WSI	Water Supply Index
WWAP	World Water Assessment Programme
Z-index	Palmer Anomaly Drought Index
α	Shape parameter of Gamma distribution
β	Scale parameter of Gamma distribution



CHAPTER 1

INTRODUCTION

1.1 Background

Throughout history, nations, cities and civilizations have grown near water resources as water is a fundamental necessity to life on Earth and crucial to social and economic development (David and Claudia, 2006). Different quantity of water has been used in various sectors including domestic, agricultural, and industrial sectors. In developed countries, water is consumed mostly in the industrial sector while in developing countries such as Cambodia, much of water is used to support agriculture (WWAP, 2003). While Cambodia is considered to have abundant water resources (MOWRAM, 2008), such resources are non-uniformly distributed in space and time (Sam and Pech, 2015) resulting in agricultural production which contributes most to Cambodia's Gross Domestic Product (GDP) (Bansok et al., 2011). Referring to the "Rectangular Strategies" of Royal Government of Cambodia (RGC) from the third to fifth legislature, the enhancement of agricultural sector has been considered as one of the main policies which covers (1) improving productivity and diversification of agriculture, (2) increasing agricultural area, (3) managing water resources and irrigation, (4) reforming fisheries. According to Saburo et al. (2006), the heart of agricultural regions in Cambodia are in the Tonle Sap and Mekong River basin where rice is the common crop. The Tonle Sap basin covers approximately 44% of Cambodia and accommodates about 32% of total population (Bansok et al., 2011). The evidence of the hydrological change in the Tonle Sap basin, reported by Australian Agency for International Development (AusAID), has caused concerns and impacts on the social, economic, and environmental development (Keskinen et al., 2011). The Tonle Sap basin has frequently experienced natural hazards such as flood, heavy storm, and drought which are related to the dominant climate system in the Southeast Asia and the Asian-Australian Monsoon (AAM) (Yihui, 2007, and Ding et al., 2015). Those natural disasters have significantly impacted the rice production in Cambodia. Based on the evaluation performed by the Ministry of Environment from 1996 to 2000, Cambodia, drought led to an approximate 20% decrease in the national rice production. Later in 2004, a severe drought damaged the paddy rice field around 300,000 hectares and reduced the potential harvesting about 82% (Chhinh and Millington, 2015). Drought has become more threatening catastrophe for the country in recent years due to a decrease in rainfall amount. According to the evidences mentioned above, drought is a major hazard which leads the country to unsustainable development and economic loss. Therefore, the evaluation of the drought

intensity, severity, frequency, duration, and distribution can help in identifying sensitive agricultural area which is less prone to the water scarcity and will eventually support the national development. More importantly, it also contributes to the Rectangular Strategies of RGC for enhancing the agricultural sector in Cambodia.

1.2 Objectives

Main objectives of this research are:

- to predict streamflow in ungauged basin for drought analysis
- to analyze spatial and temporal characteristics of meteorological, agricultural, and hydrological droughts

1.3 Scope of the Study

- This research is conducted in the Greater Baribo basin which is one out of eleven basins in the Tonle Sap basin in Cambodia.
- The study period is between 1985 and 2008 during which several drought events were found, and meteo-hydrological records are sufficient for detailed study.
- Gauged data, land use, and soil types are obtained from Ministry of Water Resources and Meteorology (MOWRAM) and Mekong River Commission (MRC); satellite data i.e. Infrared Radiation (IR) and Near-Infrared Radiation (NIR) are downloaded from National Oceanic and Atmospheric Administration's (NOAA).
- Prediction of Ungauged Basin (PUB) method is applied to predict the time-series of streamflow data.
- Three drought indices are selected for assessing the meteorological, agricultural, and hydrological droughts.
- Interpolation technique is employed to distribute the drought intensity and develop drought map.

1.4 Overall Research Framework

Research procedures consist of four main steps as shown in Figure 1.1 and briefly explained as follows:

- The data preparation covers the collection of all data required for calculation of the drought indices (e.g. rainfall, streamflow, IR, NIR, and NDVI), data pre-processing, and data quality checking and cleaning.
- The PUB technique is performed to predict the streamflow data for hydrological drought analysis.
- The selected drought indices are explored to demonstrate the characteristics of the three types of drought namely meteorological, agricultural and hydrological droughts.
- Spatial interpolation of the drought index value is examined to produce drought map for the whole Greater Baribo basin. The development of the drought map is based on the selected drought event and spatial interpolation technique.

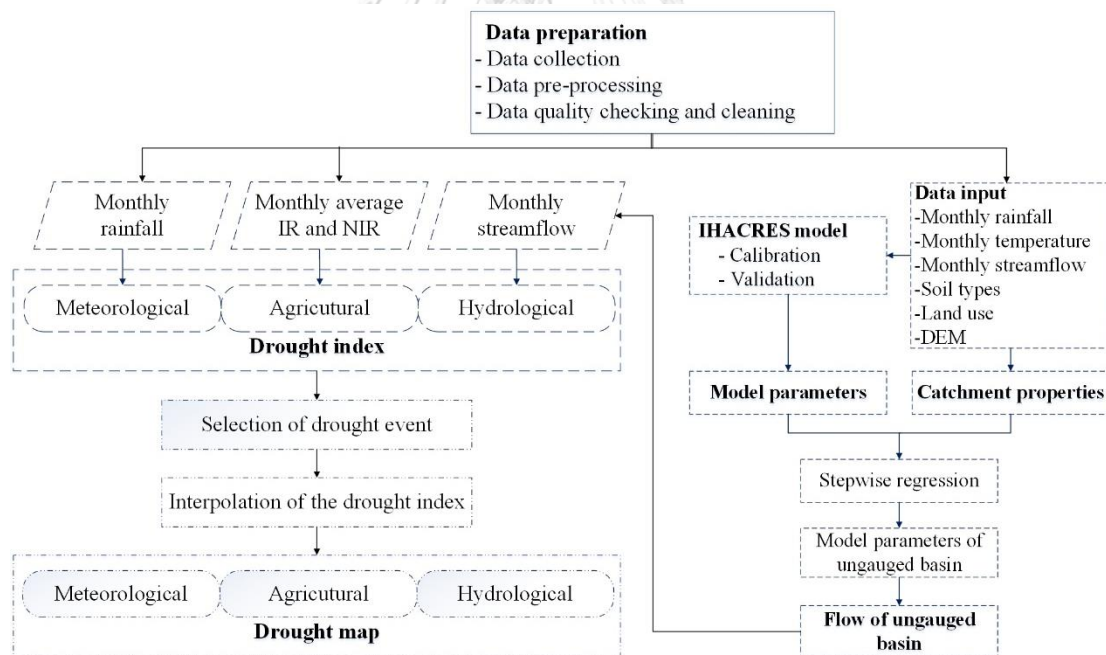


Figure 1.1 Framework of research procedure

1.5 Thesis Outline

This thesis consists of six chapters and Chapter 1 explains why this research is important and needed. Chapter 2 is literature review which refers to theories and previous studies in drought analysis. Chapter 3 describes characteristics of the study area. Chapter 4 explains the methodology used in this study. Chapter 5 shows and discuss the results obtained from this research and chapter 6 is the conclusions and recommendations.

1.6 Expected Outputs and Outcomes

1.6.1 Outputs

- Regression equations for predicting streamflow in ungauged basins
- Streamflow estimates for ungauged basins
- Drought indices
- Drought maps

1.6.2 Outcomes

- Understanding of the PUB technique
- Understanding of the development of drought and calculation of drought indices
- Ability to identify key indices which can be used as indicators of the drought characteristics
- Increased awareness of the impacts of drought on the national development

CHAPTER 2

LITERATURE REVIEW

2.1 Definitions of Drought

Many researchers attempted to give definitions of drought. According to Vlachos and James (1983), drought is one of four categories of the water deficit defined based on its process and context as shown in Figure 2.1. The process refers to an environmental transformation which can be caused by either nature or human (man-made), and the context is considered based on the duration of the existence of the process which can be either temporary or permanent. Apart from the drought, other three categories are aridity, water shortages, and desertification. Drought and aridity are caused by natural processes, but they are different in terms of the duration of the existence. Drought is a temporary water imbalance while aridity is a permanent water deficiency. When moving from the natural to man-made process, temporary water imbalance is called water shortages and permanent water deficiency is termed as the desertification.

Even more specific, Wilhite and Glantz (1985) defined drought as conceptual and operational definitions. Conceptual definitions of drought are expressed in a general description of the concepts for the overall understanding and organizing drought policy, whereas operation definitions of drought principally describe the criteria for identifying the beginning and ending of drought and severity for a specific application. World Meteorological Organization (WMO) (1986) stated that drought means a sustained and extended lack of the precipitation. General UN Secretariat (1994) defined that drought is the phenomenon of the nature which occurs when the precipitation has been much lower than the normal recorded level, leading to weighty hydrological imbalances and adversely damaged agriculture. Indeed, droughts are variably defined based on the disciplinary perspective e.g. drought characteristics, causes, effect, and stage of occurrence (Wilhite and Glantz, 1985). The four common types have been identified, namely 1) meteorological, 2) agricultural, 3) hydrological, and 4) socio-economic droughts. The detail of these four types of drought is described in the next section.

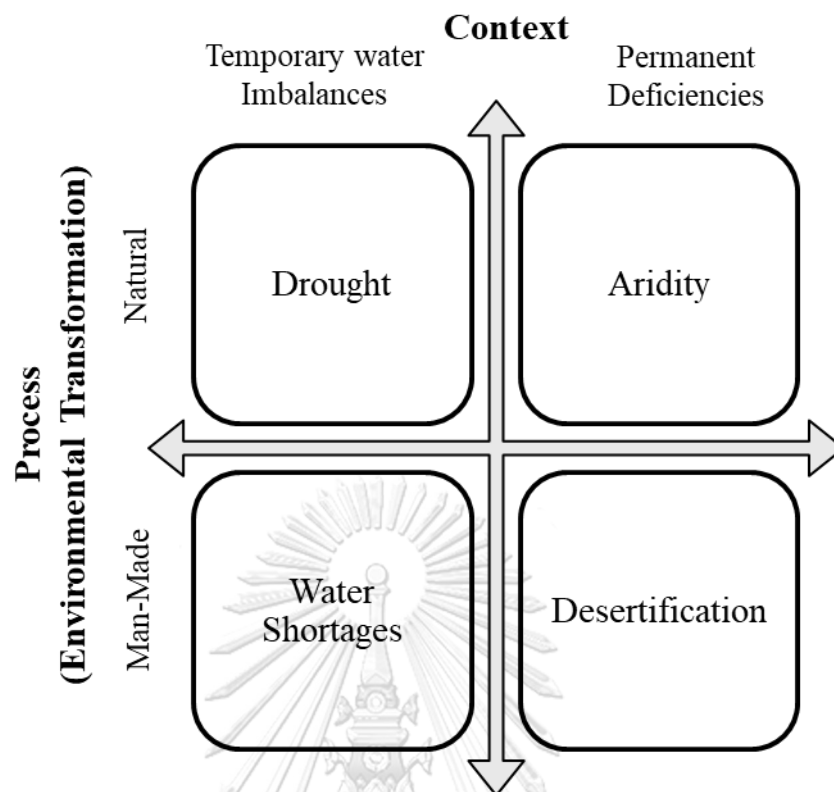


Figure 2.1. Four main terms of the water deficit (Vlachos and James, 1983)

2.2 Types of Drought

The classification of drought is different depending on viewers. However, droughts which are commonly categorized in reference with three dimensions, which are the severity, duration, and spatial distribution, can be classified into four categories comprising of the meteorological, hydrological, agriculture, and socio-economic drought (Wilhite and Glantz, 1985, and Council, 2004). As shown in Figure 2.2, droughts occur in a sequential order. The meteorological drought is caused by changes in meteorological variables such as rainfall, temperature, and frequently defined depending on the level of the dryness and the duration of the drought period (Keyantash and Dracup, 2002). The meteorological drought can be found as the shortage of the precipitation over an area for a period. The precipitation data has been principally used to assess the meteorological drought (Chang, 1991, and Eltahir, 1992) Many researchers used monthly precipitation data to determine the drought severity (Chang and Kleopa, 1991, and Estrela et al., 2000) and used the cumulative precipitation data to assess the drought intensity and duration. The meteorological drought leads to deficiency of the soil moisture content and subsequently resulting in the agricultural drought.

The agricultural drought generally refers to a period that the crop reaches the wilting point causing crop failures without the present of surface water resources. The agricultural drought is defined by the Food and Agriculture Organization (FOA) of United Nations and Land and Water Development Division (LWDD) (1983) as the probability of a year that the agriculture is damaged from the deficiency of the soil moisture. The agricultural drought is the difference between the crop water demand and the available soil moisture content (Wilhite and Glantz, 1985). Its indices rely on a combination of the rainfall, temperature, and soil moisture content (Mishra and Singh, 2010).

The hydrological drought is found when the discharge in the river, surface water, and sub-surface water is less than the usual and insufficiency to meet the demand. It is also referred to as impacts of dry spells on the surface and sub-surface hydrology. Gumbel (1963) gave another definition of the hydrological drought as the minimum annual value of discharge with the daily time step, while David (2003) stated that hydrological drought occurs when the flow rate in the river is less than usual. Streamflow is needed to indicate this type of drought. Dracup et al. (1980) found that geology is one of sensitive factors influencing the hydrological drought.

The definitions of the socio-economic drought, as stated by Kifer and Stewart (1938), normally links various features of the meteorological, agricultural, and hydrological droughts. For example, Gibbs (1975) defined the socio-economic drought as it is generally associated with the supply and demand of some economic goods. The socio-economic drought is the consequence of previous three types of drought which refers to water resources in a specific region which fail to meet the demand at the specific period of time (Kifer and Stewart, 1938). In short, the socio-economic drought takes place when the demand side for economic goods is over the supply side (Wilhite and Glantz, 1985).

Apart from mentioned four types of droughts, the groundwater drought is considered a relatively new type of drought (Mishra and Singh, 2010). It is observed when the groundwater recharge is affected by the drought which consequently lowers groundwater levels and groundwater discharges. Furthermore, Van Lanen and Peters (2000) reported that this type of drought usually occurs in months or a years. As it is difficult to identify the amount of the available underground water, the groundwater drought is defined by the decrease of the groundwater level (Chang and Teoh, 1995, and Eltahir and Yeh, 1999).

This research mainly focuses on three types of drought namely meteorological, agricultural and hydrological droughts due to unavailability of socioeconomic and ground water data.

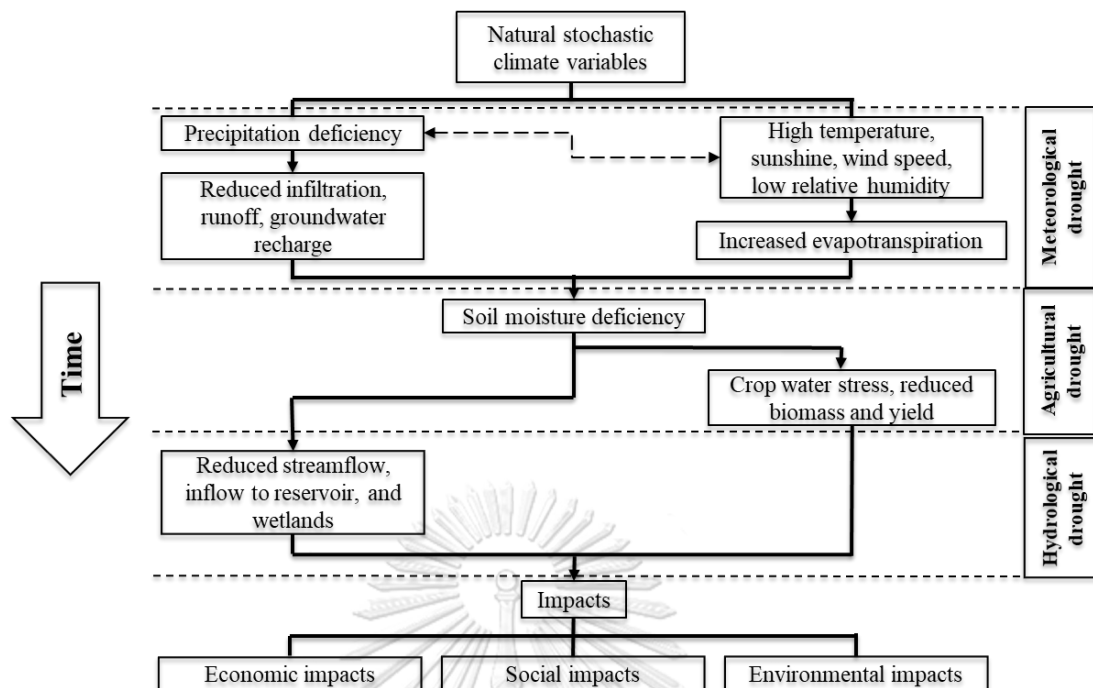


Figure 2.2. General sequence for the occurrence of different types of drought (Wilhite and Glantz, 1985)

2.3 Assessment of Drought

There are a number of researchers who assessed the drought severity using different methods (Chhinh and Millington, 2015). Likewise, Suwanwerakamtorn et al. (2006) employed the matrix overlay function in ArcViewGIS which developed by Khon Kaen University to assess the drought risk in the Nam Choen basin in the Northeast of Thailand. Seven parameters were used including 1) rainfall, 2) surface water and irrigation, 3) sub-surface water, 4) stream density, 5) slope, 6) soil drainage, and 7) land use. The value of each parameter was determined as numerical values and then inserted into the matrix overlay tool in ArcViewGIS to indicate the agricultural drought severity and drought map. The result from that research was verified against the survey data from the national rural development project at village level in 1994, 1996, 1999, 2003 and 2005 which is provided by the National Economic and Social Development Board (NESDB). Some researchers applied the Standardized Precipitation Index (SPI) in terms of the operational application to assess the agricultural drought (Mestre, 2011, Omondi, 2011, and Sarkar, 2011). Although the SPI is a meteorological drought index, it can be utilized to evaluate the agricultural drought due to its ability to examine the drought in various time scales. The seasonal time scale of the SPI was generally considered for indicating the agricultural drought. Motha (2011) mentioned that a

crop model played an important role in the agricultural management and decision-making process to cope with the drought and other natural disasters. He used the crop model to separate the yield prospects into components owing to the changing weather trends, genetic improvements, and improved technology. So, the crop simulation model can be used to analyze the reduction of crop yields by effects of drought.

MoE (2005) applied formulation of the Nation Adaptation Program of Action to climate change (NAPA) to assess the drought and flood from 1982 to 2002 in Cambodia. This assessment was based on the interview and surveying data which involved two main steps. The first step was to identify locations where were affected by both flood and drought. The second step was to assess impacts of severe floods and droughts on people, properties, and wells. The objective of the survey was to know about locations and losses caused by floods and drought hazards. They classified the Level of Vulnerability (LV) into four groups as shown in Table 2.1. LV greater than 7 means very vulnerable. LV from 3 to 7 means vulnerable. LV from 0.50 to 3 means quite vulnerable. LV equal or lower than 0.50 means not vulnerable. After that, the data was combined and grouped into three categories to calculate the LV score which considered the level of fatalities, property losses, and number of contaminated wells. Finally, the flood and drought prone areas based on the LV score were mapped, so the flood and drought risk of each geographical location in Cambodia can be identified from the LV score.

Table 2.1. Level of Vulnerability (LV) based on score value (MoE, 2005).

No.	Vulnerability Score (LV)	Level of Vulnerability
1	Above 7	Very vulnerability
2	3 to 7	Vulnerability
3	0.5 to 3	Quite vulnerability
4	Below and equal 0.5	Not vulnerability

Chhinh and Millington (2015) conducted a research on the drought monitoring for the rice production in Cambodia using the SPI. The SPI requires only the rainfall data to calculate in various time-scales. The use of the difference probability of rainfall distribution influenced the SPI value due to the fitting of the precipitation series distribution. Some of the widely used rainfall distributions to simulate the SPI's value are Gamma (McKee et al., 1993, Edwards, 1997, and Mishra et al., 2009) Pearson type III (Guttman, 1999), Lognormal, and Exponential distributions (Todorovic and Woolhiser, 1976, Madsen et al., 1998, Lloyd-

Hughes and Saunders, 2002, and Wu et al., 2007). To estimate SPI values, the Gamma distribution of the precipitation data was transformed to the standard normal distribution with the random variable Z with zero mean and variance of one. The random variable Z was then converted to SPI value by normal inverse cumulative distribution function. The value of the SPI was categorized into seven classes including 2 and above, 1.50 to 1.99, 1 to 1.49, -0.99 to 0.99, -1 to -1.49, -1.50 to -1.99, and -2 and less. This class refers to extremely wet, severely wet, moderately wet, near normal, moderately dry, severely dry, and extremely dry, respectively as shown in Table 2.2.

Table 2.2. Drought classification based on the SPI value (Guo et al., 2017)

SPI Value	Category
2.0 and above	Extremely wet (W3)
1.5 to 2.0	Severely wet (W2)
1.0 to 1.5	Moderately wet (W1)
-1.0 to 1.0	Near normal (N)
-1.0 to -1.5	Moderately dry (D1)
-1.5 to -1.0	Severely dry (D2)
-2.0 and less	Extremely dry (D3)

As the technology has updated very fast during the 1980s, the satellite has opened many ways to assess the drought severity by the remote sensing data from sensors. Guo et al. (2017) used the CHIRPS satellite precipitation dataset which was a new IR-based climatic precipitation data with the high resolution ($0.05^\circ \times 0.05^\circ$) between 1981 and 2016 to evaluate the drought severity in the Lower Mekong Basin (LMB). Filtering method was used to select the missing data and gauges which contained missing data more than 30 percentages were not considered. Normal Ratio Method (NRM) was employed to fill in the missing data in each gauge from the nearest two to three gauges. The monthly precipitation data was used to calculate the SPI. Bert and Elga (2016) analyzed precipitation and vegetation health condition in Cambodia. The remote sensing Enhanced Vegetation Index (EVI) was applied to indicate the severity of drought in this research. EVI values on the same day over different years were compared to assess the relativeness of the vegetation cover which known as the Standard Vegetation Index (SVI). The high SVI value indicated a good growth condition of vegetation, while low value showed that the vegetation faced both flood and drought issues. Son et al. (2012) applied the monthly Moderate Resolution Imaging Spectroradiometer (MODIS)-

Normalized Difference Vegetation Index (NDVI) and Land Surface Temperature (LST) data for the agriculture drought monitoring in the LMB in the dry season. The Temperature Vegetation Dryness Index (TVDI) was calculated by the parameterizing the relationship between the MODIS-NDVI and LST data. The daily volumetric surface soil moisture from the Advanced Microwave Scanning Radiometer-Earth Observing System (AMSR-E) and monthly precipitation from the Tropical Rainfall Measuring Mission (TRMM) were collected and used to verify the result. TVDI was compared with the Crop Water Stress Index (CWSI), AMSR-E, and TRMM precipitation to check the efficiency.

2.4 Drought Indices

Drought indices are quantitative measures using key raw climatological variables, or indicators, to determine characteristics of drought and to transform them into a single numerical value which is more convenient to use than the raw indicator data (Hayes, 2006). There are a large number of drought indices which were developed in the last decades to response the effect of the drought around the world (Niemeyer, 2008, and Cai et al., 2011). Many drought indices have been developed during the 20th century to indicate the water deficit condition in terms of meteorological, agricultural, hydrological droughts.

The early generation of drought indices has focused on the meteorological aspect. Examples of meteorological drought indices are the Palmer Drought Severity Index (PDSI) (Palmer, 1965), Palmer Modified Drought Index (PMDI) (Palmer, 1965), Rainfall Anomaly Index (RAI) (Van Rooy, 1965), Bhalme Mooley Drought Index (BMDI) (Bhalme and Mooley, 1980), Standardized Anomaly Index (SAI) (Katz and Glantz, 1986), Drought Severity Index (DSI) (Bryant et al., 1992), Standardized Precipitation Index (SPI) (McKee et al., 1993), Effective Drought Index (EDI) (Byun and Wilhite, 1999), Percent of Normal Precipitation (PNP) (Keyantash and Dracup, 2002), Reconnaissance Drought Index (RDI) (Tsakiris and Vangelis, 2005), and Standardized Precipitation Evapotranspiration Index (SPEI) (Vicente-Serrano et al., 2010).

The description of some widely used indices is briefly explained here. The PNP is a simple index which depends on the variation between the actual precipitation and long-term normal precipitation. The PDSI requires more data including monthly precipitation, temperature, and Available Water Content (AWC) to determine the evapotranspiration, runoff, soil recharge, and moisture from water balance equation. The PMDI is modified from the PDSI but they are different in the process of identifying the drought period. The BMDI takes into account the rainfall over four months of the monsoon. A statistical process is

applied to identify standard deviation and coefficient of variation of precipitation. The numerical value of the BMDI is then determined within the range between -4 and 4. The value of the BMDI below zero indicates the dry period and above zero indicates the wet period. The EDI drought index refers to the effective precipitation. This index addresses the weaknesses of some indices by considering the beginning, ending, and accumulated stress of the drought at the daily rather than monthly time-scale. The RDI is relatively a new drought index with the physical based and the calculation is depended on the combination of precipitation and evaporation requirement (Zargar et al., 2011). The SPI requires only the rainfall data. The value of the SPI is generated from the monthly rainfall data with the statistical transformation from the probability distribution to the standard normal distribution. The values of the SPI below zero indicate dry periods and above zero indicate wet periods. It performs well in assessing the early emergency and agricultural drought since it can be calculated at various time scales of interest. Moreover, SPI is considerable widely used worldwide (Wilhite, 2011).

Agricultural drought indices are the approach to determine impacts of the water deficit condition on the soil moisture content that lead to crop failure. Example of indices in category are the Aridity Index (Ia) (Thornthwaite, 1948), Relative Soil Moisture (RSM) (Thornthwaite, 1955), Palmer Anomaly Drought Index (Z index) (Palmer, 1965), Crop Moisture Index (CMI) (Palmer, 1968), Keetch-Byram Drought Index (KBDI) (Alexander, 1990), Soil Moisture Drought Index (SMDI) (Welford et al., 1993), Crop Specific Drought Index (CSDI) (Meyer et al., 1993), National Rainfall Index (NRI) (Gommes and Petrassi, 1996), Dry Condition and Excessive Moisture Index (DM Index) (Meshcherskaya and Blazhevich, 1997), Soil Moisture Anomaly (SMA) (Potgieter et al., 2005) Evapotranspiration Deficit Index (ETDI) (Narasimhan and Srinivasan, 2005), DTx (Matera et al., 2007).

The description of some widely used indices is briefly explained here. The Ia is a widely used index to represent the crop moisture stress, and its computation is relied on the water balance technique. The CMI principally considers on the evapotranspiration which requires the precipitation and temperature data as inputs in the water balance model. The KBDI is used for planning the fire management operation in many regions around the world. The calculation of the KBDI, which requires only the precipitation and temperature, is based on the fine fuel moisture calculation with the empirical theory. The SMDI and CSDI are drought indices which were developed and applied to indicate the drought severity on the corn (Meyer et al., 1993) and soybean (Meyer and Hubbard, 1995). The long-term statistics is applied on the SMDI to define the weekly normalized soil moisture. The strength of the SMDI and CSDI is that they can determine the soil moisture at different layers of the root

depth. The ETDI is based on the similar approach to the SMDI; the prior focuses on the water deficit while the later considers the soil moisture deficit. The NRI uses the average annual precipitation at the regional level to represent drought because of its good relationship with the agricultural production. The DM index is the combination of the drought index and the excessive moisture in an explicit form including the area of the distribution of the precipitation and temperature in given gradations. It uses a simple calculation method and specific calibration for each region. All agricultural drought indices mentioned above require the soil moisture or AWC as the input. According to the limitation of the data in the study area, these indices are not able to be assessed in this research.

As the development of new technology during the past decades, the satellite data play an important role for assessing the agricultural drought. Many agricultural drought indices using the satellite data have been developed to overcome the limitation of the indices using gauged data. They are able to indicate the state of the land surface condition and health of vegetation. Examples of drought indices developed using the data from satellites are the NDVI (Tucker, 1979), Crop Water Stress Index (CWSI) (Idso et al., 1981), Normalized Difference Infrared Index (NDII) (Hardisky et al., 1983), Soil Adjusted Vegetation Index (SAVI) (Huete, 1988), Vegetation Condition Index (VCI) (Kogan, 1990), Vegetation Index/Temperature Trapezoid (VITT) (Moran et al., 1994), Temperature Condition Index (TCI) (Kogan, 1995), Enhanced Vegetation Index (EVI) (Huete et al., 2002), Standardized Vegetation Index (SVI) (Peters et al., 2002), Vegetation Condition Albedo Drought Index (VCADI) (Ghulam et al., 2007a), Perpendicular Drought Index (PDI) (Ghulam et al., 2007b), Modified Perpendicular Drought Index (MPDI) (Ghulam et al., 2007c), and Remote Sensing Drought Risk Index (RDRI) (Liu et al., 2008).

The description of some widely used indices is briefly explained here. The NDVI is a well-known drought index used to assess the health of the vegetation on the land surface, which was firstly applied to indicate the drought by Tucker and Choudhury (1987). The CWSI provided the information of the crop water status which depends on the minimum and maximum level of the stress, which was preliminarily applied by Jackson et al. (1981). After the remote sensing data was made available, the VITT was introduced. The VITT is an extension of the CWSI instead the remote sensing data was inputted. The VCI uses the NDVI value as the input in corresponding to the changes in vegetation conditions from the extremely unfavorable condition to optimal condition. The EVI is more responsive to canopy structural variations including leaf area index (LAI), canopy type, plant physiognomy, and canopy architecture. It was developed to optimize the vegetation signal with improved sensitivity in high biomass regions and improved vegetation monitoring. The VCADI requires

large amount and variety of the input data, so its application has a limitation. The VCADI was developed to the new index called PDI which can be calculated from the near-infrared and red spectral reflectance space data. After years of improvement, the MPDI was eventually and successfully developed indicating a well performance in comparison with the VCADI and PDI on vegetation surfaces. The MPDI includes the fraction of the vegetation of a pixel that accounted for the soil moisture and vegetation growth. The RDRI is a drought index developed from a linear combination of three cloud indices which describe the length of the continuous absence of clouds, the ratio between cloudy and non-cloudy days, and the length of the longest continuous cloud cover. The SVI uses the greenness probability to evaluate the health condition of the vegetation. The main input of SVI is NDVI by normalized to normal distribution with zero mean and standard deviation one. The cumulative probability of the NDVI normalized value is the SVI. Moreover, SVI can detect the failure or unhealthy condition of vegetation by all causes such as drought, flood, crop rotation, and unseasonable coolness.

Hydrological drought indices have been mainly developed to represent impacts of the drought on streamflow. Generally, the main input of the hydrological drought index is the time-series streamflow data; however, a common problem has always raised up with the data shortage in the developing country; therefore, estimating streamflow in the ungauged basin is recommended to overcome the data shortage problem. Hundedcha et al. (2002) stated that the prediction of streamflow in the ungauged basin is the most challenging tasks in hydrology of the 21st century. He also mentioned that there are many methods of the prediction of the ungauged basin, which are different from each other owing to the region of interest and envisaged goals. After getting the streamflow data, the hydrological drought is able to analyze its indices including the Palmer Hydrological Drought Index (PHDI) (Palmer, 1965), Surface Water Supply Index (SWSI) (Shafer and Dezman, 1982), Reclamation Drought Index (RDI) (Weghorst, 1996), Regional Streamflow Deficiency Index (RSDI) (Stahl, 2001), Water Balance Derived Drought Index (Loukas et al., 2007), and Streamflow Drought Index (SDI) (Nalbantis and Tsakiris, 2009).

The description of some widely used indices is briefly explained here. The PHDI and SWSI were developed to indicate the complete picture of the water balance in the basin for water management purposes. In fact, the PHDI does not consider the snow accumulation while the SWSI does. The RDI was developed for the operational detection of drought events and for the triggering of the relief when the severity level was reached. The RSDI utilizes the discharge to examine regional drought events, and it is detected when the substantial number of stations shows a similar low streamflow pattern. The Water Balance Derived Drought

Index which was applied by Loukas et al. (2007) with UTHBAL water balance model to determine the discharge in the river. Then this index was derived by normalizing and standardizing the synthetic runoff to the mean runoff. The SDI is a hydrological drought index which uses monthly streamflow as the input. The calculation of SDI is simple, but it provides a satisfactory result. The calculation of SDI mainly relies on the probability distribution of monthly streamflow and it can be calculated at any time-scales of interest.

According to the description above, we found that each drought index has their own special features. There is no a single drought index which can be applied to assess the drought at all climate regimes, sectors affected and types of droughts. However, the selection of suitable index is of high importance because there is no absolute definition of drought. Thus, the following questions suggested by WMO and Global Water Partnership (GWP) could assist the selection an appropriate drought index for particular situation (WMO and GWP, 2016):

- Do the indicators or indices allow for timely detection of drought to trigger appropriate communication and coordination of drought response or mitigation actions?
- Are the indicators or indices sensitive to climate, space and time in order to determine drought onset and termination?
- Are the indicators or indices and various severity levels responsive and reflective of the impacts occurring on the ground for a given location or region?
- Are the chosen indicators, indices and triggers the same, or different, for going into and coming out of drought? It is critical to account for both situations.
- Are composite (hybrid) indicators being used in order to take many factors and inputs into account?
- Are the data and resultant indices or indicators available and stable? In other words, is there a long period of record for the data source that can give planners and decision-makers a strong historical and statistical marker?
- Are the indicators or indices easy to implement? Do the users have the resources (time and human) to dedicate to efforts and will they be maintained diligently when not in a drought situation? This can be better justified if such a system is set up for monitoring all aspects of the hydrologic or climatic cycles, not just droughts.

The SPI, SVI, and SDI are used to assess the meteorological, agricultural, and hydrological droughts in this research since they able to response to questions above. They are able to assess the drought at any time-scales of interest allowing timely detection. Based

on the literature the SPI and SVI were applied for drought assessment in Cambodia and were able to provide reliable result (Chhinh and Millington, 2015, Bert and Elga, 2016, and Sok et al., 2017).

2.5 Previous Studies of Drought

Drought is a global issue which has spread all over the world. In last decades, the large scale intensive drought has occurred in many locations and caused large scale effects in Asia, Africa, South America, Central America, North America, Europe, and Australia (Le Comte, 1994). According to the research of Intergovernmental Panel on Climate Change (IPCC), the agriculture area in many parts of Asia was damaged in the past few decades as the result of increasing water stress due to increasing temperature, the effect of El Niño, and the reduction in the number of rainy days (Bates, 2009). As the result of the worst effect of drought, there are several studies conducted to assess the drought prone area, intensity, severity, duration, and frequency. India was one among those countries most vulnerable to drought. Lester and Gurenko (2003) found that since the mid of 1990s drought occurred in consecutive years with prolonged and widespread over the entire country. Moreover, the frequency of drought in recent years has increased.

Furthermore, many researches were conducted on the drought issue in the tropical region. For example, Zou et al. (2005) conducted a research to assess the variation in drought over China using the PDSI. The monthly data set of the precipitation and temperature from 1951 to 2003 were used in which the result showed that the drought was significant in the northern part of China. During the late 1990s, most part of the northern China (except northwest China) had experienced severe and long period of drought. Furthermore, the yellow river was dried (no streamflow) for 226 days in 1997 which was the longest and driest duration of the record. Suwanwerakamtorn et al. (2006) conducted a study on the drought assessment using the GIS technology in the Nam Choen basin in the northeastern of Thailand. Matrix overlay function in ArcViewGIS developed by Khon Kaen University was applied to indicate drought risk areas from seven types of data including 1) slope, 2) soil drainage, 3) stream density, 4) precipitation, 5) surface water irrigation, 6) sub-surface water, and 7) land use. It was found that 13.47%, 40.88%, 37.87%, and 7.78% on the entire region were very mild risk, mild risk, moderate risk, and severe risk, respectively. Wattanakij et al. (2006) applied the multi-temporal SPI to evaluate the characteristics and pattern of drought in the northern of Thailand between 1976 and 2004 from 308 rainfall stations. The Kriging method was applied for the spatial interpolation of the average annual precipitation and pattern of the

drought intensity for the whole region. The result showed that the amount of the precipitation increased from the southwest to the northeast region. The moderate and severe drought often occurred in the south and southwest region.

There were several studies of drought in Cambodia. For example, MoE (2005) conducted a study of the vulnerability and adaptation to climate hazards and the climate change using the formulation of the National Adaptation Program of Action to climate change (NAPA). The evaluation was based on the survey of rural Cambodian households between 1982 and 2002. It was found that several provinces which are in the south of Phnom Penh, downstream along the Mekong, and the Tonle Bassac rivers faced the problem of the flood while the Upper part of the Tonle Sap faced drought problem. Chhinh and Millington (2015) conducted a research regarding impacts of drought on rice production by using the SPI in Kompong Speu province, Cambodia. It was found that more than 1000 Hectares (ha) of the paddy field were damaged by the drought from 1994 to 2006 and the late season of drought causing a greater damage than the early and mid-season. Bert and Elga (2016) analyzed the precipitation and vegetation data in all major basins over the entire Cambodia from April 2015 to May 2016 using the rainfall data from Climate Hazards Group InfraRed Precipitation with Station data (CHIRPS) and the precipitation data from rain gauges. The SVI and EVI were assessed. The result showed 17% decrease in the average rainfall over the entire Cambodia and 22% decrease in rainfall for the Upper Mekong 1 basin located in the northeast of Cambodia. The most drought prone area was in the upstream part of the Tonle Sap, Upper Mekong basin 1, and 3S (Sekong, Sesan, and Srepok) basin. Guo et al. (2017) conducted a meteorological drought analysis in the Lower Mekong Basin (LMB) using the satellite-based long-term CHIRPS product which used the latest update of CHIRPS in 2016 with long term record and high resolution. The SPI was selected to analyze the drought at various time scales from January 1981 to July 2016. According to the result, CHIRPS could capture the drought characteristics at various time scales. The best performance was found when assessing at 3-month time-scale. The LMB experienced several drought problems in the last 30 years. The longest period of the drought was from 1991 to 1994 which was around 38 consecutive months of drought. The driest period was between 2015 and 2016 when 75.6% of the entire LMB were affected.

The literature review in this chapter is used as a guideline to select the drought indices which are suitable for the study area and help develop understanding of the characteristic and application of the drought indices. More importantly, it helps to identify the gap in research particularly the drought assessment in the Greater Baribo basin. According to the discussion about the previous study of drought, we found that the meteorological and

agricultural drought assessment was used different index and input data. However, there was no the assessment of the impact of drought on agriculture in the Tonle Sap basin. At the best knowledge of the author, there was no research on the hydrological drought in Cambodia. This is probably because the impact of drought on streamflow has not been clearly seen until the last decade when some main rivers in Cambodia experienced dry and low streamflow condition. Furthermore, the assessment of three types of drought is high of important to endorse the “Rectangular Strategies” of the RGC policy for enhancement of agricultural sector.



CHAPTER 3

STUDY CATCHMENT

3.1 General Catchment Characteristics

The Tonle Sap basin is the biggest basin which covers about 44% of the entire Cambodia. It is located between latitude 11°30'10" N - 14°26'16" N and longitude 102°9'57" E - 105°48'32" E. The elevation varies between 0 and 1779 msl (Meter above mean Sea Level). It covers six provinces i.e. Battambang, Pursat, Banteay Meanchey, Siem Reap, Kompong Thom, and Kompong Chhnang. The area of Tonle Sap basin is about 82140 km² covering 11 sub-basins which are Sen, Mongkol Borey, Sreng, Chinit, Greater Baribo, Pursat, Staung, Dauntri, Siem Reap, Chikreng, and Sangker basin as shown in Figure 3.1. The Greater Baribo basin was selected as the study area since it is rich in rainfall station and the duration of the data is longer than other basins. Furthermore, it is the fifth biggest among 11 basins covering three provinces i.e. Kompong Chhnang, Kompong Speu, and Pursat. It has the area of 7155 km² and covers by the agricultural area about 34% (mostly paddy rice field). The major economic drivers in the Greater Baribo basin are agriculture and aquaculture. The eastern part of the Greater Baribo basin is the flood plain area where the agriculture and aquaculture activity are found. The farmers plant only rice during the wet season while the dry season can be found a mixed crop, rice and vegetation. There are hundreds of small reservoirs which belong to the private sector and located in the floodplain area of the basin. Those small reservoirs play an important role to both agriculture and aquaculture during the dry season. The agricultural area which located far away from the floodplain area strongly relies on the rainfall and some existing small and poorly designed irrigation schemes during Pol Pot regime (1975 to 1978). In case the drought is expected to happen, possible consequences may result to a reduction in not only the agricultural, aquaculture productivity and related sectors but also rural people within the basin and the regional and national economic loss. It also impacts on the RGC policy of "Rectangular Strategies". Thus, the Greater Baribo basin is considered suitable for testing the assessment of spatial and temporal of drought intensity which affecting the agriculture productivity.

The Greater Baribo basin is divided into three sub-basins which are the Bannak, Baribo and Kraing Ponley sub-basins and the area of sub-basins are, 1091 km², 2995 km², and 3006 km², respectively as showed in Figure 3.1. The elevation varies from 0 to 1779 msl and the direction of flow is from the west to the east to the Tonle Sap Great lake.

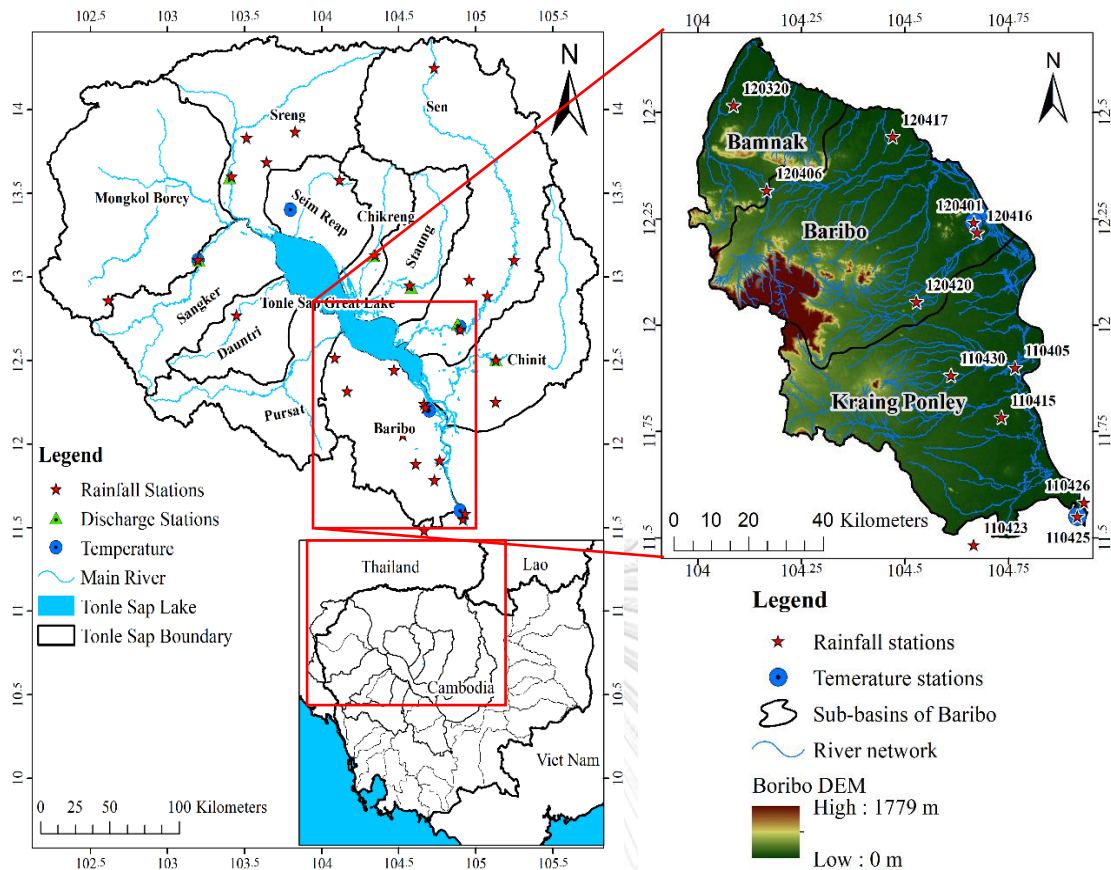


Figure 3.1. Tonle Sap and Greater Baribo basins with sub-basins, main river, and elevation.

3.2 Geographical Characteristics

3.2.1 Land Use

According to the land use data in 2003 obtained from MOWRAM, there are 20 land use types in the Greater Baribo basin, yet they are grouped into six types of land use i.e. agriculture, forest, water body, and urban area as illustrated in Table 3.1. Besides, the Greater Baribo basin covers approximately 34.36% of the agriculture, 63.20% of the forest and flooded forest, 2.15% of water body, and 0.29% of the urban area. More than 95% of the agricultural area is the paddy field yet the distribution and description of the land use in the Greater Baribo basin can refer to Figure 3.2.

Table 3.1. Description of the land use in the Greater Baribo basin.

No	Land Use Original	Land Use Regroup	Area (km ²)	Area (%)
1	Rice Field	Agriculture	2045.42	28.59
2	Receding Rice Fields and Floating Rice Fields		175.00	2.45
3	Village Garden Crops		160.42	2.24
4	Field Crops		74.38	1.04
5	Swidden Agriculture		3.09	0.04
6	Shrubland	Forest	1578.35	22.06
7	Deciduous Forest		1140.57	15.94
8	Woodland and Scattered trees		643.99	9.00
9	Evergreen Broad-Leafed Forest		501.95	7.02
11	Mixed Evergreen/Deciduous Forest		400.30	5.59
12	Other Forest		31.97	0.45
10	Grassland	Grassland	26.66	0.37
13	Barren Land		3.50	0.05
14	Flooded Shrub	Flooded forest	127.80	1.79
15	Flooded Grassland		44.10	0.62
16	Flooded Forest		20.02	0.28
17	Marsh or Swamp		3.25	0.05
18	Open Water (oceans, large lakes and rivers)	Water body	80.76	1.13
19	Lake or Pond (Perennial)		73.27	1.02
20	Urban, and Built-up Areas	Urban	20.54	0.29

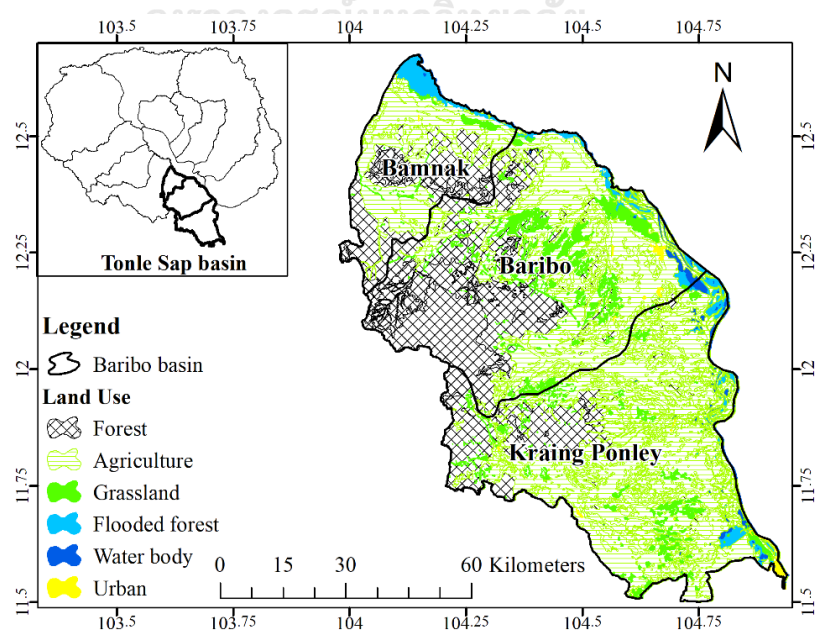


Figure 3.2. Land use map of the Greater Baribo basin

3.2.2 Soil Types

Soil types in the Greater Baribo basin in 2003 were obtained from MOWRAM. From Table 3.2, there are three main soil types found in the Greater Baribo basin i.e. clay (45.7%), sand (31.1%), loamy (23.2%). Figure 3.3, the western part is mostly covered by loamy and the middle part of the Baribo and Kraing Ponley sub-basins are occupied by sand. Clay is usually found in the Bannak, eastern part of the Baribo, and Kraing Ponley sub-basins. For detailed about the soil types distribution and description in the Greater Baribo basin can be illustrated in Figure 3.3 and Table 3.2.

Table 3.2. Description of major soil types in the Greater Baribo basin

No	Soil Types	Area (km ²)	Area (%)
1	Clay	3269.36	45.69
2	Loamy	1659.21	23.19
3	Sand	2226.43	31.12

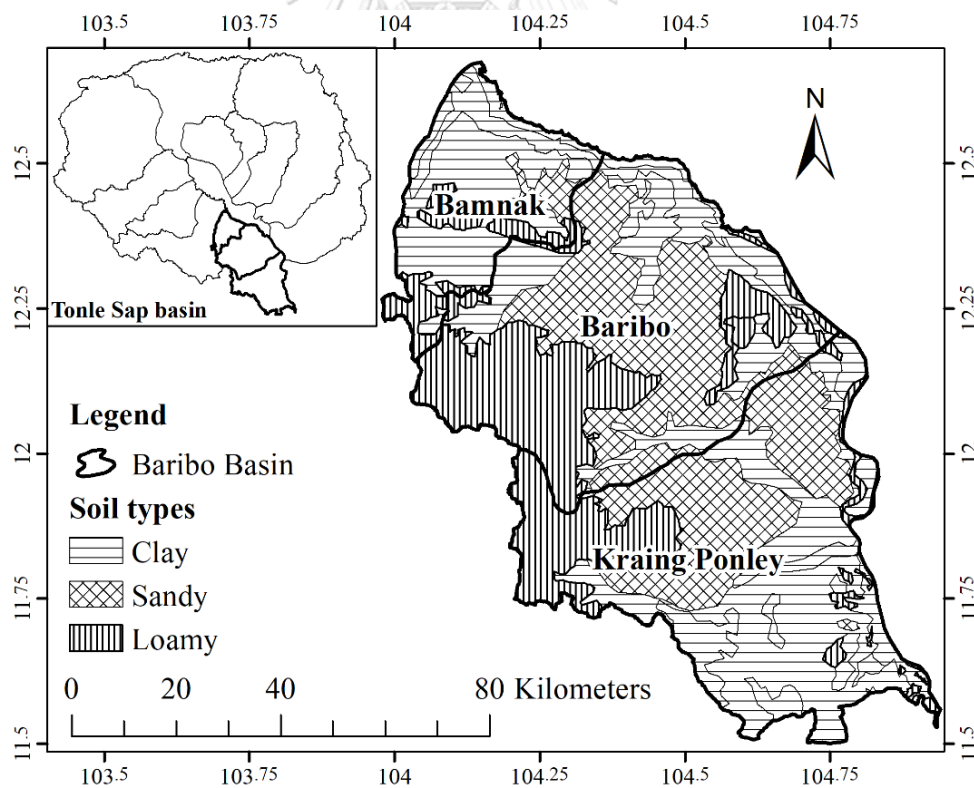


Figure 3.3. Soil types map of the Greater Baribo basin

3.3 Rainfall Data in the Greater Baribo Basin

3.3.1 Rainfall Consistency Test

The consistency test is needed to check the consistency of the rainfall data over a long time period of record. Double Mass Curve (DMC) is a well-known consistency test of the hydrologic data to guarantee that any trends detected are owing to meteorological causes and not to change in observational methods, exposure, or location of gauge. The description of DMC is as follows.

The consistency test using DMC is used to verify the quality of many types of the hydrologic data based on comparing an individual station with the pattern of the surrounding stations. The two variables are plotted as a straight line if the data are proportional. In contrast, a changing in slope of the DMC refers to the inconsistency of the data and the variation of the slope defines the level of change in the relation. The DMC was employed to test the quality of the 12 observed rainfall stations which are located inside and near by the Greater Baribo basin from 1985 to 2008. For example, while the DMC was applied to test the consistency of a rainfall station, the other 11 rainfall stations were employed as the surrounding stations. There were 11 rainfall stations identified as the surrounding stations since they are located at similar elevation and the rainfall characteristics such as annual rainfall (max, mean, min, and SD) and seasonality (wettest and driest months) are not significantly different from each other (see section 3.3.2).

The DMC result of the 12 rainfall stations in the Greater Baribo basin showed that the DMC of rainfall stations 110405, 110415, 110426, 120401 and 120416 captured a notable break in slope in 1992 (see Figure 3.4). It was more likely to be caused by a permanent change of upgrading gauging equipment according to the interview with Mr. Sat Song, a staff in the Department of Water Resources and Meteorology in Kompong Chhnang province. Mr. Sat Song who is responsible for data management and collection, said that some rainfall stations in the province were changed the method of data collection from manual to computer base. According to historical evidence explained above, we can assume that the data after changing in slope of the DMC is more reliable and accurate. Thus, the observed rainfall before the changing in slope (1985-1991) was adjusted by multiplying them by the ratio of the DMC slope after change in 1992 to the slope before change in 1992 as illustrated in equation 3.1.

$$P_a = \frac{a_2}{a_1} P_o \quad \text{Eq. 3.1}$$

Where P_a is the adjusted annual rainfall, P_o is the observed annual rainfall, a_1 is the DMC slope for 1985-1991 (before changing in slope), and a_2 is the DMC slope for 1992-2008 (after changing in slope). The result of adjusted DMC of the five inconsistent rainfall stations are shown in Figure 3.5

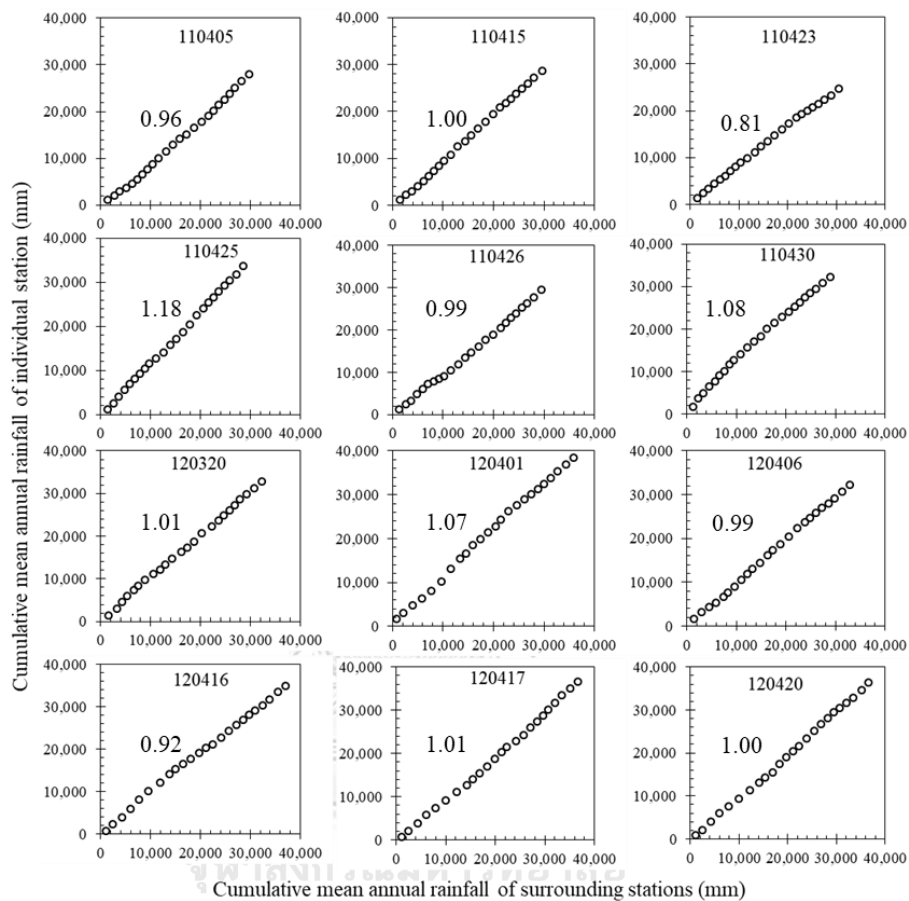


Figure 3.4. Consistency test by double mass curve of the 12 rainfall stations

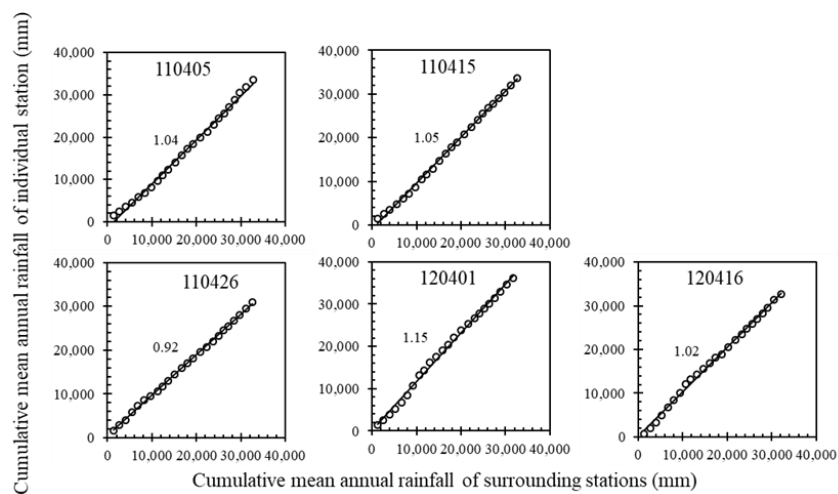


Figure 3.5. DMC of rainfall data of the inconsistent station after adjusted

3.3.2 Rainfall Characteristic

The rainfall stations which are located inside and nearby each sub-basin, are analyzed. There are two, four, and six rainfall stations located inside and nearby the Bamnak (120320 and 120406), Baribo (120401, 120416, 120417, and 120420), and Kraing Ponley sub-basins (110405, 110415, 110423, 110425, 110426 and 110430), respectively. The daily rainfall from 1985 to 2008 of the stations in the Bamnak, Baribo, and Kraing Ponley sub-basins are shown from Figure 3.6 to Figure 3.8. The maximum daily rainfall of the 12 rainfall stations range between 198 and 217 mm in the Bamnak, 143 and 226 mm in the Baribo, and 103 and 182 mm in the Kraing Ponley sub-basins. The maximum rainfall of 226 mm is found in August 1992 at station 120401. In 1990, the rainfall stations i.e. 120320, 120406, 110405, 110415, and 110430 indicate low rainfall. Later in 1993, the low rainfall is found for the rainfall stations 120401, 110405, 110415, 110423, 110426, and 110430.

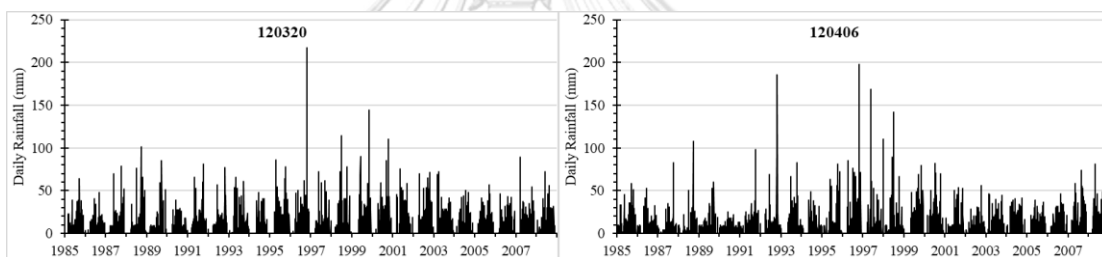


Figure 3.6. Daily rainfall of stations in the Bamnak sub-basin

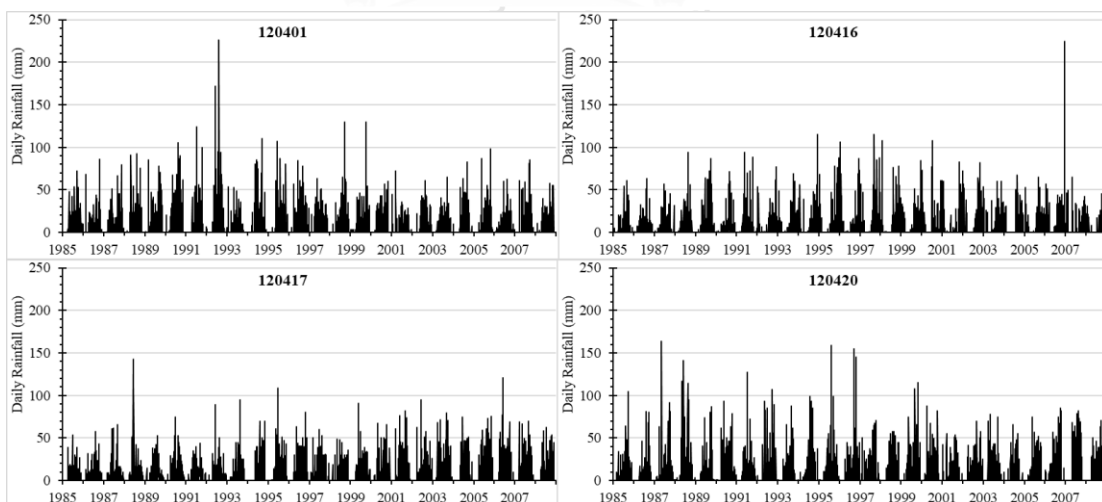


Figure 3.7. Daily rainfall of stations in the Baribo sub-basin from

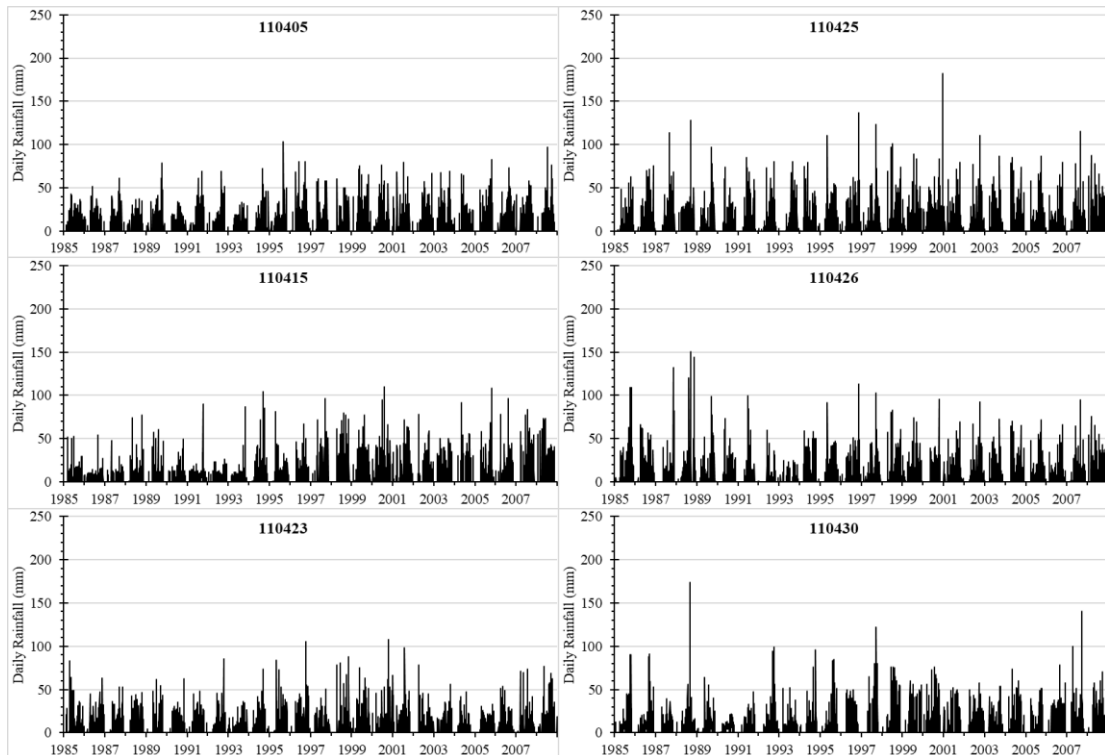


Figure 3.8. Daily rainfall of stations in the Kraing Ponley sub-basin

The monthly rainfall between 1985 and 2008 for the 12 rainfall stations in the Bamnak, Baribo, and Kraing Ponley sub-basins are shown in Figure 3.9 to Figure 3.11, from which a wide range of monthly rainfall variation can be seen. The monthly rainfall in the Kraing Ponley and Bamnak sub-basins are normally less than 500 mm but the Baribo sub-basin has many months which the monthly rainfall is greater than 500 mm. The highest monthly rainfall of 665.3 and 687.5 mm in July 1991 and August 1992, respectively are found in the Baribo sub-basin. The variation in the monthly rainfall in the Bamnak and Baribo sub-basins are higher than the Kraing Ponley sub-basin. The lowest monthly rainfall of the three sub-basins is in 1990 and 1993. The monthly rainfall of the station in the same basin have less variation in monthly rainfall from 2000 to 2008.

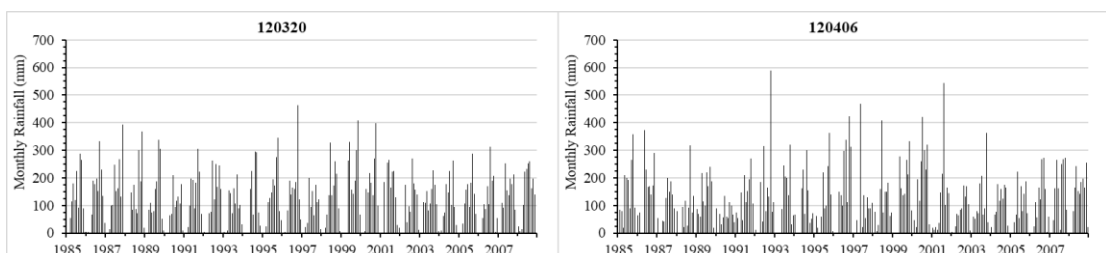


Figure 3.9. Monthly rainfall of stations in the Bamnak sub-basin

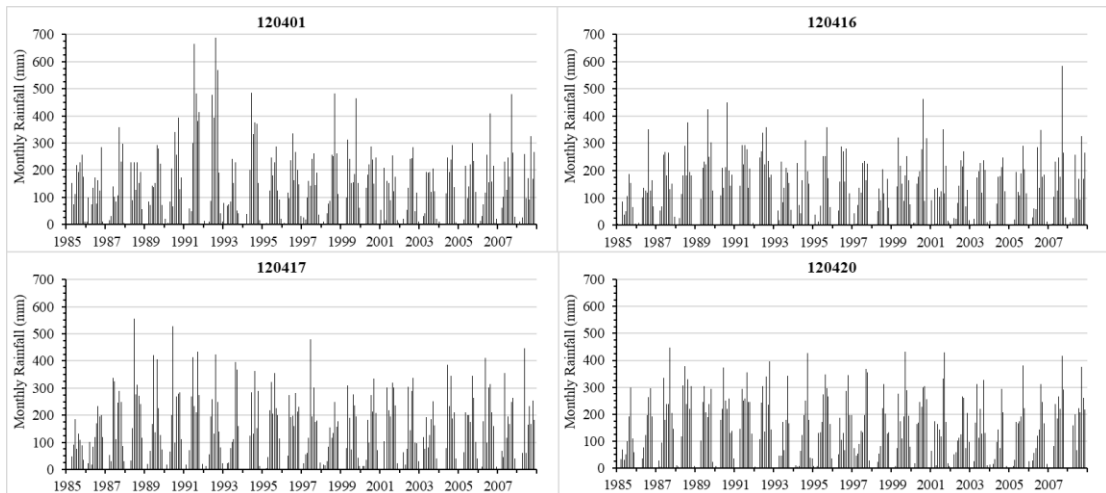


Figure 3.10. Monthly rainfall of stations in the Baribo sub-basin

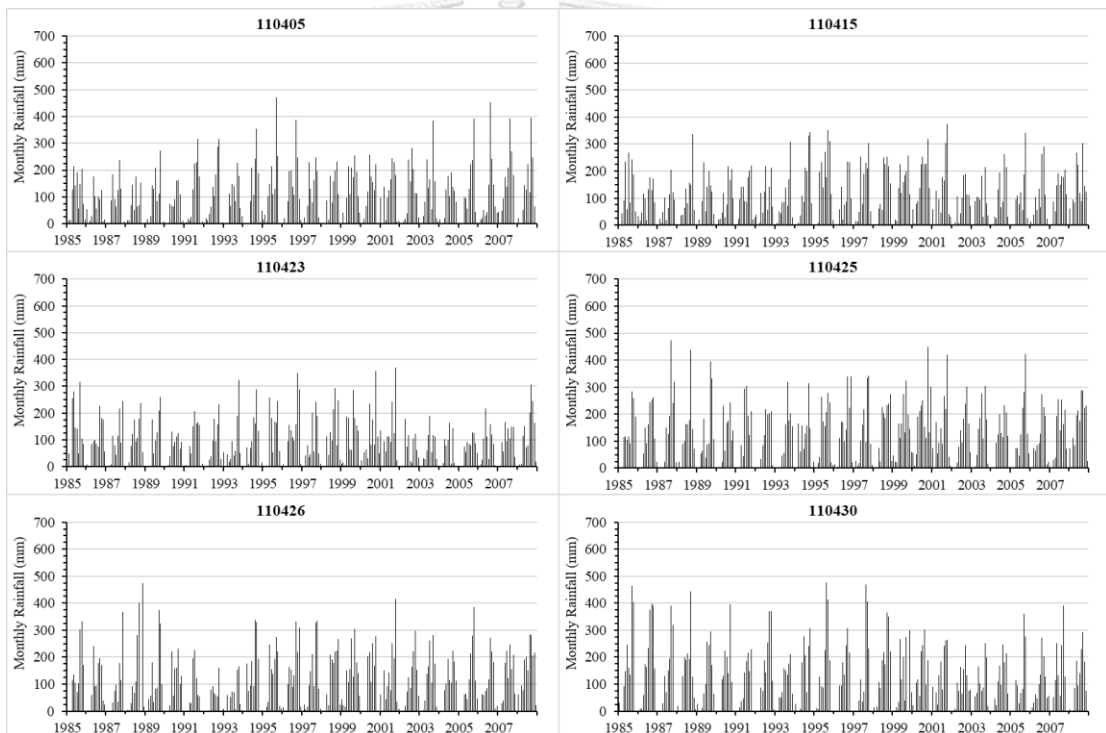


Figure 3.11. Monthly rainfall of stations in the Kraing Ponley sub-basin

Figure 3.12 to Figure 3.14 show the annual rainfall of the 12 rainfall stations in the three sub-basins between 1985 and 2008 while Table 3.3 shows the inter-variability (the difference between the maximum and minimum), minimum, mean, maximum and SD of the annual rainfall. According to Figure 3.12 to Figure 3.14, the pattern of annual rainfall of the Bamnak and Kraing Ponley sub-basins are very similar to each other. Between 1985 and 1992, the Baribo sub-basin has high annual rainfall while the other sub-basins are not and later from 1993 to 2008, the three sub-basins show similar pattern

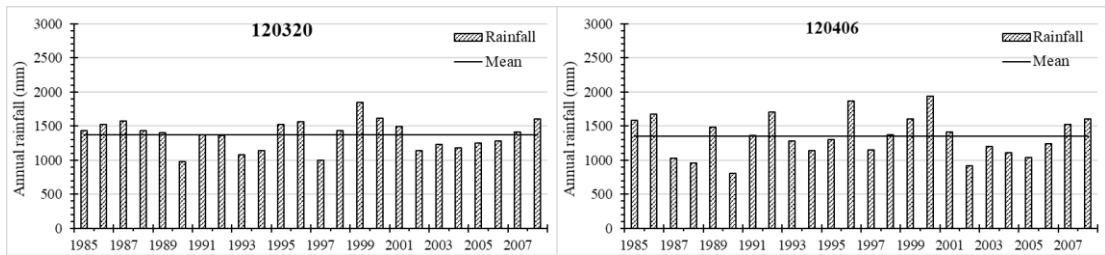


Figure 3.12. Annual rainfall of stations in the Bamnak sub-basin

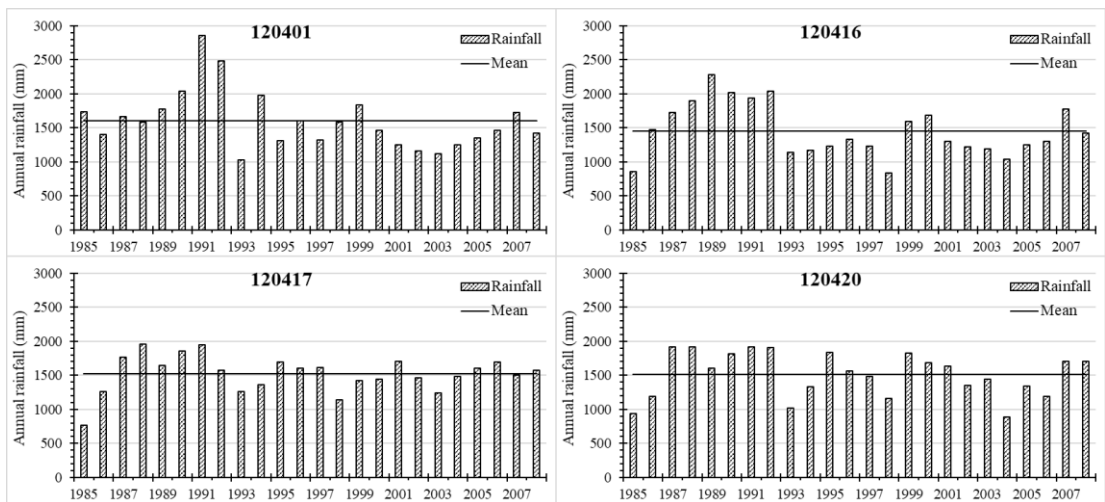


Figure 3.13. Annual rainfall of stations in the Baribo sub-basin

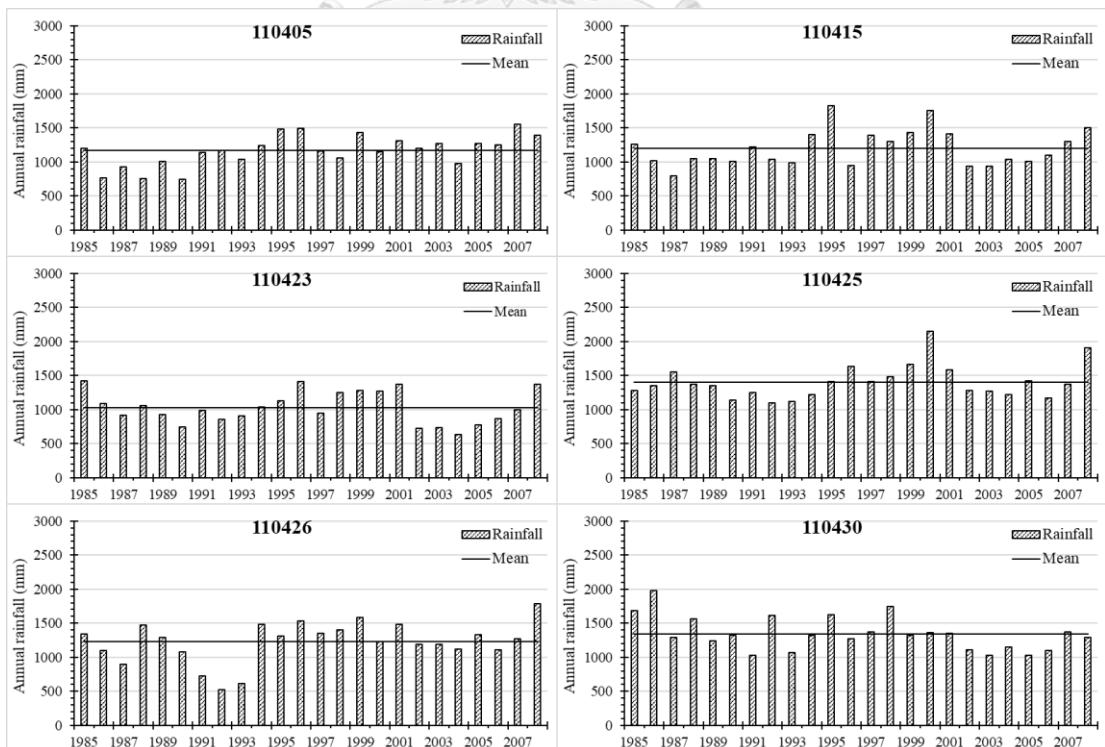


Figure 3.14. Annual rainfall of stations in the Kraing Ponley sub-basin

of annual rainfall. As shown in Table 3.3, the highest inter-variation, minimum, mean, maximum, and SD of annual rainfall can be seen in the Baribo sub-basin and the lowest is generally found in the Kraing Ponley sub-basin. It can be considered that the Baribo sub-basin is prone to both extreme flood and drought issues because it receives high mean annual rainfall with high inter-variation and SD.

Table 3.3. Description of rainfall stations in the Greater Baribo basin

Sub-basin	Station ID	Coordinate		Inter-variation (mm)	Min (mm)	Mean (mm)	Max (mm)	SD (mm)
		Lat	Lon					
Bamnak	120320	12.5	104.1	872.4	979	1369.5	1851.4	214.6
	120406	12.3	104.2	1132.2	808.3	1346.8	1940.5	302
Baribo	120401	12.2	104.7	1454.5	1027.3	1504.1	2481.8	361.6
	120416	12.2	104.7	1333.6	704.4	1364	2038	313
	120417	12.4	104.5	1189	767	1523.3	1956	268.2
	120420	12.1	104.5	1038	883	1514.9	1921	327.4
Kraing Ponley	110405	11.9	104.8	804.6	747	1166	1551.6	226.5
	110415	11.8	104.7	1027	797	1197.6	1824	265.4
	110423	11.5	104.7	794.8	631.7	1030.3	1426.5	237.1
	110425	11.6	104.9	1052.5	1094.8	1406	2147.3	250
	110426	11.6	104.9	1264.2	522.4	1225.8	1786.6	302.6
	110430	11.9	104.6	950.3	1023.7	1341.9	1974	249.9

Figure 3.15 to Figure 3.17 show the monthly average rainfall of the 12 rainfall stations in the Bamnak, Baribo, and Kraing Ponley sub-basins. In the tropical region like Cambodia, the rainy season starts from May to October, whereas the dry season is between November and April. The wettest month is found in September or October when the monthly rainfall of three sub-basins are about 200 mm/month. The reduction in rainfall is usually noticeable in July or August due to the shift of the Inter-Tropical Convergence Zone (ITCZ), but this reduction is less evident to station 120401 in the Baribo sub-basin compared to the Kraing Ponley and Bamnak sub-basins.

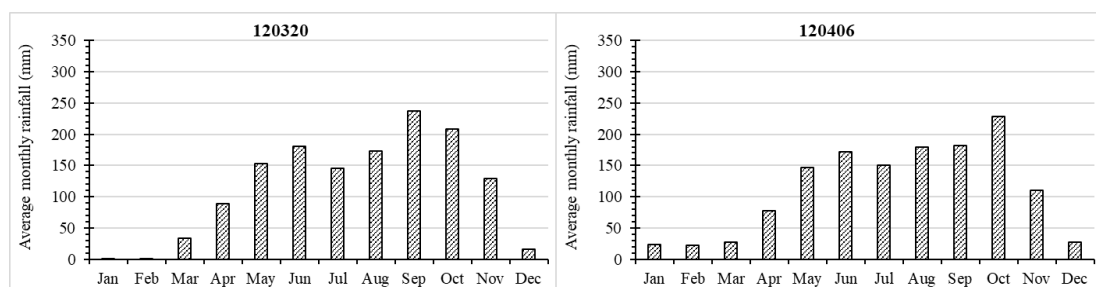


Figure 3.15. Monthly average rainfall of stations in the Kraing Ponley sub-basin

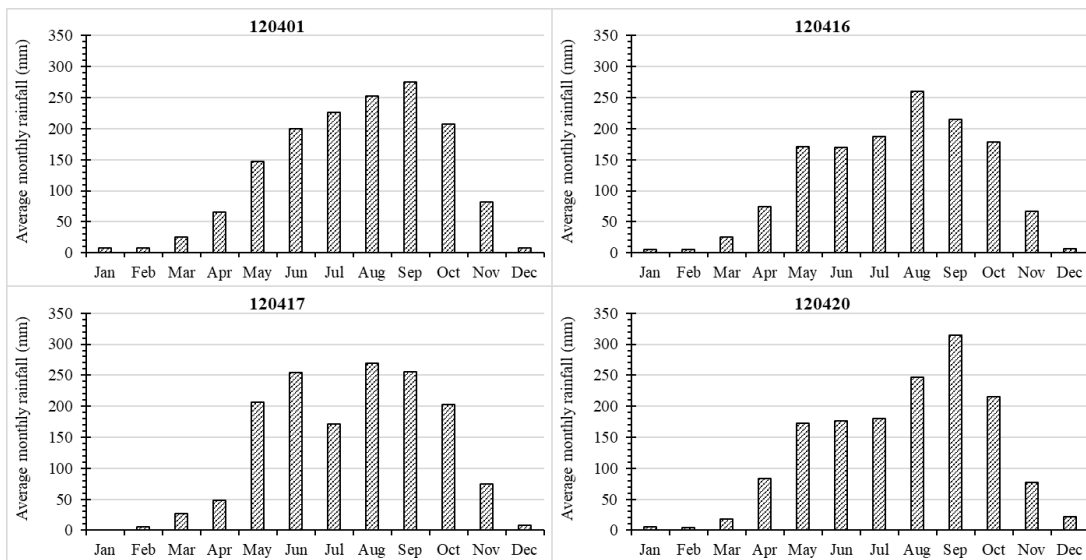


Figure 3.16. Monthly average rainfall of stations in the Bamnak sub-basin

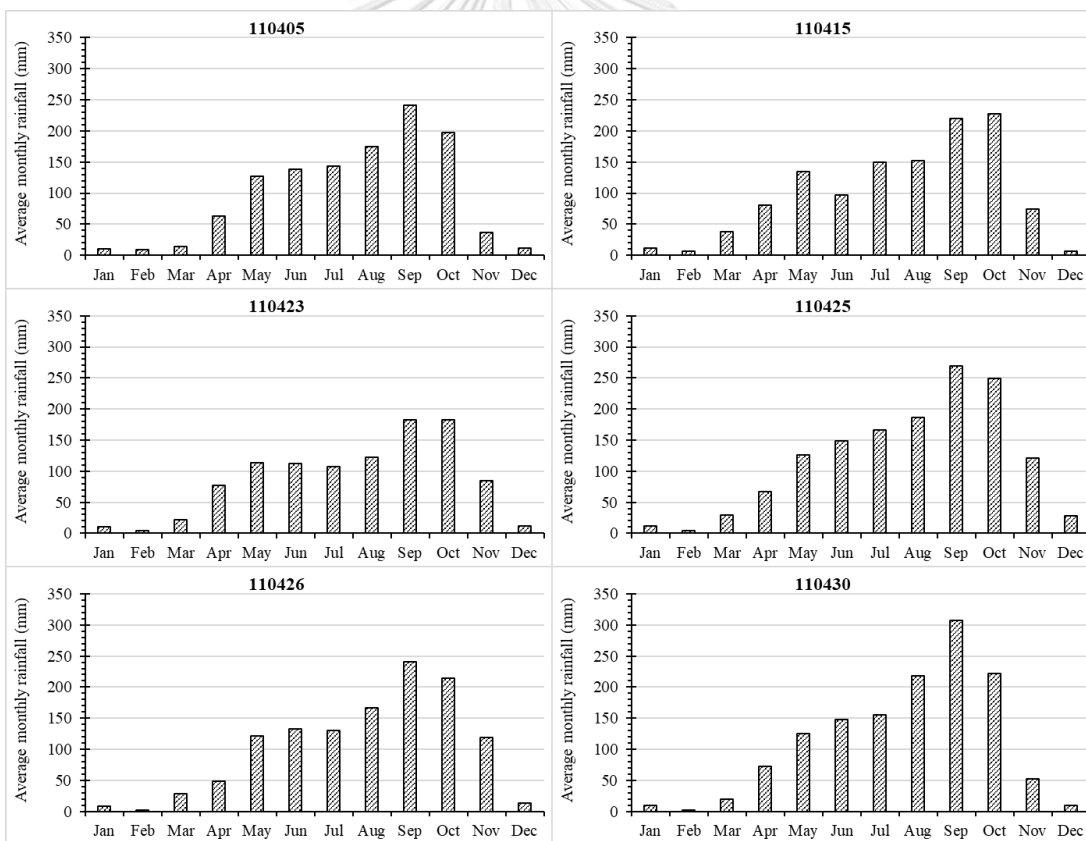


Figure 3.17. Monthly average rainfall of stations in the Kraing Ponley sub-basin

3.3.3 Mean Annual Rainfall Distribution

The daily rainfall data from 12 stations across the entire Greater Baribo basin covering between 1985 and 2008 was compiled as a point database for the analysis. Inverse Distance Weighting (IDW) interpolation method was selected to indicate the spatial average annual rainfall across the whole basin due to it is a widely used method for estimation of missing data in hydrology and geographical. According to Yang et al. (2015) and Chen et al. (2017), IDW performs well for mean annual rainfall distribution mapping. The mean annual rainfall in the Greater Baribo basin is governed mainly by the southwest monsoon, isolated tropical cyclones from the northeast across the South-China Sea and Viet Nam and topography and general approach direction (MRC, 2011). Figure 3.18 shows the distribution of the mean annual rainfall in the Greater Baribo basin and it varies from 1040 to 1525 mm. The Baribo sub-basin has highest mean annual rainfall while the lowest is found in the Kraing Ponley sub-basin. This implies that the Kraing Ponley sub-basin is probably subject to higher level of drought hazard compared to the other two sub-basins. Figure 3.16 shows that the mean annual rainfall in the Bamnak and Baribo sub-basins tends to increase from the north to south. In the Kraing Ponley sub-basin, the mean annual rainfall increases from the south to north. The evaporation from the Tonle Sap Great lake and the isolated tropical cyclones from the northeast across the South-China Sea and Viet Nam can be the main factors causing higher mean annual rainfall in the Baribo sub-basin. The lowest mean annual rainfall is found in the southern part of the Kraing Ponley sub-basin because it is mostly covered by the low-gradient and low-relief landscape. The mean annual rainfall distribution in the Greater Baribo basin obtained here is similar with that of the regional rainfall in MRC (2011).

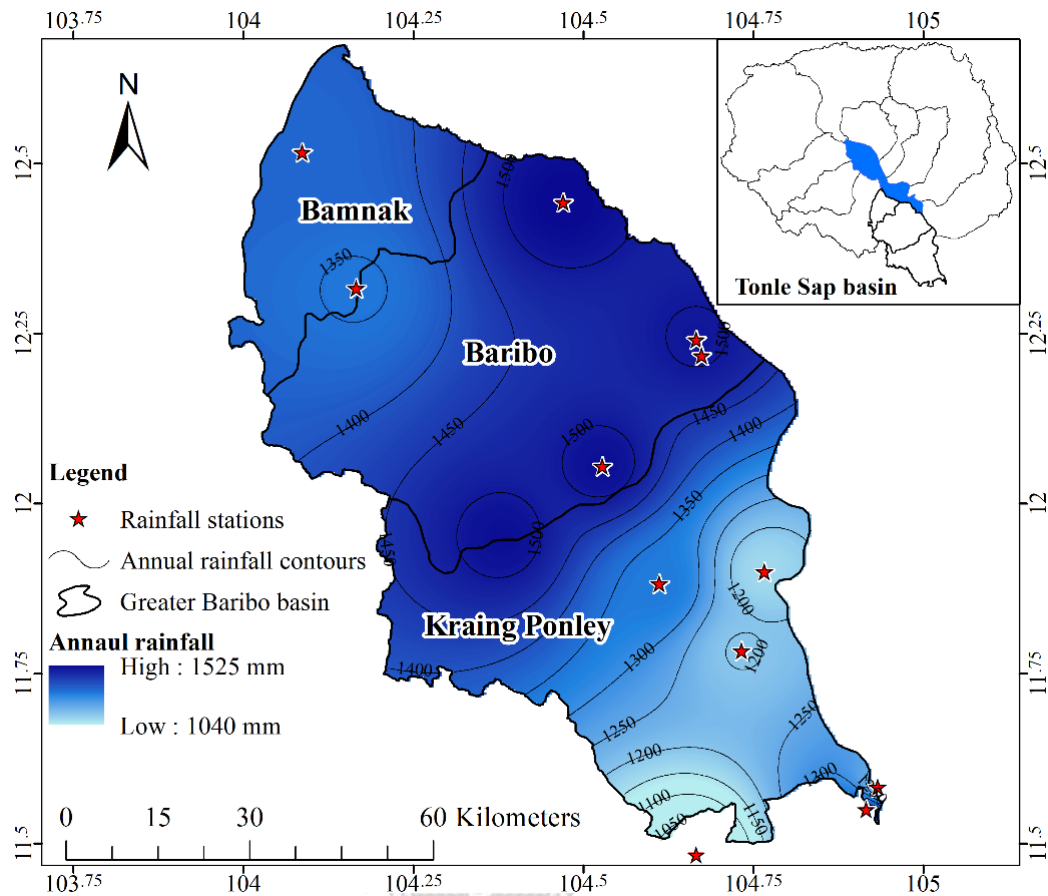


Figure 3.18. Annual rainfall distribution of the Greater Baribo basin

3.4 Satellite Images Data

Infrared Radiation (IR) and Near-Infrared Radiation (NIR) used in this study are the land surface reflectance products of NOAA with resolution of $0.05^{\circ} \times 0.05^{\circ}$. IR and NIR are recorded using the AVHRR imager channel 1 at wavelength of $0.63 \mu\text{m}$ and channel 2 at wavelength of $0.83 \mu\text{m}$, accordingly. In this study, the monthly average data of IR and NIR are converted from their daily time series data. The catchment monthly IR and NIR of the three sub-basins are determined by average the value of pixels in the same sub-basin. Figure 3.19 and Figure 3.20 show the pattern of the IR and NIR of the three sub-basins which are similar to each other. The monthly average IR and NIR alter from 0.09 to 0.64 and 0.20 to 0.73, respectively. They are the major inputs for computing the NDVI and the detail of the computation is as following.

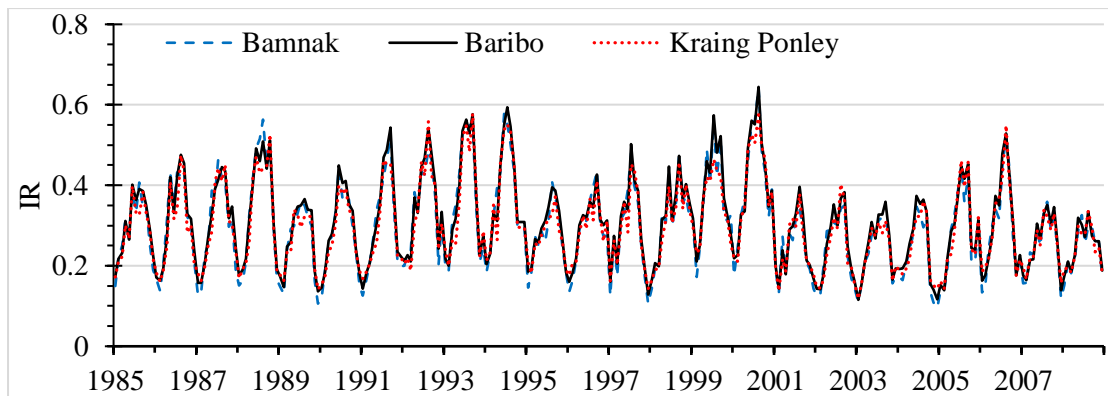


Figure 3.19. Monthly average of Infrared Radiation (IR)

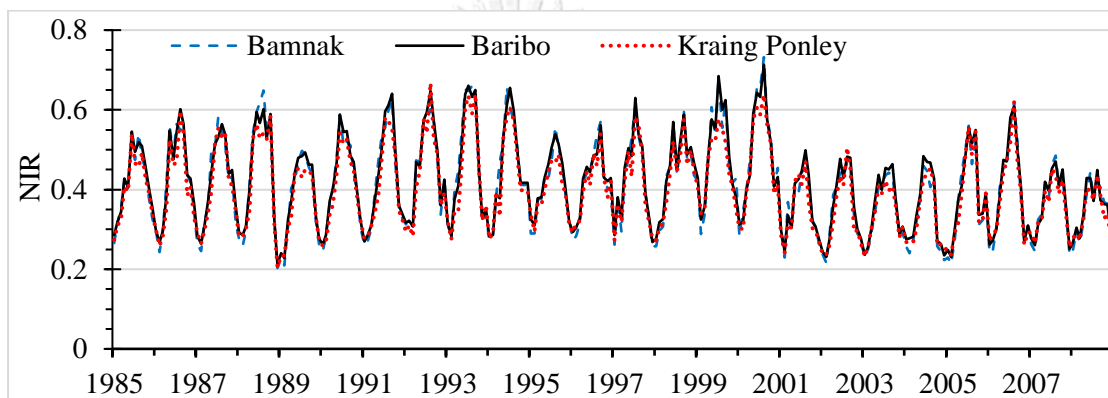


Figure 3.20. Monthly average of Near-Infrared Radiation (NIR)

The NDVI is developed to quantify the vegetation condition (greenness density) based on the difference between IR and NIR and the calculation is as shown in equation 3.2. Figure 3.21 shows that the vegetation in a good condition have high reflection of NIR and less reflection of IR and in contrast to the vegetation in a poor condition. The monthly average of NDVI is converted from their daily time series data. The NDVI value is normally changed between -1 to 1. The positive NDVI value refers to the area which is covered by vegetation while the negative value is not. Generally, NDVI is used for assessing the greenness density of the vegetation and high NDVI value refers to good condition of vegetation. In this research, area NDVI value of the three sub-basins is determined by averaging the value of pixels in the same sub-basin. The pattern of NDVI in the three sub-basins are similar to each other. Based on Figure 3.22, the value of NDVI of the three sub-basins change between 0.08 to 0.43. High NDVI value in the Bamnak sub-basin indicates that its vegetation condition is better than other sub-basins.

$$NDVI = \frac{NIR - IR}{NIR + IR} \quad \text{Eq. 3.2}$$

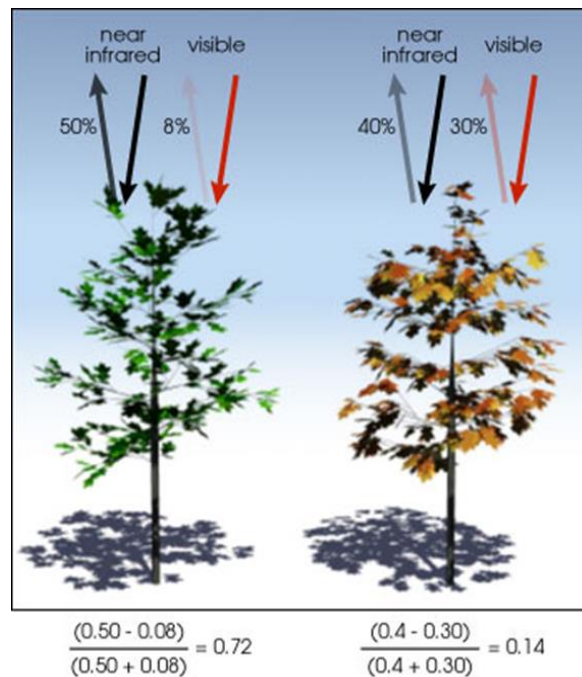


Figure 3.21. Pictorial description of IR, NIR and NDVI calculation.

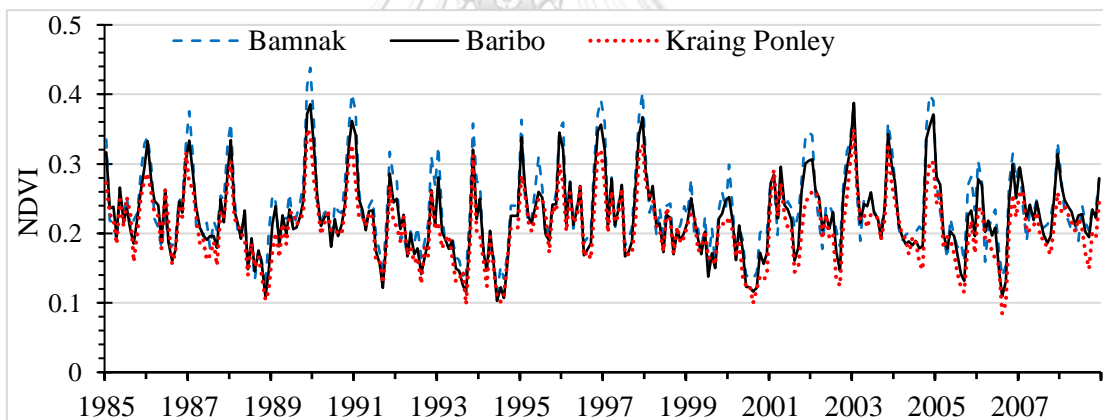


Figure 3.22. Monthly average of NDVI

3.5 Hydrological Characteristic of Gauged Basins

There are eleven basins in the Tonle Sap basin as shown in Figure 3.1. Six gauged basins i.e. Chikreng, Chinit, Sangker, Sen, Sreng, and Staung basin are used for predicting the streamflow for the ungauged basin in the Greater Baribo basin. There are 17 rainfall and 5 temperature stations which are employed to determine the area rainfall and temperature of each gauged basin as illustrated in Figure 3.1. The point rainfall and temperature at stations inside and nearby the six gauged basins between 2000 and 2006 are employed to determine the area rainfall and temperature using Thiessen polygon method. The analysis of hydrological data in the six gauged basins are performed in the following sections.

3.5.1 Rainfall Characteristic

Figure 3.23 shows the daily area rainfall for the six gauged basins between 2000 and 2006. The rainfall patterns of the gauged basins are similar, but the rainfall amount is different. According to Figure 3.23, the Chikreng basin has the highest daily rainfall while the other five gauged basins are comparable to each other. Normally, the maximum daily rainfall is less than 89.2 mm except in the Chikreng basin, the rainfall of 106 mm is found in August 2006.

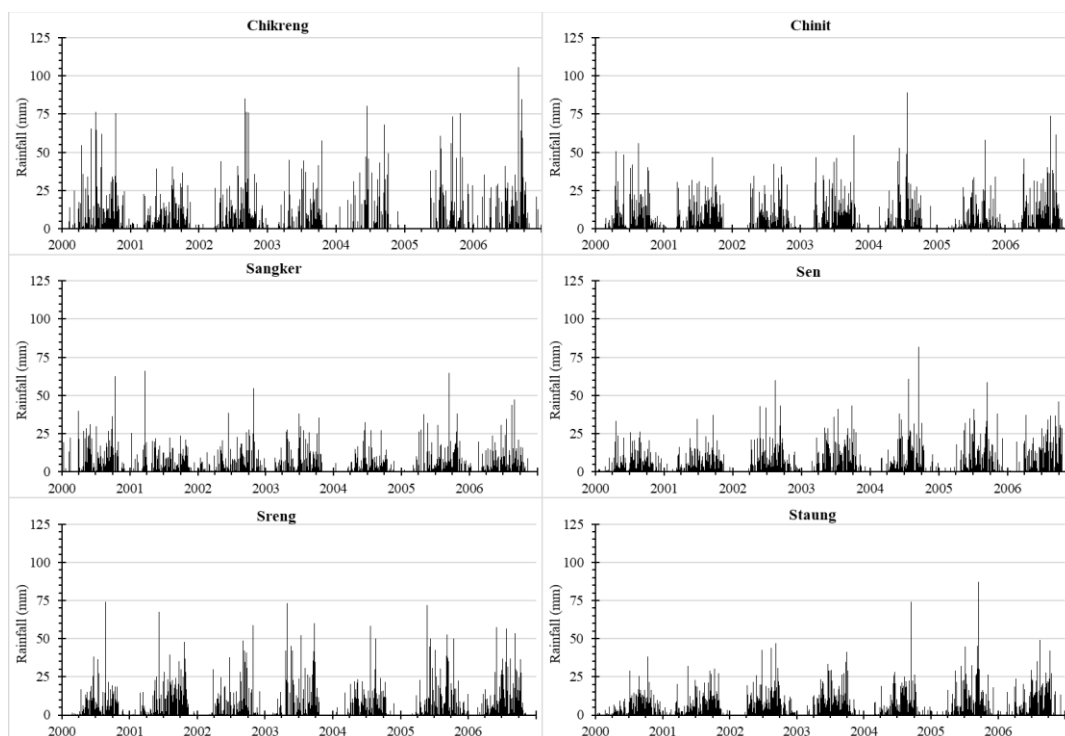


Figure 3.23. Daily rainfall data of gauged basins in the Tonle Sap basin

Figure 3.24 shows the monthly catchment rainfall between 2000 and 2006 of the six gauged basins. The monthly rainfall, the six gauged basins have similar pattern, but they are different in rainfall amount. According to Figure 3.24, the wet month of the gauged basin is between May and November and the wettest month is found in September or October. The variation of the monthly rainfall is not notable in the six basins. When comparing to other basins, the Sangker basin commonly has lower monthly rainfall which is less than 300 mm. The monthly rainfall of 583.6 mm is captured in September 2002 in Chikreng basin which is the most extreme monthly rainfall of the six gauged basins. It is caused by several extreme daily rainfall occurred in the same month which can be illustrated in Figure 3.23.

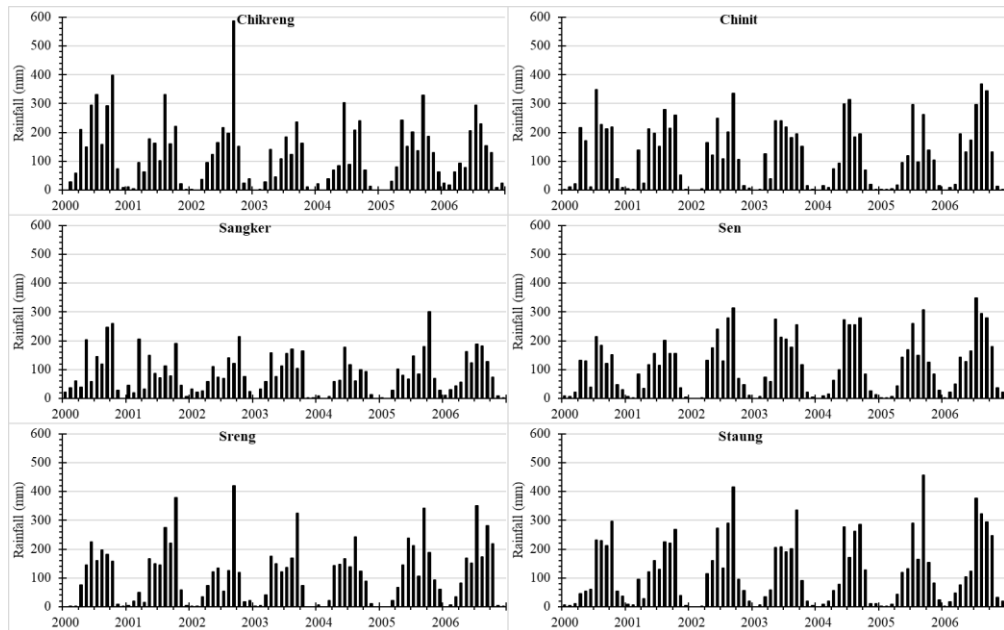


Figure 3.24. Monthly rainfall data of gauged basins in the Tonle Sap basin

Figure 3.25 shows the annual area rainfall of the six gauged basins. The inter-variation on the annual rainfall of the six basins are not high and normally less than 596 mm except the Chikreng basin which has the inter-variation about 960 mm. It can be seen from Figure 3.25 that the Sangker basin has the lower annual rainfall than other basins while the lowest annual rainfall of 960 mm captured in 2004.

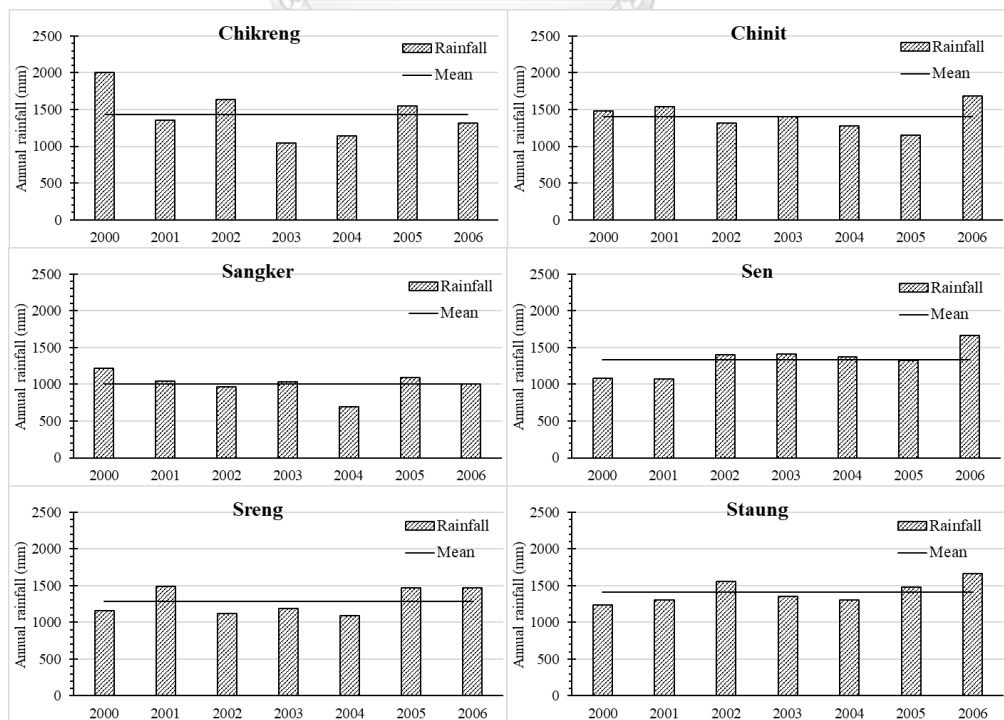


Figure 3.25. Annual rainfall data of gauged basins in the Tonle Sap basin

3.5.2 Temperature Characteristic

There is some missing temperature data in the gauged basin. Simple average of temperature value at same day in different year is employed for filling missing data. Based on Figure 3.26, the daily temperature of gauged basins has the same pattern. Generally, the daily temperature of the six gauged basins varies between 20.05 and 36.7 °C.

Figure 3.27 shows the monthly average temperature of the gauged basins. It clearly shows that the six gauged basins have similar pattern and normally range between 24.4 and 31.2 °C. The low and high temperatures are generally found in December and April, accordingly. The temperature of the gauged basins in 2006 is lower than other years.

Figure 3.28 pictures annual average temperature between 2000 and 2006. It indicates that the annual temperature of the gauged basins changes between 27.1 and 28.5 °C. Moreover, they have similar pattern to each other.

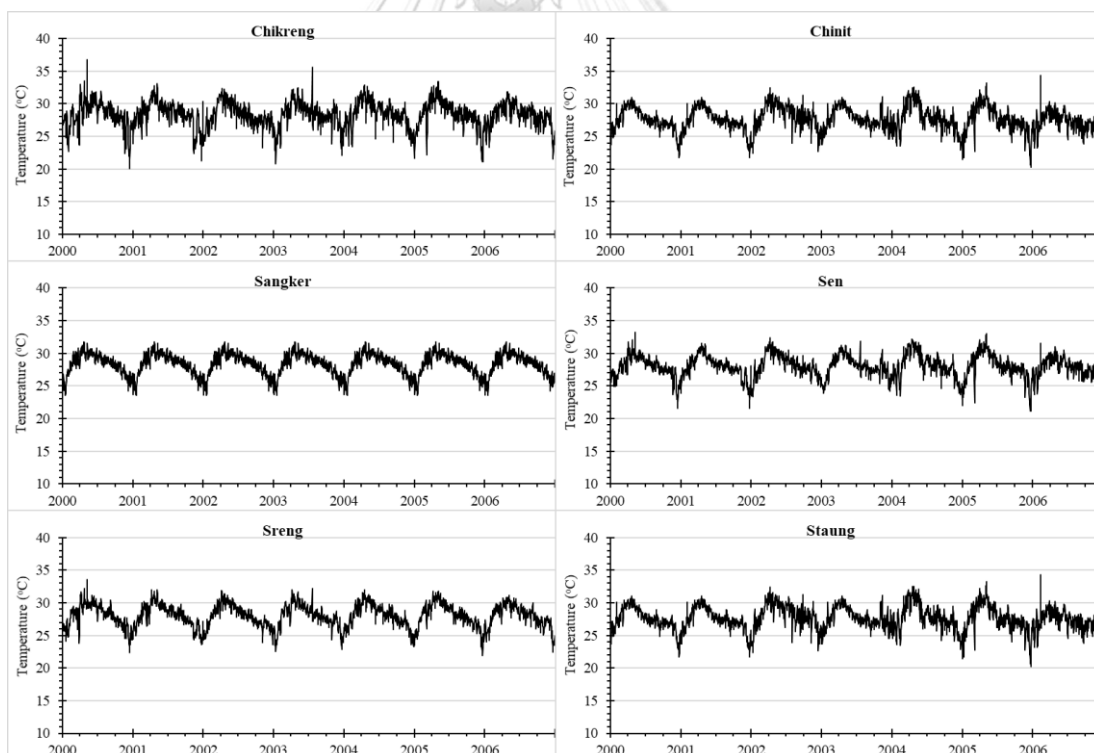


Figure 3.26. Daily temperature of gauged basins in the Tonle Sap basin

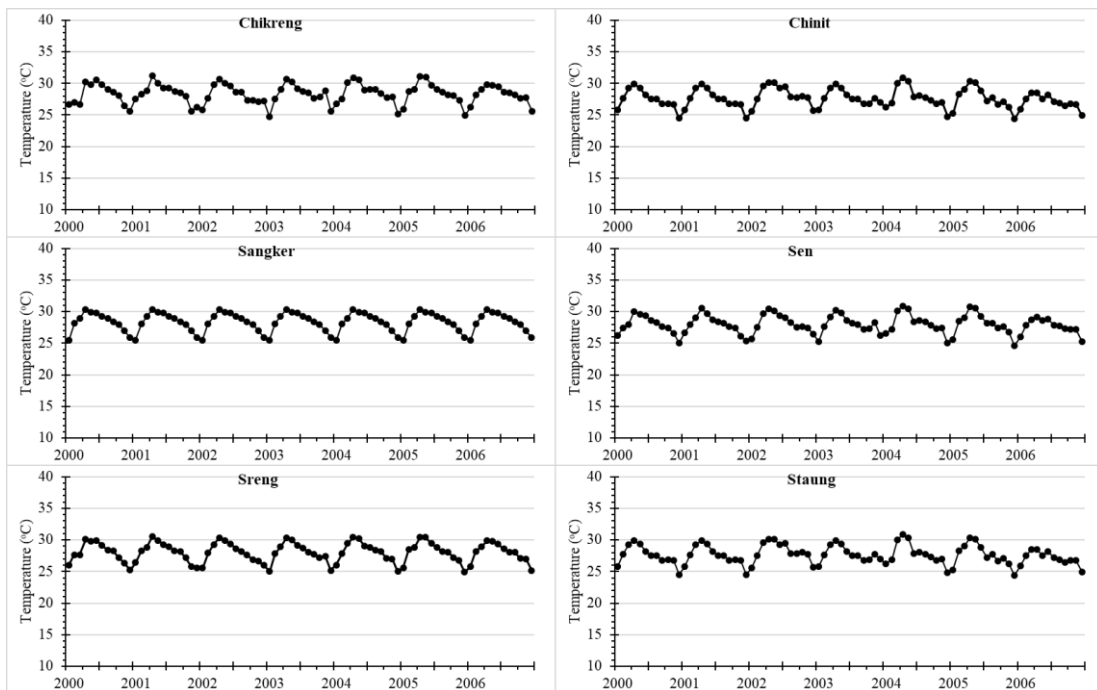


Figure 3.27. Monthly average temperature of gauged basins in the Tonle Sap basin

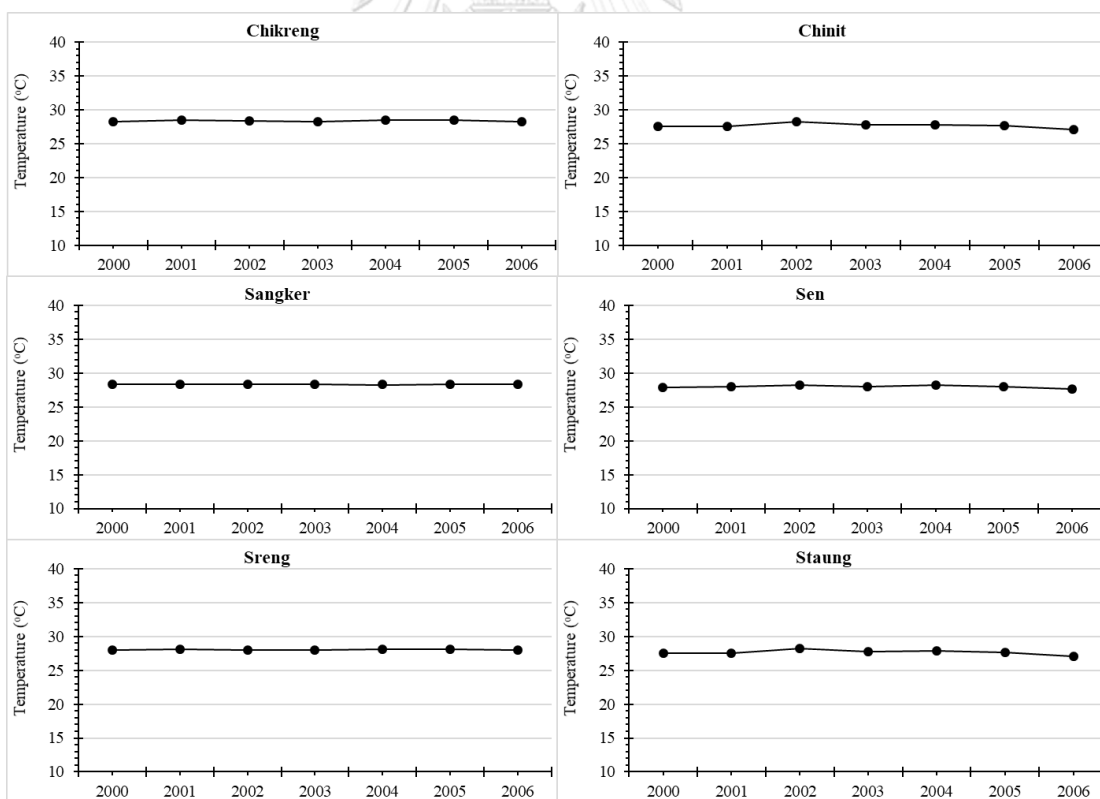


Figure 3.28. Annual average temperature of gauged basins in the Tonle Sap basin

3.5.3 Streamflow Characteristic

The daily, monthly and annual streamflow of the six gauged basins are shown in Figure 3.29 to Figure 3.31. Figure 3.29 depicts that the daily streamflow in the six gauged basins has similar pattern of wet and dry months but they are different in amount. The variation of the streamflow in the Sangker basin is higher compared to other basins. This is probably because the upstream part of the Sangker basin is the mountainous area with steep slope and less forest causing the Sangker basin to have more chance of high rainfall, high runoff velocity, and low losses. The Sreng basin has lowest daily streamflow which can probably be caused by the physical characteristics of the basin e.g. size, shape, density of river network and land use. The size of the Sreng basin is two to four times bigger than the other gauged basins (see Appendix A). The Sreng basin is a very wide basin (see Figure 3.1) and mainly covered by forest at the upstream area. This leads to long travel time of runoff to the outlet and high infiltration and evaporation.

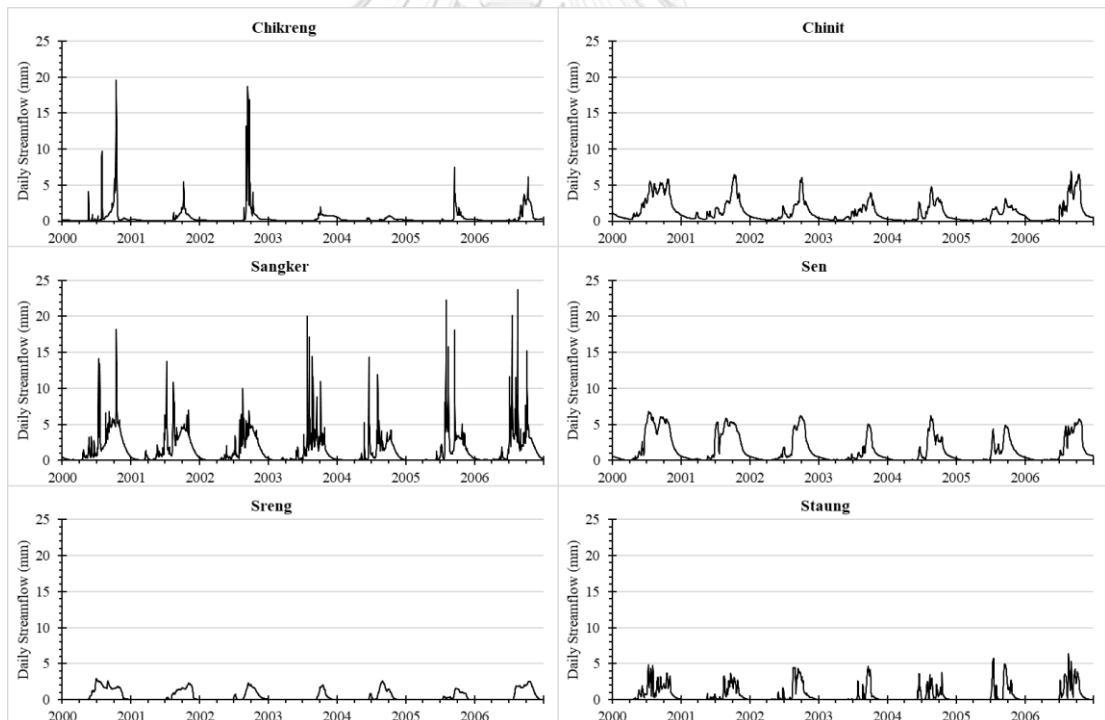


Figure 3.29. Yield of daily streamflow of gauged basins in the Tonle Sap basin

Figure 3.30 shows monthly streamflow of the six gauged basins. The gauged basins show similar pattern on the monthly streamflow, but they are different in amount of streamflow. It can be drawn from Figure 3.30 that the reduction in streamflow is usually noticeable in July or August due to the shift of the Inter-Tropical Convergence Zone (ITCZ). The wet month can be found between May to October and dry month is between November to April while the wettest month normally occurred in September or October.

Figure 3.31 shows the yield of the annual streamflow of the six gauged basins. The graphs show that the yield of the annual streamflow of Chinit, Sangker, Sen, and Staung basin have similar pattern with the lowest annual streamflow occurring in 2003 and 2004. The Chikreng and Sreng basins have relatively low annual streamflow. Referring to the analysis above, the major factors which could cause the Sreng river basin to have less streamflow, are river network, percentage of forest, shape and size of the basin. In contrast to Sreng basin, the Chikreng basin has smaller basin size but higher in percentage of forest (see Appendix A). Thus, forest can be the major factor causing the Chikreng river basin to have low streamflow.

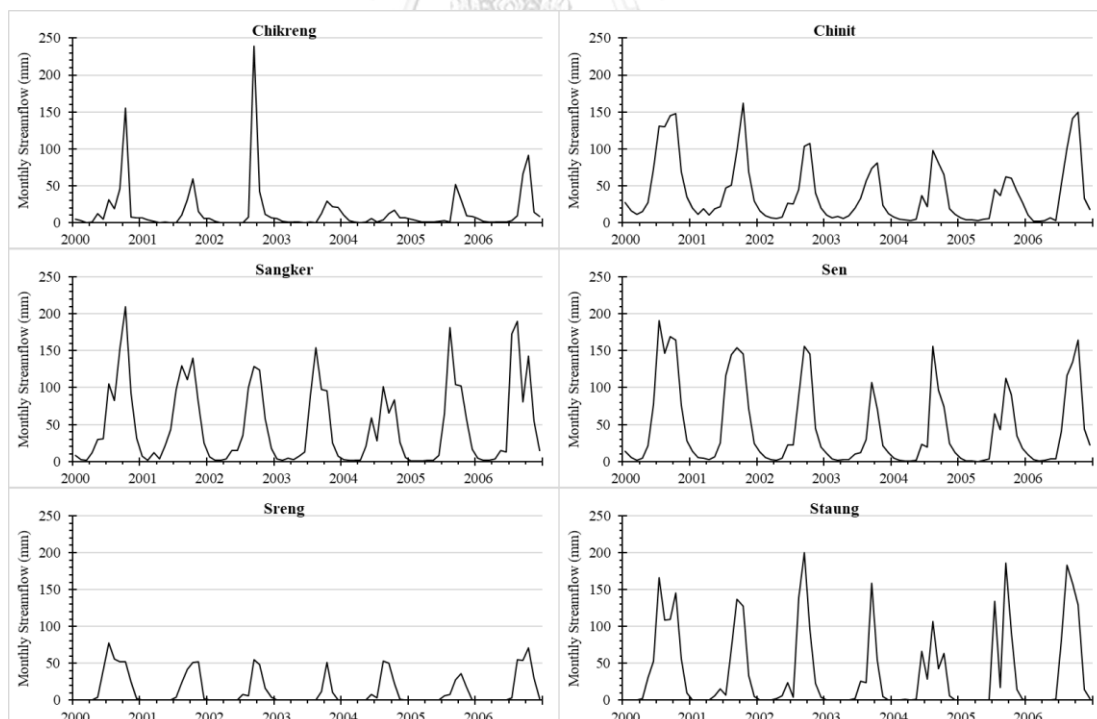


Figure 3.30. Yield of monthly streamflow of gauged basins in the Tonle Sap basin

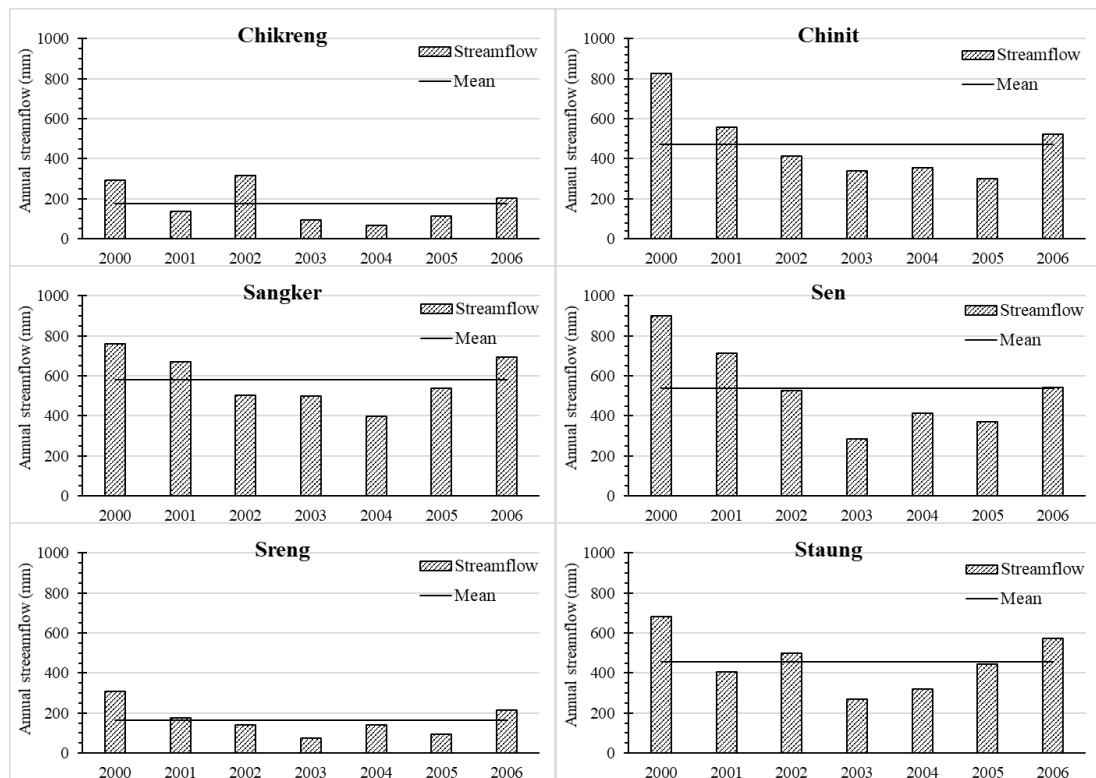


Figure 3.31. Yield of annual streamflow of gauged basins in the Tonle Sap basin

According to the analysis of the hydrological characteristics in the six gauged basins above, it clearly shows that the rainfall and streamflow change from year to year whereas the temperature does not vary much. High variations in rainfall and streamflow lead to challenging water management. The assessment of drought is focused in this study due to limited number of previous studies in Cambodia. The methodology for the analysis of drought is explained in Chapter 4.

CHAPTER 4

METHODOLOGY

The methodology used in this research to achieve desired objectives is presented in this chapter. The overall framework consists of four main steps, including data preparation, prediction streamflow in ungauged basins, drought index estimation and development of drought map as shown in Figure 1.1. The detail procedure is described in the following sections.

4.1 Data Preparation

4.1.1 Data Collection

The meteorological (rainfall and temperature), hydrological (streamflow), and geospatial (soil types and land use) data are obtained from the MOWRAM and MRC as mentioned earlier in Chapter 3 and summarized here in Table 4.1. The Advanced Very High-Resolution Radiometer (AVHRR) surface reflectance data of infrared radiation (IR) and near-infrared radiation (NIR) (channel 1 and channel 2, accordingly) at daily time series from 1985 to 2008 were obtained from NOAA Climate Data Record (CDR). They are gridded data with the special resolution of 0.05 degree and array with longitude and latitude dimensions of 7200×3600. The IR and NIR data are the important input which used to assess the vegetation condition. Prior to the calculation of the drought indices, the quality of the collected data is examined as explained in the following sections.

4.1.2 Data Quality Checking and Cleaning

The consistency of the rainfall data obtained from 12 rainfall stations in the Greater Baribo basin between 1985 and 2008 were performed using DMC as described in section 3.3.1. There is no missing data for rainfall and streamflow but there is for temperature, IR, and NIR data. The missing temperature, IR, and NIR are filled using the simple average of the temperature at the same day and month but in different year.

Table 4.1. Description of the data collection

Type	Station Name	Station ID	Lat	Lon	Duration	Sources
Rainfall	Kompong Tralach	110405	11.9	104.8	1985-2008	MOWRAM and MRC
	Oudong	110415	11.8	104.7	1985-2008	
	Thnal Tetung	110423	11.5	104.7	1985-2008	
	Pochentong	110425	11.6	104.9	1985-2008	
	Chruy Changvar	110426	11.6	104.9	1985-2008	
	Samaki Meanchey	110430	11.9	104.6	1985-2008	
	Beoung Kantot	120320	12.5	104.1	1985-2008	
	Kompong Chhnang	120401	12.2	104.7	1985-2008	
	Bamnak	120406	12.3	104.2	1985-2008	
	Rolar Phear	120416	12.2	104.7	1985-2008	
	Ponley	120417	12.4	104.5	1985-2008	
	Tuk Phos	120420	12.1	104.5	1985-2008	
	Pailin	120202	12.9	102.6	2000-2006	
	Maung Russey	120303	12.8	103.5	2000-2006	
	Staung	120402	12.9	104.6	2000-2006	
	Kompong Thom	120404	12.7	104.9	2000-2006	
	Prasat Balang	120422	13	105	2000-2006	
	Prasat Sambo	120516	12.9	105.1	2000-2006	
	Taing Kok	120517	12.3	105.1	2000-2006	
	Battambang	130305	13.1	103.2	2000-2006	
	Kralanh	130307	13.6	103.4	2000-2006	
	Angkor Chum	130320	13.7	103.7	2000-2006	
	Srey Snam	130326	13.8	103.5	2000-2006	
	Varin	130328	13.8	103.8	2000-2006	
	Phnom Koulen	130403	13.6	104.1	2000-2006	
	Kompong Kdei	130405	13.1	104.3	2000-2006	
	Sondan	130505	13.1	105.2	2000-2006	
	Kompong Thmar	NaN	12.5	105.1	2000-2006	
	Presh Vihear	NaN	14.2	104.7	2000-2006	
	Temperature	Battambang	NaN	13.1	103.2	
Kompong Chhnang		NaN	12.2	104.7	2012-2017	
Kompong Thom		NaN	12.7	104.9	1998-2011	
Pochentong		NaN	11.6	104.9	1985-2008	
Siem Reap		NaN	13.4	103.8	2012-2016	
Discharge	Kralanh	540101	13.6	103.4	2000-2006	
	Battambang	550102	13.1	103.2	2000-2006	
	Prasat Keo	560102	13.1	104.6	2000-2006	
	Kampong Chen	600101	12.9	104.6	2000-2006	
	Kampong Thom	610101	12.7	104.9	2000-2006	
	Kampong Thmar	620101	12.5	105.1	2000-2006	

4.1.3 Data Pre-processing

This research assesses the drought at five time-scales including 3-, 6-, 12-, 24- and 48-month. The rainfall, streamflow, and NDVI are computed at five time-scales of interest in particular month. For example, the calculation of the drought indices for January at a 3-month timescale, the data (rainfall, streamflow, or NDVI) must be cumulated from the three consecutive month consisting two preceding months to the month of analysis as shown in Table 4.2. The same procedure is applied for other time-scales but need to change the number of cumulated month basin on time-scale.

Table 4.2. Converting data to the time-scale of 3-, 6-, 12-, 24-, and 48-month

Month of interest	3-month	6-month	12-month	24-month	48-month
Jan	Nov	Aug	consecutive 12 months from Feb last year up to Jan	consecutive 24 months from Feb last 2 years up to Jan	consecutive 48 months from Feb last 4 years up to Jan
	Dec	Sep			
	Jan	Oct			
	-	Nov			
	-	Dec			
	-	Jan			

4.2 Drought Indices

4.2.1 Selection of Drought Index

Three types of droughts i.e. meteorological, agricultural, and hydrological are assessed within the Greater Baribo basin. Since there are numerous drought indices of each type of drought, it is very important to select the indices which can represent each form of drought with different advantages and disadvantages and the data requirement. Based on available data, there are 20 drought indices which possible to be assessed as listed in Table 4.3.

There are 3 out of 20 drought indices (see Table 4.3) which are selected to represent the three types of droughts in this research. The selection of these drought indices are based on their data requirement and ability to answer the seven equations which stated by WMO and GWP (2016) as detailed in section 2.4. The brief methodology of the three selected indices is separated into three main groups of droughts such as meteorological, agricultural, and hydrological. The description for calculating the selected indices is summarized in the following section.

Table 4.3. Brief process and main features of widely used drought indices

No.	Drought index and Source	Type	Input Data	Brief process*	Main features
1	Palmer Severity Drought Index (PSDI) (Palmer, 1965)	M	P, T, AWC	The PSDI considers the water supply and demand instead of the precipitation anomaly. The value of the PSDI is between -4 and 4. The principal equation is: $PSDI_k = \frac{Z_k}{3} - 0.897PSDI_{k-1}$	The first and widely used combined drought index. The PSDI provides reliable result than the precipitation only index, and it is the most effective where impacts are sensitive to the soil moisture.
2	Palmer Modified Drought Index (PMDI) (Palmer, 1965)	M	P, T, AWC	The calculation and possible range of the PMDI is same to those of the PSDI. $PMDI_i = \frac{Z_k}{3} - 0.897.PMDI_{i-1}$	The PMDI was modified from the PSDI, whereas its main difference is the identification of the time of the drought.
3	Rainfall Anomaly Index (RAI) (Van Rooy, 1965)	M	P	The RAI uses normalized precipitation values based upon the station history of a location. It compares the precipitation in current period with the historical precipitation. The value of the RAI is ranked between -3 and 3, and its equation of this index is as follows: $RAI = \pm 3 \frac{P - \bar{P}}{\bar{E} - \bar{P}}$	The RAI is used to indicate the impact of the drought on the agriculture, seasonal rainfall variability, pattern of onset and length for the rainy season, and the overall variability of the seasonal rainfall intensity.
4	Bhalme and Mooley Drought Index (BMDI) (Bhalme and Mooley, 1980)	M	P	The BMDI is calculated using statistics of the rainfall, rainfall anomaly, and moisture index, and it varies between -4 and 4. The principal equation is illustrated as follows: $BMDI = \frac{\sum_1^n i_k}{n}$	The BMDI is an empirical index that uses the monthly rainfall as the core climatological input as it considers the rainfall during the southwest monsoon (Jun-Sep).

Table 4.3. Brief process and main features of widely used drought indices (Cont.)

No.	Drought index and Source	Type	Input Data	Brief process*	Main features
5	Standardize Precipitation Index (SPI) (McKee et al., 1993)	M	P	<p>The calculation of the SPI relies on the transformation of the precipitation probability distribution to the normal distribution. The value of the SPI generally varies from -3 to 3, and its principal equation is as follows:</p> $SPI = \frac{x_i - \bar{x}}{S}$	<p>The SPI is a simple index which is able to demonstrate the drought at various time scales, and it can be applied to assess the agricultural and hydrological drought. It is the standardized drought index which has been widely adopted for research and operational modes and can represent both the wet and the dry condition.</p>
6	Effective Drought Index (EDI) (Byun and Wilhite, 1999)	M	P	<p>The EDI mainly relies on the effective rainfall (EP) which is computed from three variables including mean of EP (MEP), deviation of EP (DEP), and the standard deviation (SD) value of DEP (SEP). The value of the EDI normally varies from -2.5 to 2.5. The principal equation is as follows:</p> $EDI = \left[\frac{DEP}{ST(DEP)} \right] \text{ or}$	<p>The EDI is a simple and transparent index which was developed to overcome the limitation of the SPI. The calculation of the SPI cannot be performed until all daily record of rainfall data for the particular timescales are available, but the EDI can be computed at daily time-scale.</p>
7	Percentage of Normalized Precipitation (PNP) (Keyantash and Dracup, 2002)	M	P	<p>The PNP is calculated by dividing a given precipitation by the normal precipitation (NP) and time by 100. The NP usually corresponds to the mean of the past 30 years. The main equation to determine this index is as follows:</p> $PNP = \frac{P}{NP} \times 100$	<p>The PNP uses a simple calculation, which is able to indicate the drought from monthly to yearly time scales and is also effective for a single region or season. Especially, it is convenient to use the PNP to communicate with the public.</p>

Table 4.3. Brief process and main features of widely used drought indices (Cont.)

No.	Drought index and Source	Type	Input Data	Brief process*	Main features
8	Standardize Precipitation Evapotranspiration Index (SPEI) (Vicente-Serrano et al., 2010)	M	P, T	The SPEI uses the basis of the SPI but it includes the temperature as a component. The value of the SPEI ranges between -5 and 5. The main equation as is as follows: $SPEI_{Aj} = 1.756 \times W_t - 1.704$	It is required to overcome the shortcoming of the SPI in addressing the consequence of the climate change on the drought behavior. It mostly relies on the water balance and evapotranspiration.
9	Palmer Anomaly Drought Index (Z index) (Palmer, 1965)	A	P, T, AWC	The Z index is actually an intermediate term in the computation of the PSDI. The value of the Z normally ranges between -3.5 and 3.5. The formula of the Z index is given as: $Z = K_j d$	The Z index can track the agricultural drought as it responds quickly to change in soil moisture values. The calculation of Z index really complicates because there are many assumptions used in the water balance computation. It is slightly less complex than the PSDI.
10	Aridity Index Anomaly (Ia) (Thornthwaite, 1948)	A	P, T, WS, SR	Ia uses the water balance technique to monitor the agricultural drought. The value of Ia varies from 1 to 100 and it is computed as: $I_a = \frac{PE - ET}{PE}$	This index is one of tools to monitor the agricultural drought, and it is a commonly used index to represent the crop moisture stress.
11	Crop Moisture Index (CMI) (Palmer, 1968)	A	P, T, AWC	The CMI was derived from the PSDI and could indicate the moisture supply in the short term. The CMI is the cumulative of the evapotranspiration and soil water recharge. $CMI_i = CMI_{i-1} + 1.8 \frac{ET \times ET}{\sqrt{\alpha}}$	The CMI is not performed well to indicate the long-term drought, but it is effective for assessing the short-term (weekly) drought. The CMI can assess present conditions for crops, but it can rapidly change.

Table 4.3. Brief process and main features of widely used drought indices (Cont.)

No.	Drought index and Source	Type	Input Data	Brief process*	Main features
12	Palmer Hydrological Drought Index (PHDI) (Palmer, 1965)	H	P, T, AWC	<p>The PHDI is modified from PSDI to quantify the long-term impact of the hydrological drought, and it considers the soil moisture and reservoir deficit. The value of the PHDI is the same as that of the PSDI. The main equation for calculating the PHDI is:</p> $PHDI_k = \frac{Z_k}{3} - 0.897I_{k-1}$	The PHDI has a more stringent criterion for the elimination of the drought/wet spell, which is slower than the PSDI toward the normal state. This retardation is appropriate for the assessment of the hydrological drought, which is a slower developing phenomenon than the meteorological drought.
13	Streamflow Drought Index (SDI) (Nalbantis and Tsakiris, 2009)	H	SF	<p>The SDI uses the same calculation procedure as the SPI, but it uses the streamflow instead of the precipitation data. The value of the SDI is ranked between -2 and 0. Based on the summation of $V_{i,k}$ the streamflow volume, the SDI is indicated for each reference period k of the i-th hydrological year as the equation below:</p> $SDI_{i,k} = \frac{V_{i,k} - \bar{V}_k}{s_k}$	The SDI is used to monitor and identify hydrological drought in a particular basin. The calculation of SDI is simple and longer streamflow data helps to give more accurate result. SDI can be calculated at various timescales using the same procedure as that of the SPI.
14	Normalized Difference Vegetation Index (NDVI) (Tucker, 1979)	A, RS	NIR, IR	<p>The NDVI uses the advanced very high-resolution radiometer (AVHRR), reflected red (Red), and near-infrared (NIR) channels to calculate. The value of the NDVI varies from -1 to 1. The formula for the NDVI is given as:</p> $NDVI = \frac{NIR - Red}{NIR + Red}$	The NDVI indicates and predicts the agricultural production, and it is preferred for the global vegetation monitoring because it helps compensating for changing illumination conditions, surface slope, aspect, and other extraneous factors.

Table 4.3. Brief process and main features of widely used drought indices (Cont.)

No.	Drought index and Source	Type	Input Data	Brief process*	Main features
15	Normalized Difference Infrared Index (NDII) (Hardisky et al., 1983)	A, RS	NIR, SWIR	<p>The NDII uses the ratio of different values of the near infrared reflectance (NIR), short-wave infrared reflectance (SWIR), and the satellite data of the MODIS level 3 surface reflectance product (MOD09A1). The NDII is a normalized index in which its theoretical values vary between -1 and 1. The formula of this index is:</p> $NDII = \frac{\rho_{0.85} - \rho_{1.65}}{\rho_{0.85} + \rho_{1.65}}$	<p>The NDII was developed to monitor the leaf water content. It can be effectively used to detect the plant water stress according to the property of the shortwave infrared reflectance, which is negatively related to the leaf water content due to the large absorption by the leaf.</p>
16	Soil Adjusted Vegetation Index (SAVI) (Huete, 1988)	A, RS	NIR, IR	<p>The SAVI uses the same procedure as the NDVI, but it is adjusted by the multiplication factor. The value of the SVAI is between -1 and 1. The equation used to determine the SAVI is as follows:</p> $SAVI = \left(\frac{NIR - Red}{NIR + Red} + L \right) (1 + L)$	<p>The SAVI is useful for monitoring the soil and vegetation which can provide the high-resolution and high-density data associated with the remote sensing data allowing a good spatial coverage. The computation procedure is complex as it requires data to run operationally. A short-recorded period associated with the satellite data can hamper climate analyses.</p>
17	Vegetation Condition Index (VCI) (Kogan, 1990)	A, RS	NIR, IR	<p>The VCI is a pixel-wise normalization of the VI that is useful for making relative assessments of changes in the VI signal by filtering out the contribution of local geographic resources to the spatial variability of VI. The value of the VCI ranges from -1 to 1, and it is computed as:</p>	<p>The VCI is applied to identify drought situations and determine the onset, especially in areas where drought episodes are localized and ill defined. It focuses on the impact of the drought on the vegetation, and it can also provide the information on the onset, duration and severity of</p>

Table 4.3. Brief process and main features of widely used drought indices (Cont.)

No.	Drought index and Source	Type	Input Data	Brief process*	Main features
17				$VCI = \frac{NDVI - NDVI_{min}}{NDVI_{max} - NDVI_{min}}$	the drought by noting vegetation changes and comparing them with historical values. It allows high resolution and good spatial coverage of the analysis.
18	Enhanced Vegetation Index (EVI) (Huete et al., 2002)	A, RS	NIR, IR	<p>The EVI was developed to optimize the vegetation signal with the improved sensitivity in high biomass regions and improved vegetation monitoring. The value of the EVI is between 0 to 1 and it is computed as:</p> $EVI = G \frac{\rho_{NIR} - \rho_{Red}}{\rho_{NIR} + C_1 \rho_{Red} - C_2 \rho_{Blue} + 1}$	The EVI is more responsive to canopy structural variations including the Leaf Area Index (LAI), canopy type, plant physiognomy, and canopy architecture
19	Modified Perpendicular Drought Index (MPDI) (Ghulam et al., 2007c)	A, RS	NIR, IR	<p>The MPDI is a real time operational drought index which is based on the NIR-red spectral reflectance space. The main limitation of this approach is the assumption of the invariant soil color. The equation of the MPDI is as:</p> $MPDI = \frac{1}{(1 - f_v)} (PDI - f_v PDI_v)$	The MPDI is modified from the PDI which is developed to assess the vegetation fraction and takes into account both the soil moisture and the vegetation growth. The MPDI is an in-situ drought index derived from the 0-20 cm mean soil moisture. It has the potential to provide a simple and real-time drought monitoring method in the remote estimation of the drought phenomena.

Table 4.3. Brief process and main features of widely used drought indices (Cont.)

No.	Drought index and Source	Type	Input Data	Brief process*	Main features
20	Standardized Vegetation Index (SVI) (Nalbantis and Tsakiris, 2009)	A, RS	NDVI, IR, and NIR	The SVI is a cumulative probability density of the Z-score of the NDVI which can be computed as follows: $z_i = \frac{NDVI_i - \overline{NDVI}}{\sigma}$ $SVI = P(Z < z_i)$	The SVI is the transformation of the probability of the NDVI as it can indicate the greenness probability term using the relative vegetation greenness.

Note: *Readers are suggested to refer to the source for full explanation of the variables used for calculating the indices.

M = Meteorological, A = Agricultural, H = Hydrological, RS = Remote Sensing, P = Precipitation, T = Temperature, AWC = Available Water Capacity, SF = Streamflow, IR = infrared, NIR = Near Infrared, SWIR = Short Wave Infrared, SR = Solar Radiation, WS = Wind Speed

SPI, SVI, and SDI are employed for assessing the meteorological, agricultural, and hydrological droughts, respectively. These indices are selected because they are widely used, require less input data, use simple principle, give effectiveness result, and can be computed at any time-scales of interest (Wilhite, 2011, Hong et al., 2015, and Bert and Elga, 2016). Furthermore, SPI and SVI use rainfall and NDVI, accordingly as key input. They are commonly used in Cambodia and provided reliable result (Chhinh and Millington, 2015, Guo et al., 2017, and Sok et al., 2017). SVI can provide a near real time indicator and the calculation is based on the greenness probability term. Moreover, it can be assessed the vegetation in many aspects including drought, flood, crop rotation, and unseasonable coolness. For hydrological drought, SDI is a well-known drought index which uses only streamflow as the key input (Hong et al., 2015). Because the Greater Baribo basin is a data-sparse basin, the assessment of hydrological drought via SDI cannot be performed directly from the gauged data; predictions of streamflow using the PUB technique is needed as explained in section 4.2.4.

4.2.2 Meteorological Drought Index

The SPI was developed by McKee et al. (1993). It allows users to define the severity, intensity, frequency, and duration of the drought at various time scales. Figure 4.1 shows the 6 steps for calculating the SPI.

First, the daily rainfall was converted to monthly rainfall. The monthly rainfall was cumulated to the time-scales of interest as shown in section 4.1.3. After that, cumulative monthly rainfall is grouped into 12 groups of difference months (i.e. January, February, March, ..., December). The computation of the SPI involves the distribution fitting. Gamma distribution is found to fit well with the monthly rainfall data in Cambodia (Chhinh and Millington, 2015, Guo et al., 2017, and Sok et al., 2017). Figure 4.2 is shown here as an example of fitting Gamma distribution for monthly rainfall of station 110405. It can be seen that Gamma distribution fits well with both high and low rainfall in most months. Gamma distribution is found to underperform for some months i.e. April, June, July, August, and November. However, Gamma distribution is considered acceptable for this research because the error is small for low rainfall which is critical for drought analysis. Moreover, Gamma distribution is found to fit best with rainfall comparing to other e.g. Lognormal and Exponential distributions. The probability density function (PDF) of the Gamma distribution is characterized by shape (α) and scale (β) parameters which can be estimated from the empirical rainfall distribution for each rain gauge at any time scales of interest. The example of fitting Gamma distribution for each month at rainfall station 110405 is illustrated in Figure 4.2. The cumulative probability of the observed precipitation data for the period of study and time scale is then obtained. However, due to the large number of zero rainfall values, the cumulative probability is transformed to the standard normal random variable Z with zero mean and unit variance. Finally, the value of Z is converted to the SPI as shown in the example of equiprobability transformation from fitted Gamma distribution to the standard normal distribution in June at rainfall station 110405 (see Figure 4.3).

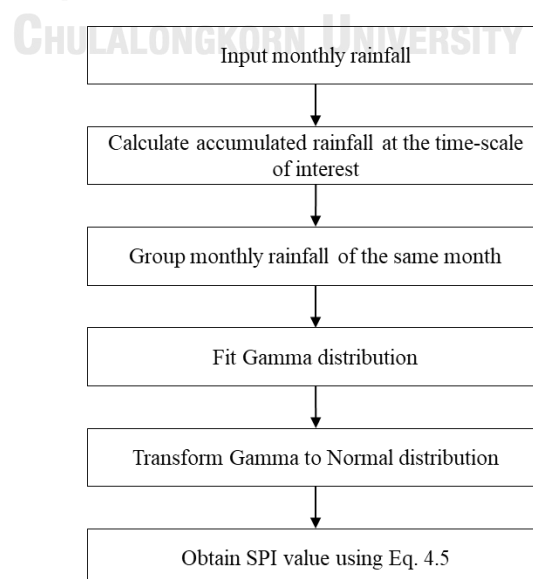


Figure 4.1. Framework for computing SPI

The equation 4.1 is the probability distribution function (PDF) of the Gamma distribution which represents for the distribution of rainfall of each month with no zero value because the Gamma cannot define the rainfall at zero. $\Gamma(\alpha)$ is the gamma function which evaluated at α .

$$g(x) = \frac{1}{\beta^\alpha \Gamma(\alpha)} x^{\alpha-1} e^{-\frac{x}{\beta}} \quad \text{for } x, \alpha, \beta > 0 \quad \text{Eq. 4.1}$$

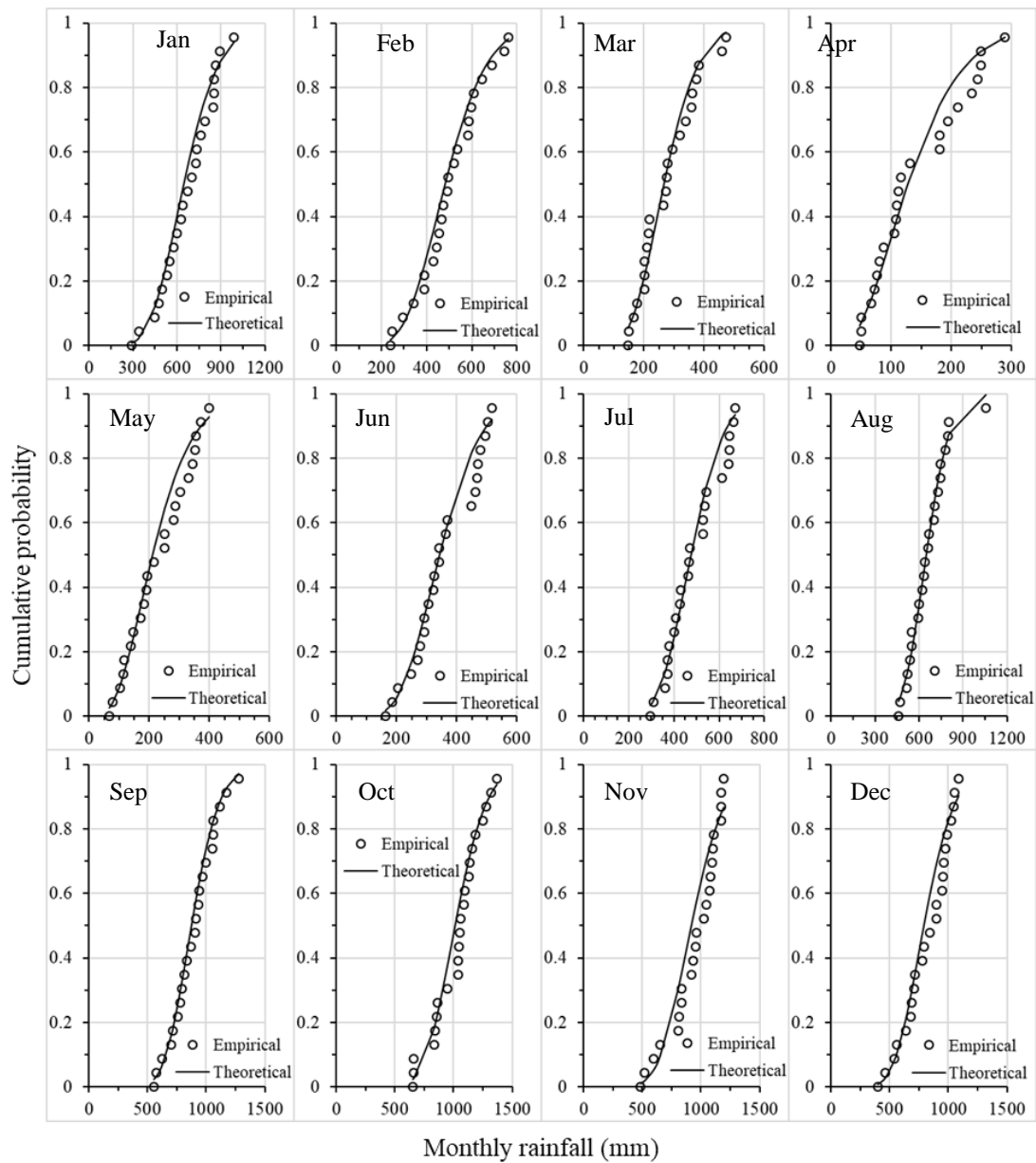


Figure 4.2. Fitting gamma distribution of each month in 110405

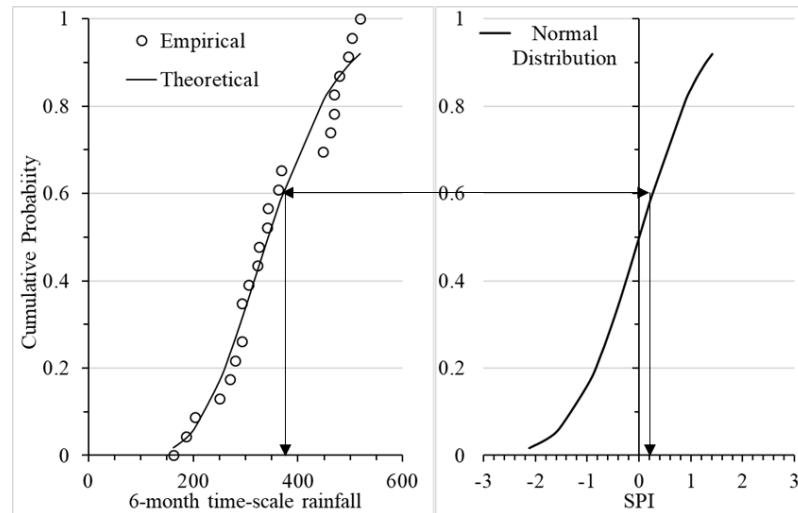


Figure 4.3. Example of equiprobability transformation from fitted gamma distribution to the standard normal distribution in June at 110405

After that calculate the cumulative distribution function (CDF) ($G(x)$) of the observed rainfall data for the period of study, the equation 4.2 which is based on the selected rainfall distribution in the equation 4.1 is applied.

$$G(x) = \int_0^x g(x)dx = \frac{1}{\hat{\beta}\hat{\alpha}\Gamma(\hat{\alpha})} \int_0^x x^{\hat{\alpha}-1} e^{-\frac{x}{\hat{\beta}}} dx \quad \text{Eq. 4.2}$$

$$\hat{\alpha} = \frac{1}{4A} \left(1 + \sqrt{1 + \frac{4A}{3}} \right) \quad \text{Eq. 4.3}$$

$$\hat{\beta} = \frac{\bar{x}}{\hat{\alpha}} \quad \text{Eq. 4.4}$$

$$A = \ln(\bar{x}) - \frac{\sum \ln(x)}{n} \quad \text{Eq. 4.5}$$

Owing to the exclusion of zero values of the rainfall in the PDF of the Gamma distribution; thus, the recalculation of the observed rainfall for the CDF ($H(x)$) is needed.

This can be referred to the equation 4.6.

$$H(x) = q + (1 + q)G(x) \quad \text{Eq. 4.6}$$

$$q = -\frac{m}{n} \quad \text{Eq. 4.7}$$

where,

q = the probability of the rainfall of the zero value

m = the numbers of zeros in the rainfall time series

n = the total number time series of the rainfall

Next, the new CDF of the observed rainfall is converted to the standard normal random (Z-score) with zero mean and unit variance. The value of the SPI can be calculated from equation 4.8.

$$SPI = \frac{x_i - \bar{x}}{SD} \quad Eq. 4.8$$

where, \bar{x} and SD are the mean and standard deviation of monthly rainfall, respectively. The values of the SPI normally range from -3 to +3 which are divided into seven categories as illustrated in Table 2.2. The value above zero represents the wet period, and the value below zero represents the dry period. For example, the SPI value of -2 refers to the monthly rainfall at the time-scale of interest is less than mean with two times of variance and +2 refers to the monthly rainfall at the time-scale of interest is greater than mean with two time of variance.

4.2.3 Agricultural Drought Index

SVI is an index developed based on the satellite images data. It is developed by Peters et al. (2002). It allows the assessment of the vegetation health condition by relative greenness probability. The framework for calculating SVI is shown in Figure 4.4 and explained below.

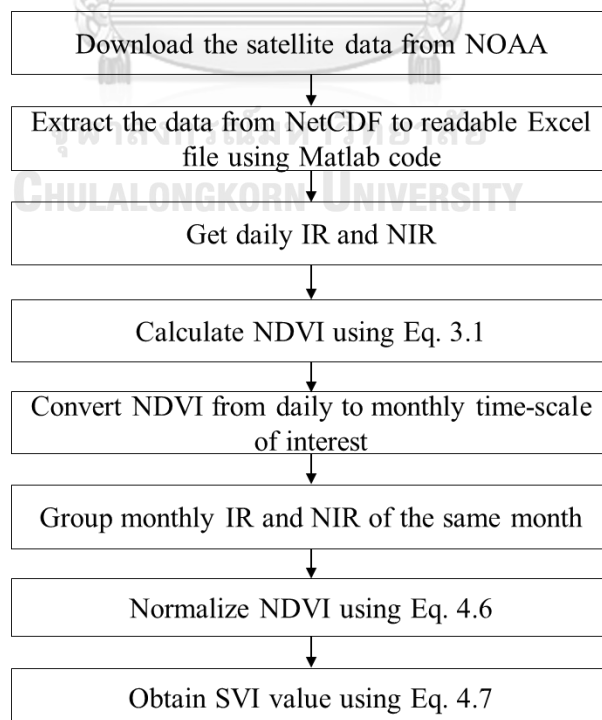


Figure 4.4. Framework for calculating SVI

The IR and NIR are downloaded from NOAA as mentioned in section 4.1.1 and they are extracted from NetCDF file to readable Excel file using MATLAB code. Then, the extracted daily IR and NIR are used to compute the daily NDVI using equation 3.1 and converted to monthly NDVI. After that, the monthly of NDVI for the time-scale of interest as detailed in section 4.1.3 are grouped into 12 groups of difference months. Each group of the monthly NDVI are transformed to normal distribution with zero mean and unit variance using equation 4.9. Then, the cumulative density function (CDF) of the Z score is calculated as in equation 4.10. SVI is the CDF of the Z score as depicted in Figure 4.5. The classification of vegetation health condition based on the SVI is shown in Table 4.4. The value of SVI ranges between 0 and 1. The value of SVI from 0.00 to 0.05 and 0.05 to 0.25 refer to very poor and poor greenness condition of the vegetation, respectively. The value of SVI from 0.25 to 0.75 refers to near normal condition of the vegetation, accordingly. The value of SVI from 0.75 to 0.95 and 0.95 to 1.00 refer to good and very good condition of the vegetation, accordingly.

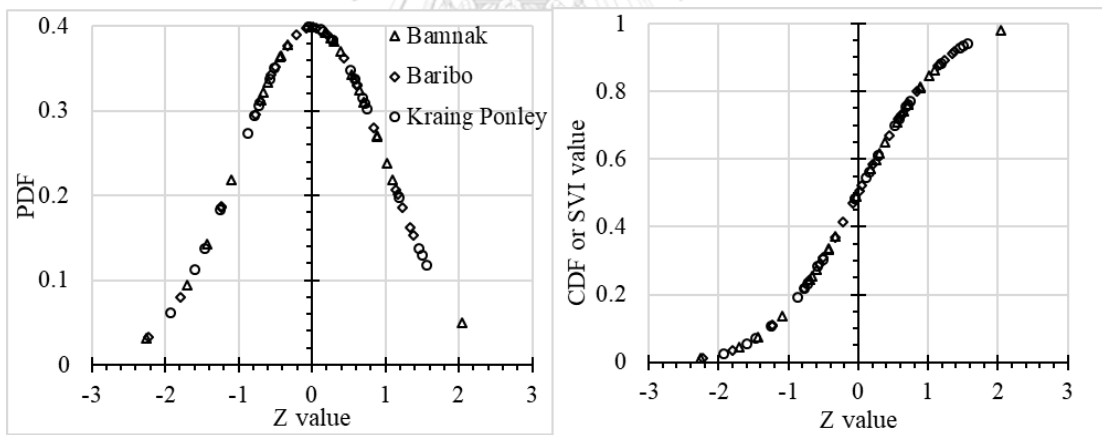


Figure 4.5. Example of PDF and CDF of normal distribution of NDVI value for three sub-basins in June

$$Z_i = \frac{NDVI_i - \overline{NDVI}}{\sigma} \quad \text{Eq. 4.9}$$

$$SVI = P(Z < z_i) \quad \text{Eq. 4.10}$$

Table 4.4. Classification of vegetation condition based on SVI value

SVI value	Category
0.00 - 0.05	Very Poor
0.05 - 0.25	Poor
0.25 - 0.75	Near Normal
0.75 - 0.95	Good
0.95 - 1.00	Very Good

4.2.4 Hydrological Drought Index

SDI is a hydrological drought index which uses time series of the monthly flow as the major input. The developing country as Cambodia, the shortage of the streamflow data is the major problem for assessing the hydrological drought. The Greater Baribo basin also meets such problem. Due to the shortage of the streamflow data in the Greater Baribo basin, the prediction of streamflow in this ungauged basin will lead an important role for the hydrological drought assessment in this research. The PUB using the correlation between model parameters and basin properties is employed to predict the streamflow in the Greater Baribo basin. The pictorial description of PUB technique is shown in Figure 4.6. There are six surrounding gauged basins within the Tonle Sap basin. The Greater Baribo basin itself is divided into 9 sub-basins as illustrated Figure 4.7. They are employed to generate the time-series streamflow data in the Greater Baribo basin. There are 19 basin properties parameters which are computed from soil types, land use, basin characteristic and rainfall characteristic of the gauged and ungauged basins as shown in Appendix A.

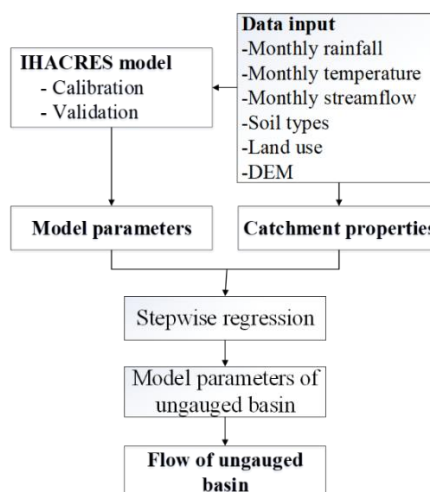


Figure 4.6. Framework for PUB technique

For the rainfall-runoff model, the physical-basin models are not used in this research. Despite the benefit of using such models that is, the use of measurable properties potentially decreases the need for calibration data limitations in the catchment studied here prevent application of physics-based models. The IHACRES is a conceptual-metric rainfall-runoff model which is selected to perform the PUB technique because it has some special features. It is a simple and friendly rainfall-runoff model and has been widely used in tropical region and many basin size (Croke et al., 2004, and Visessri and McIntyre, 2016). It contains only six parameters which is parsimonious for applying the PUB technique. It has been used to predict the model parameters and streamflow data in the ungauged basin in many regions (Post and Jakeman, 1999) including tropical region (Visessri and McIntyre, 2016). It consists of two main components which are the non-linear component (loss) for converting the rainfall to the effective rainfall and the linear component (routing) for transforming the effective rainfall to the streamflow. The non-linear component has three parameters including the volumetric storage coefficient (c), drying rate of catchment (t_w), and temperature modulation of the drying rate (f) while the linear component has other three parameters which are the relative volume of the quick flow response (v_q), the time constant for the quick flow (t_q), and the slow flow (t_s). The general structure of the model is shown in Figure 4.8.

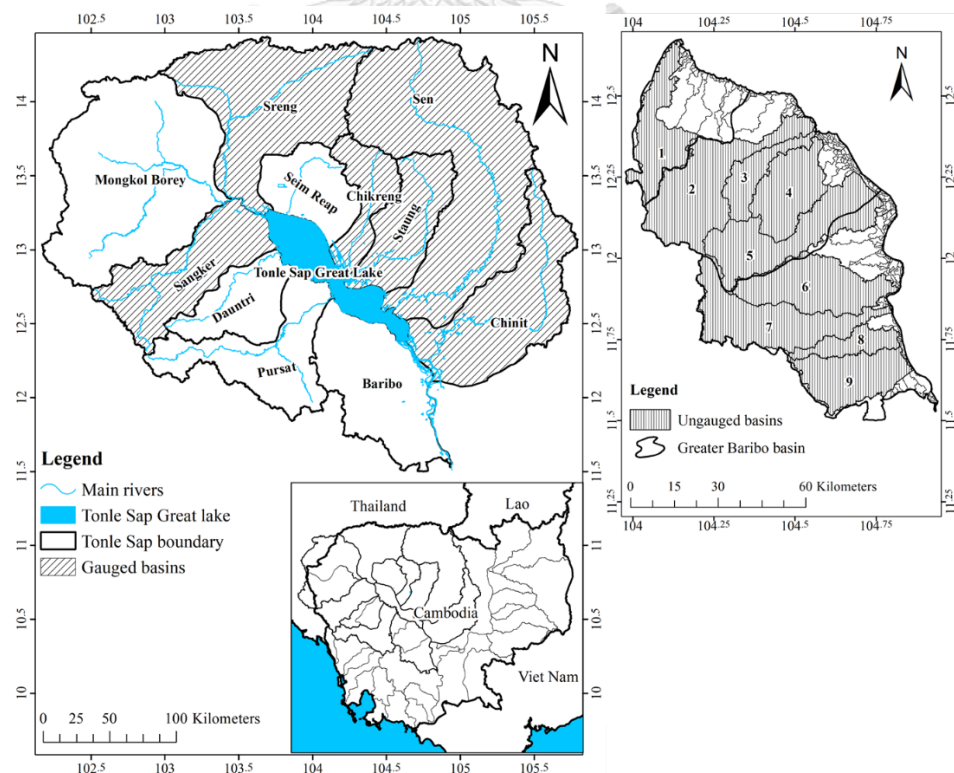


Figure 4.7. Map of the gauged and ungauged basins.

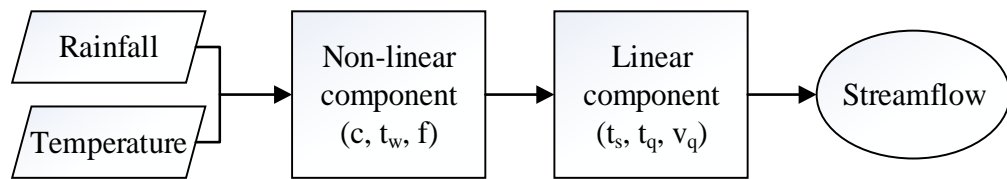


Figure 4.8. General structure of IHACRES model.

The calibration and validation periods were from 2001 to 2003 and 2004 to 2006, accordingly while at 2000 is the warmup period. After that, the relationship between the model's parameters and basin properties are explored using the stepwise regression method from which the equation could be used to estimate the model's parameters of the ungauged basin. The reliability of the regressed model parameters to generate streamflow was firstly tested by calibration and validation at gauged sites. After the calibration and validation at gauged sites were satisfied, the model's parameters of the ungauged basins are estimated, and the streamflow is generated.

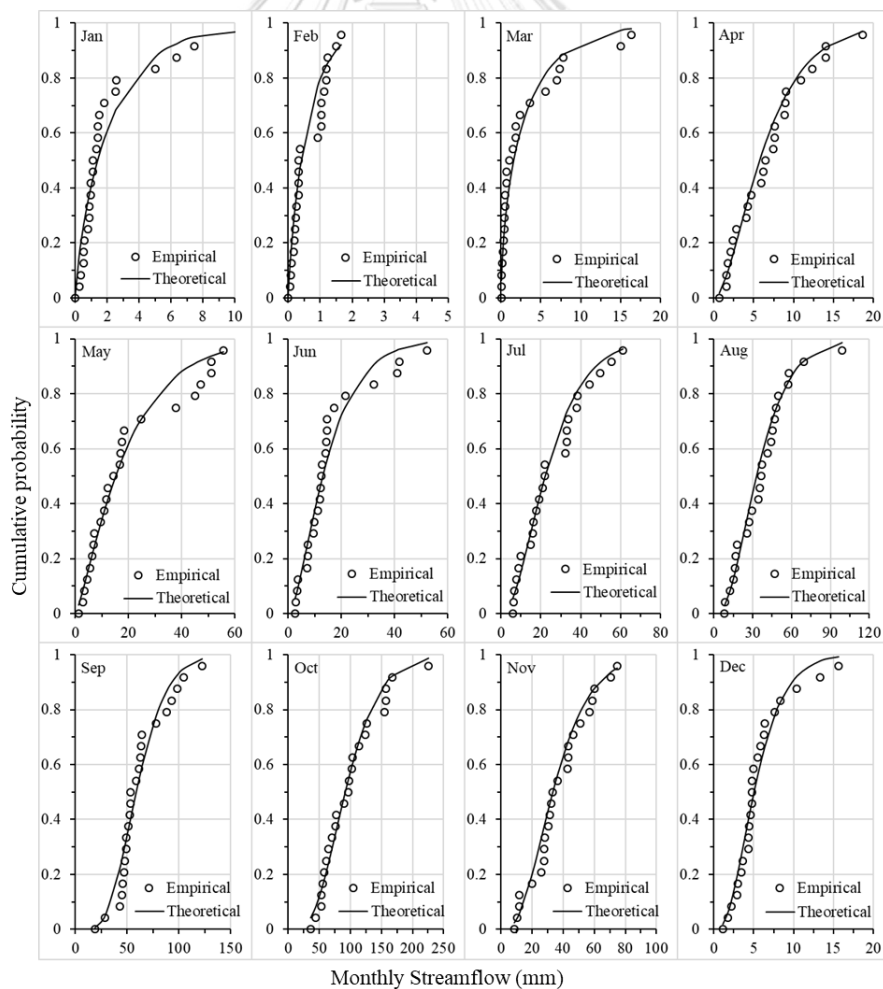


Figure 4.9. Fitting Gamma distribution of each month in sub-basin 1

After applying the prediction of the ungauged basin technique, the streamflow of nine ungauged basins in the Greater Baribo basin are generated allowing the assessment of the hydrological drought index. The calculation of the SDI is analogous with the SPI, yet the inputs are different. Furthermore, Figure 4.9 shows that the streamflow data in the Greater Baribo basin is fit well with Gamma distribution at most of the months. The error mostly found at high streamflow in January, May, and June. However, The Gamma distribution is employed for the calculation of SDI as SPI too. The brief calculation can be found in the section 4.3.1 and the drought classification of the SDI can be illustrated in Table 4.5.

Table 4.5. Drought classification based on the SDI value

SDI value	Description
above 2.0	Extremely Wet (W3)
1.5 to 2.0	Severely Wet (W2)
1.0 to 1.5	Moderately Wet (W1)
0 to -1.0	Near Normal (N)
-1.5 to -1.0	Moderately Drought (D1)
-2.0 to -1.5	Severely Drought (D2)
Below -2	Extremely Drought (D3)

4.2.5 Theory of Runs (ToR)

Theory of Runs (ToR) is a statistical properties of sequences which is applied to define the drought characteristic including drought event (DE), duration (DD), severity (DS) and intensity (DI). It has been explored frequently in the drought assessment by many researches since it helps to make the analysis more understandable (Yevjevich, 1967, Rahmat et al., 2014, and Guo et al., 2017). A DE is a period which the value of drought index is consecutively lower than the critical threshold value. Once drought events can be defined, the drought characteristics can be indicated using ToR. For SPI or SDI, a DE is a period where SPI or SDI values are continuously below 0 with the lowest SPI or SDI value is less than -1. For SVI, a drought event is a period of poor vegetation condition, possibly caused by drought, when SVI is continuously below 0.5 with the lowest value less than 0.25. DD is the number of months in a DE. DS is the absolute value of summation of the index value per drought event (see equation 4.11). DI has two types of definition which DI1 refers to the lowest value

of the index and DI2 is the ratio between DS and DD (see equation 4.12) in a DE. The brief detail of each ToR's property is shown in Figure 4.10.

$$DS = \left| \sum_{i=1}^{DD} X_i \right| \quad \text{Eq. 4.11}$$

$$DI2 = \frac{DS}{DD} \quad \text{Eq. 4.12}$$

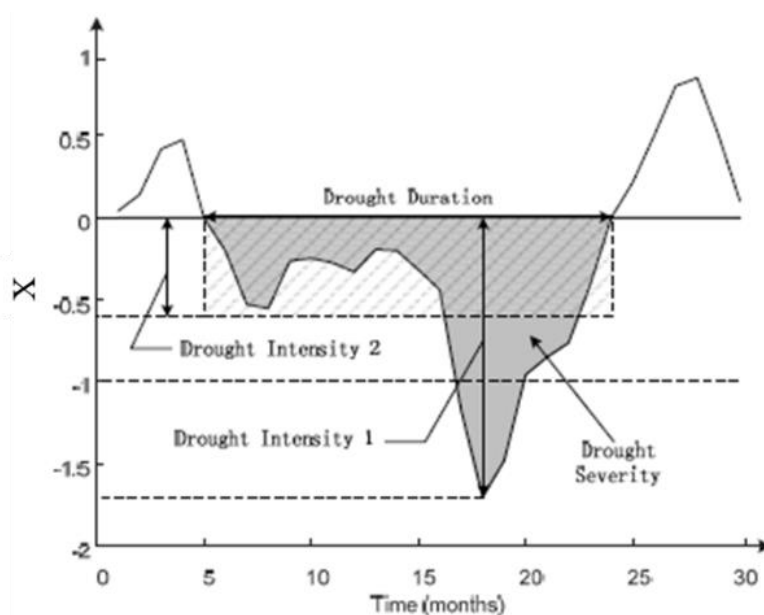


Figure 4.10. Properties of the ToR.

The ToR analysis helps to identify the potential drought event during the study period. Next, the IDW interpolation method is performed for developing drought map and learning about the drought distribution in the Greater Baribo basin. The reason and explanation of IDW method is provided in section 3.3.3.

The detail of methodology for calculating the three selected drought indices is applied to estimate the three types of drought for the Greater Baribo basin and the results are discussed in Chapter 5.

CHAPTER 5

RESULTS AND DISCUSSION

5.1 Meteorological Drought

The meteorological drought was assessed using SPI at five different time-scales i.e. 3-, 6-, 12-, 24-, and 48-month. The five time-scales of SPI were used for different purposes. The SPI at 3-, 6-, and 12-month time-scales (SPI3, SPI6, and SPI12) can be used to evaluate the seasonal and annual variation of rainfall. The 24- and 48-month time-scales (SPI24 and SPI48) can be used to monitor long term variation of rainfall. The SPI value was grouped into seven classification as shown in Table 2.2. The SPI value of the three sub-basins were calculated using the data from 12 rainfall stations. The ToR was used to analyze the drought characteristics. The drought map over the whole Greater Baribo basin was developed by interpolating the values of rainfall from 12 stations inside and nearby by the basin using Inverse Distance Weighted (IDW) technique. The analysis of meteorological drought by SPI is described as in following sections:

5.1.1 Analysis of Meteorological Drought

The value of SPI of the three sub-basins at 3-, 6-, 12-, 24-, and 48-month time-scales shown from Figure 5.1 to Figure 5.5, respectively. The value of SPI normally changed between -3 and 3. There are three graphs in each figure for the Bamnak, Baribo, and Kraing Ponley sub-basins locate in the northern, central and southern parts of the Greater Baribo basin, accordingly. There are three different lines on each graph the solid line (moderate drought), dashed line (severe drought) and dotted line (extreme drought) refer to SPI value of -1, -1.5, and -2, respectively.

It can be drawn from Figure 5.1 to Figure 5.5 that the variation of the SPI decreased with longer time-scale. The SPI3 and SPI6 varied frequently below and above zero while the value of the SPI12, SPI24 and SPI48 changed slower, last longer and less frequent. For the short time-scale, one to three extreme droughts ($SPI \leq -2$) were found in the Bamnak sub-basin but not the Baribo and Kraing Ponley sub-basins. For the long time-scale, the extreme drought did not occur in the three sub-basins. The three sub-basins showed different pattern at all time-scales between 1987 and 1993. For example, the negative values of SPI were frequently found in the Bamnak and Kraing Ponley sub-basins while the Baribo sub-basin showed positive values between 1987 and 1993. The

three sub-basins showed similar pattern from 2001 to 2005 when the SPI was frequently negative.

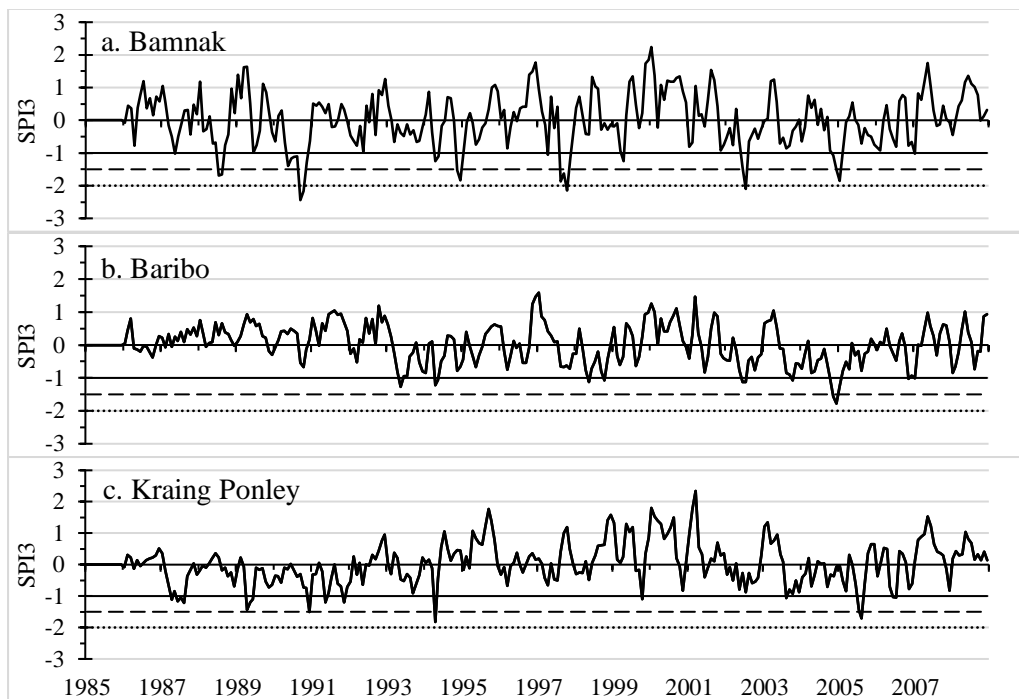


Figure 5.1. SPI3 between 1985 and 2008 of the three sub-basins

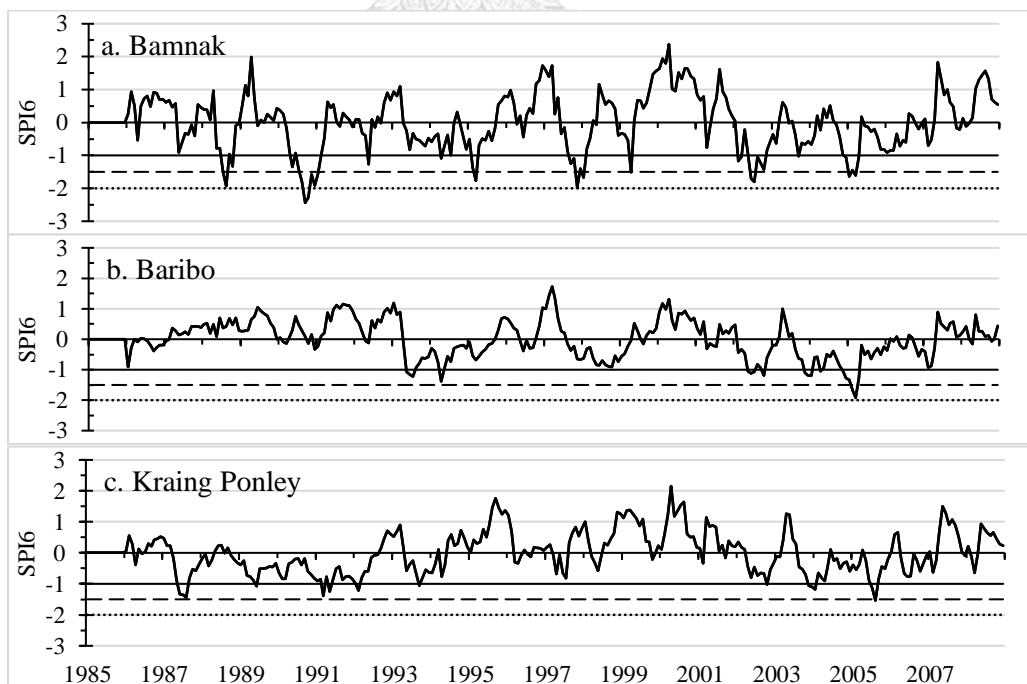


Figure 5.2. SPI6 between 1985 and 2008 of the three sub-basins

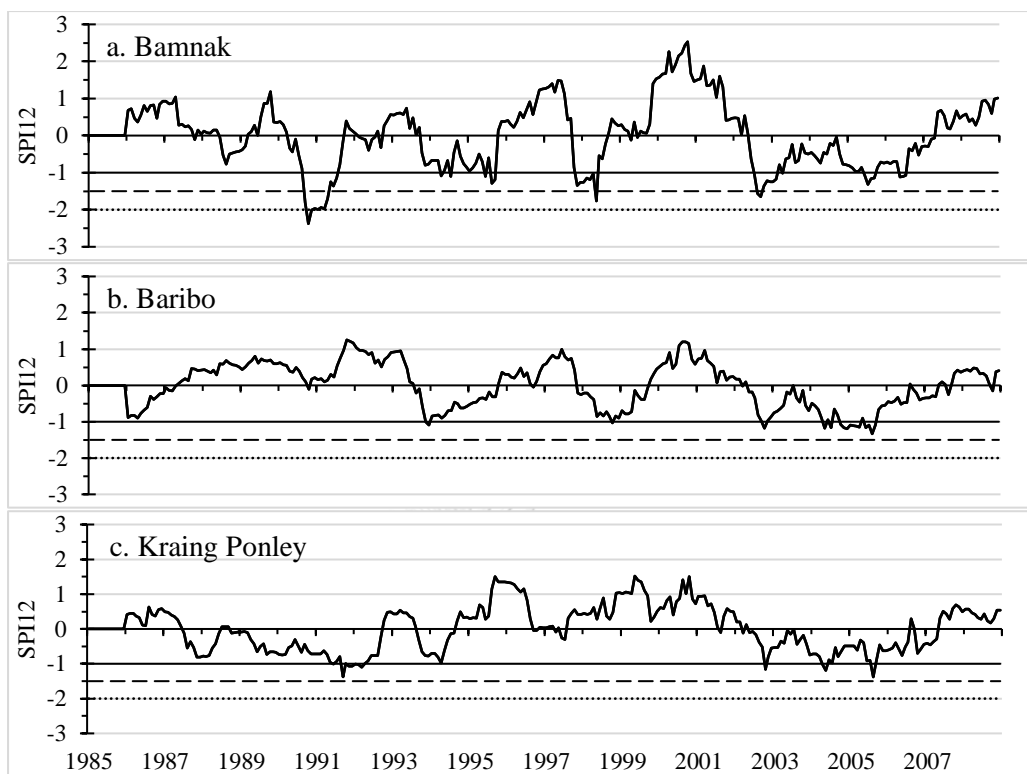


Figure 5.3. SPI12 between 1985 and 2008 of the three sub-basins

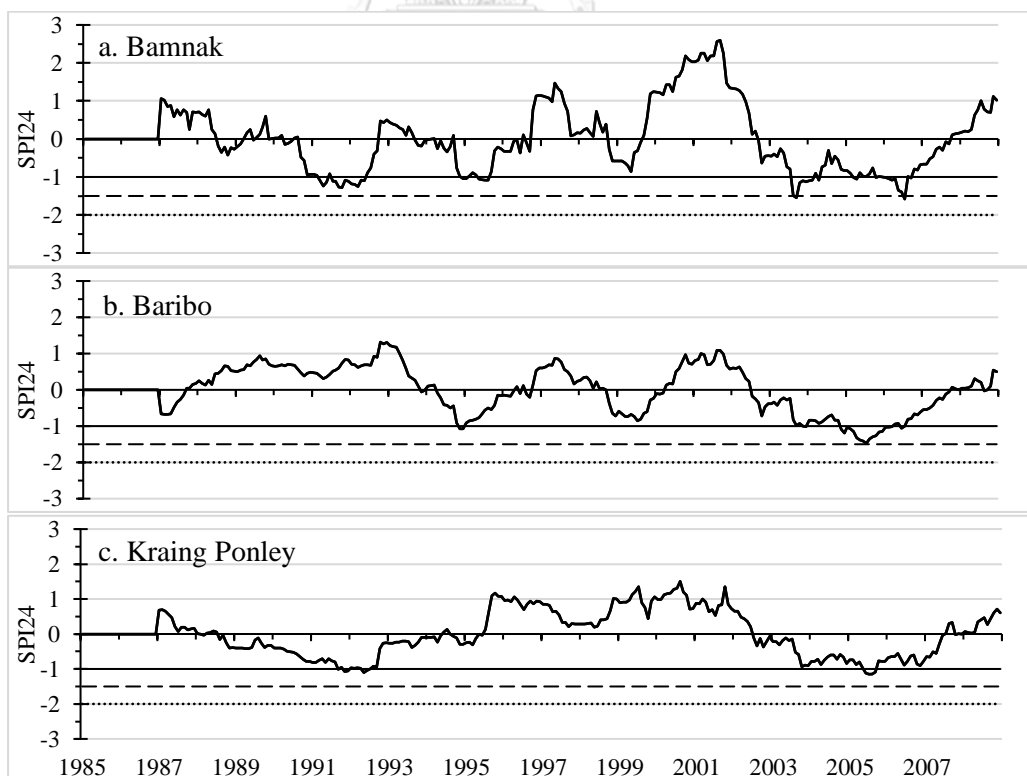


Figure 5.4. SPI24 between 1985 and 2008 of the three sub-basins

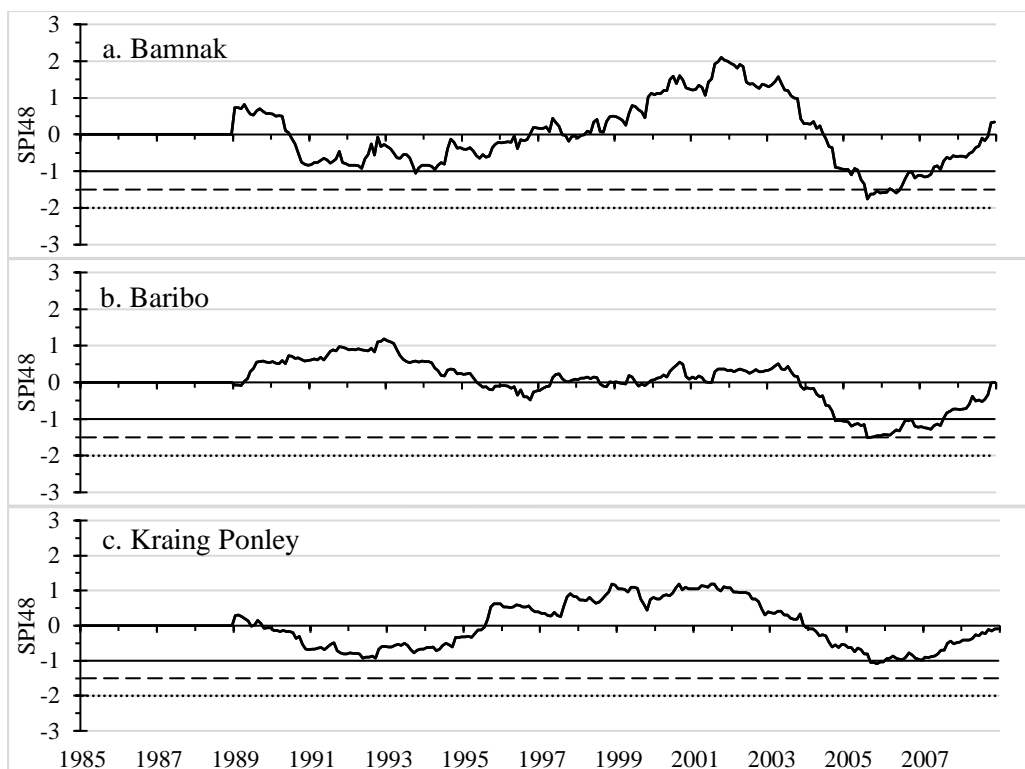


Figure 5.5. SPI48 between 1985 and 2008 of the three sub-basins

5.1.2 Theory of Runs for SPI

Table 5.1 to Table 5.5 show the properties of each DE in terms of DD, DS, DI1, and DI2 at the five time-scales in the three sub-basins using ToR method. The result indicated that the drought occurred more frequently in the Bamnak sub-basin as the DE in the Bamnak sub-basin were greater than the other sub-basins at all time-scales being assessed. For example, the SPI3 showed that there were 11 DEs in the Bamnak sub-basin while there were 7 and 9 DEs in the Baribo and Kraing Ponley sub-basins, respectively.

It was found that the length of DD in the three sub-basins strongly changed from shorter to longer time-scales. The length of DD increased from the north to south of the Greater Baribo basin at SPI3, SPI6, and SPI24. In contrast, the length of DD increased from the south to north at SPI12 and SPI48. For example, the longest length of DD in the Bamnak, Baribo, and Kraing Ponley sub-basins were 9, 13, and 15 months at SPI3 and 59, 51, and 51 months at SPI12, respectively. When considered the DD, the length of DD increased with longer time-scale. For example, the longest length of DD at SPI3 to SPI48 increased from 9 to 75, 13 to 63, and 15 to 70 in the Bamnak, Baribo and Kraing Ponley sub-basins, accordingly.

When considering the DS, the maximum DS value in the three sub-basins increased from the south to north at SPI3, SPI12, and SPI24 of the Greater Baribo basin. It was notable that the maximum DS in the Bamnak sub-basin was higher than other sub-basins at SPI3, SPI12, and SPI24 (12.01, 43.03, and 48.70, accordingly). The Baribo and Kraing Ponley sub-basins were found to have the highest DS at SPI48 (DS = 55.3) and SPI6 (DS = 28.19), accordingly. From SPI3 to SPI48, the maximum DS increased with longer time-scale. The three sub-basins experienced the drought from 1993 to 1994 and 2001 to 2006 with different severity. SPI3 to SPI48 indicated that degree of drought in the three sub-basins became more severe from 2002 to 2006.

In terms of DI1 and DI2, they indicated that the Bamnak sub-basin was impacted by more severe drought than the Baribo and Kraing Ponley sub-basins. For DI1, the extreme DE ($DI1 \geq 2$) occurred in the Bamnak sub-basin triple at SPI3 (DI1 = 2.44, 2.15, and 2.10), once at SPI6 (DI1 = 2.44) and once at SPI12 (DI1 = 2.38). The extreme drought did not occur in other sub-basins except in the Baribo sub-basin at SPI3 (DI1 = 2.10). From SPI3 to SPI48, the highest DI2 was found between 1990 and 1997 in the Bamnak sub-basin and between 2003 and 2006 in the Baribo and Kraing Ponley sub-basins.

According to the analysis of drought characteristics above, the result showed that the DE, DI1 and DI2 at the short time-scale were greater than those of the long time-scale. In contrast to the DE and DI, the DS and DD increased with longer time-scale. Besides, the drought characteristics i.e. DE, DS, and DI in the Bamnak sub-basin were more severe than other sub-basins and the most severe DE was found in 1990. The DI in the Kraing Ponley sub-basin was the lowest but the length of DD was the longest. The investigation of the SPI showed that the Bamnak sub-basin was the most drought prone area since it captured the highest DE, DS, and DI. Moreover, the SPI suggested that the Kraing Ponley sub-basin was also severely impacted by drought since long DD causes higher impact.

Table 5.1. Characteristics of the drought event in the three sub-basins for SPI3

Sub-basin	DE	DD	DS	DI1	DI2
Bamnak	1. Mar-1987 to Jul-1987	5	2.27	1.03	0.45
	2. May-1988 to Oct-1988	6	5.94	1.70	0.99
	3. Apr-1990 to Dec-1990	9	12.01	2.44	1.33
	4. Mar-1994 to Jul-1994	5	2.91	1.25	0.58
	5. Oct-1994 to Feb-1995	5	4.39	1.83	0.88
	6. Mar-1997 to Apr-1997	2	1.20	1.05	0.60
	7. Aug-1997 to Dec-1997	5	7.29	2.15	1.46
	8. Sep-1998 to Apr-1999	8	3.26	1.25	0.41
	9. May-2002 to Jan-2003	9	6.41	2.10	0.71
	10. Oct-2005 to Mar-2006	6	6.37	1.85	1.06
	11. Nov-2006 to Jan-2007	3	2.47	1.02	0.82
Baribo	1. Mar-1993 to Sep-1993	7	4.82	1.27	0.69
	2. Apr-1994 to Jul-1994	4	3.10	1.22	0.78
	3. Mar-1998 to Nov-1998	9	5.73	1.13	0.64
	4. Apr-2002 to Dec-2002	9	5.43	2.10	0.60
	5. Jun-2003 to Feb 2004	9	5.15	1.08	0.57
	6. Mar-2004 to Apr 2005	13	10.77	1.78	0.83
	7. Oct-2006 to Jan 2007	4	3.03	1.03	0.76
Kraing Ponley	1. Feb-1987 to Oct-1987	9	6.77	1.22	0.75
	2. Mar-1989 to May-1990	15	7.62	1.43	0.51
	3. Jul-1990 to Feb-1991	8	4.45	1.50	0.56
	4. Apr-1991 to Jan-1992	10	6.49	1.20	0.65
	5. Mar-1994 to May-1994	3	2.37	1.82	0.79
	6. Aug-1999 to Oct 1999	3	1.47	1.10	0.49
	7. Aug-2003 to Feb-2004	7	4.84	1.07	0.69
	8. Jun-2005 to Sep 2005	4	4.38	1.71	1.10
	9. May 2006 to Jul 2006	3	2.78	1.05	0.93

Table 5.2. Characteristics of the drought event in the three sub-basins for SPI6

Sub-basin	DE	DD	DS	DI1	DI2
Bamnak	1. May-1988 to Dec 1998	8	7.43	1.94	0.93
	2. Mar-1990 to Mar-1991	13	17.83	2.44	1.37
	3. Apr-1992 to Jun-1992	3	1.99	1.26	0.66
	4. Apr-1993 to Aug-1994	17	8.82	1.09	0.52
	5. Oct-1994 to Sep-1995	12	7.70	1.76	0.64
	6. Jun-1997 to Mar-1998	10	10.06	1.96	1.01
	7. Dec-1998 to Apr-1999	5	3.12	1.51	0.62
	8. Feb-2002 to Feb-2003	13	12.99	1.80	1.00
	9. Aug-2003 to Feb-2004	7	4.32	1.03	0.62
	10. Sep-2004 to Jul-2006	14	7.62	1.65	0.54
Baribo	1. Apr-1993 to Sep-1995	30	16.35	1.39	0.55
	2. Feb-2002 to Feb-2003	13	8.80	1.19	0.68
	3. Aug-2003 to Jan-2006	30	23.26	1.92	0.78
Kraing Ponley	1. Apr-1987 to Apr-1988	13	8.35	1.43	0.64
	2. Oct-1988 to Aug-1992	47	28.19	1.39	0.60
	3. May-1993 to Feb-1994	10	5.91	1.07	0.59
	4. Apr-2002 to Feb-2003	11	5.91	1.02	0.54
	5. Aug-2003 to May-2004	10	7.86	1.18	0.79
	6. May-2005 to Dec-2005	8	5.77	1.54	0.72

Table 5.3. Characteristics of the drought event in the three sub-basins for SPI12

Sub-basin	DE	DD	DS	DI1	DI2
Bamnak	1. Apr-1990 to Sep-1991	18	22.76	2.38	1.26
	2. Oct-1993 to Sep-1992	24	18.58	1.29	0.77
	3. Oct-1997 to Aug-1998	11	11.24	1.76	1.02
	4. Jun-2002 to Apr-2007	59	43.03	1.65	0.73
Baribo	1. Aug-1993 to Sep-1995	26	14.73	1.09	0.57
	2. Nov-1997 to Sep-1999	23	12.67	1.04	0.55
	3. May-2002 to Jul-2006	51	36.63	1.19	0.72
Kraing	1. Oct-1988 to Sep-1992	48	31.41	1.37	0.65
Ponley	2. May-2002 to Jul-2006	51	29.10	1.38	0.57

Table 5.4. Characteristics of the drought event in the three sub-basins for SPI24

Sub-basin	DE	DD	DS	DI1	DI2
Bamnak	1. Sep-1990 to Sep-1992	25	24.32	1.28	0.97
	2. Oct-1994 to Jun-1996	21	14.02	1.09	0.67
	3. Sep-2002 to Sep-2007	61	48.70	1.54	0.80
Baribo	1. Apr-1994 to Apr-1996	25	12.83	1.08	0.51
	2. Jul-2002 to Sep-2007	63	48.42	1.48	0.77
Kraing	1. Aug-1988 to May-1994	70	35.31	1.10	0.50
Ponley	2. Jul-2002 to Jun-2007	60	37.36	1.15	0.62

Table 5.5. Characteristics of the drought event in the three sub-basins for SPI48

Sub-basin	DE	DD	DS	DI1	DI2
Bamnak	1. Jul-1990 to Sep-1996	75	41.18	1.05	0.55
	2. Jul-2004 to Oct-2008	52	49.49	1.76	0.95
Baribo	1. Nov-2003 to Dec-2008	62	55.30	1.50	0.89
Kraing Ponley	1. Dec-2003 to Dec-2008	61	36.95	1.09	0.61

5.2 Agricultural Drought Index

The agricultural drought was assessed using SVI at five different time-scales i.e. 3-, 6-, 12-, 24-, and 48-month. The SVI value was grouped into five classes with different condition for good or poor of the vegetation as illustrated in Table 4.4. The SVI was calculated as grid value with the resolution of $0.05^\circ \times 0.05^\circ$. The value of SVI of the three sub-basins were demonstrated by averaging the value of each grid in the same sub-basin. The ToR was used to analyze the vegetation characteristics over the period of study for the three sub-basins. The analysis of the vegetation condition by SVI is described in the following sections:

5.2.1 Analysis of Agricultural Drought

The values of SVI at 3-, 6-, 12-, 24- and 48-month time-scales (SVI3, SVI6, SVI12, SVI24 and SVI48) are illustrated from Figure 5.6 to Figure 5.10, respectively. There are three graphs in each figure for the Bamnak, Baribo, and Kraing Ponley sub-basins locate in the northern, central and southern parts of the Greater Baribo basin, accordingly. In each graph, there are three different lines, solid line ($0.5 \geq SVI > 0.25$), dashed line ($0.25 \geq SVI > 0.05$) and dotted line ($0.05 \geq SVI$) that refer to near normal,

poor and very poor condition of the vegetation, respectively. The SVI value can range between 0 and 1. One of the most important notification of the SVI is that the drought is not the only reason but also the flood, crop rotation, and unseasonal coolness (snow region only) which lead to poor vegetation condition.

The result showed that the pattern of the vegetation condition of the three sub-basins were similar, but they were slightly different in intensity. The short time-scale analysis (Figure 5.6 to Figure 5.8) showed that the very poor condition of vegetation was found in the Baribo and Kraing Ponley sub-basins. The very poor condition of the vegetation did not occur in the Bamnak sub-basin. Furthermore, the three sub-basins experienced the poor condition of vegetation at the same period while the vegetation between 2004 and 2006 was less severe than the previous events. The long time-scale (Figure 5.9 and Figure 5.10) indicated that the vegetation in the Baribo sub-basin was poorer than other sub-basins. Since the very poor condition of the vegetation captured at all time-scales in the Baribo sub-basin but did not in the Bamnak and Kraing Ponley sub-basins.

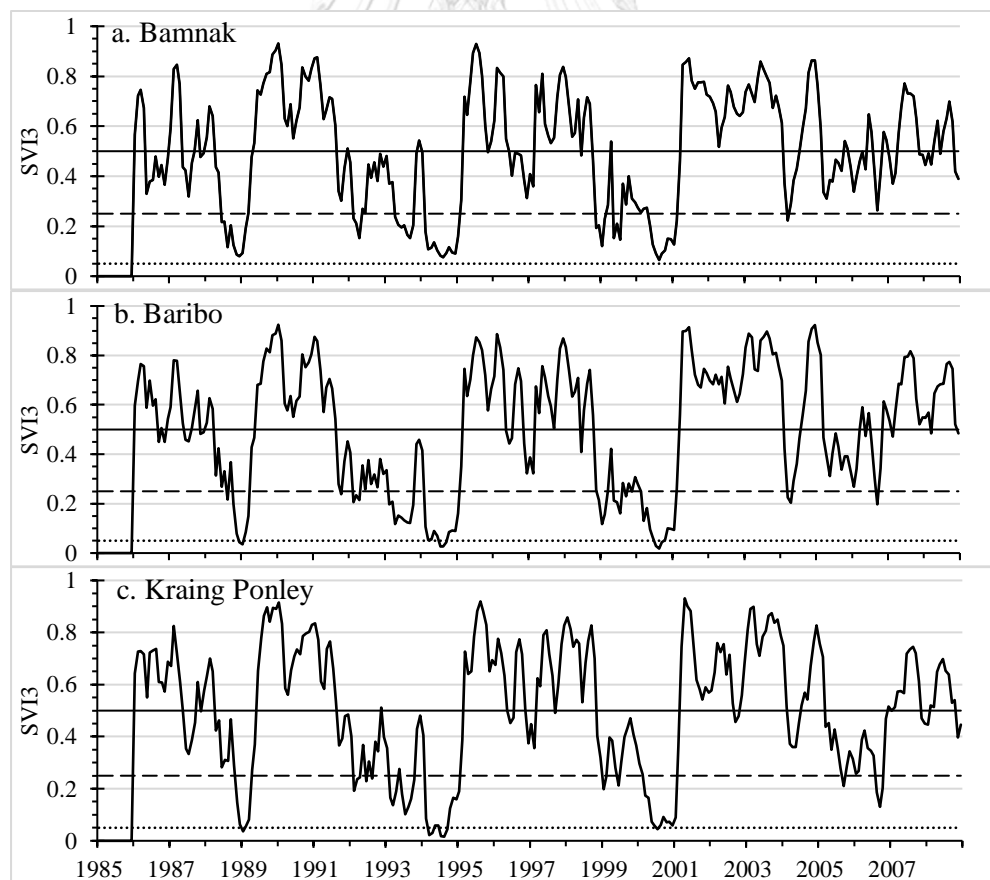


Figure 5.6. SVI3 between 1985 and 2008 of the three sub-basins

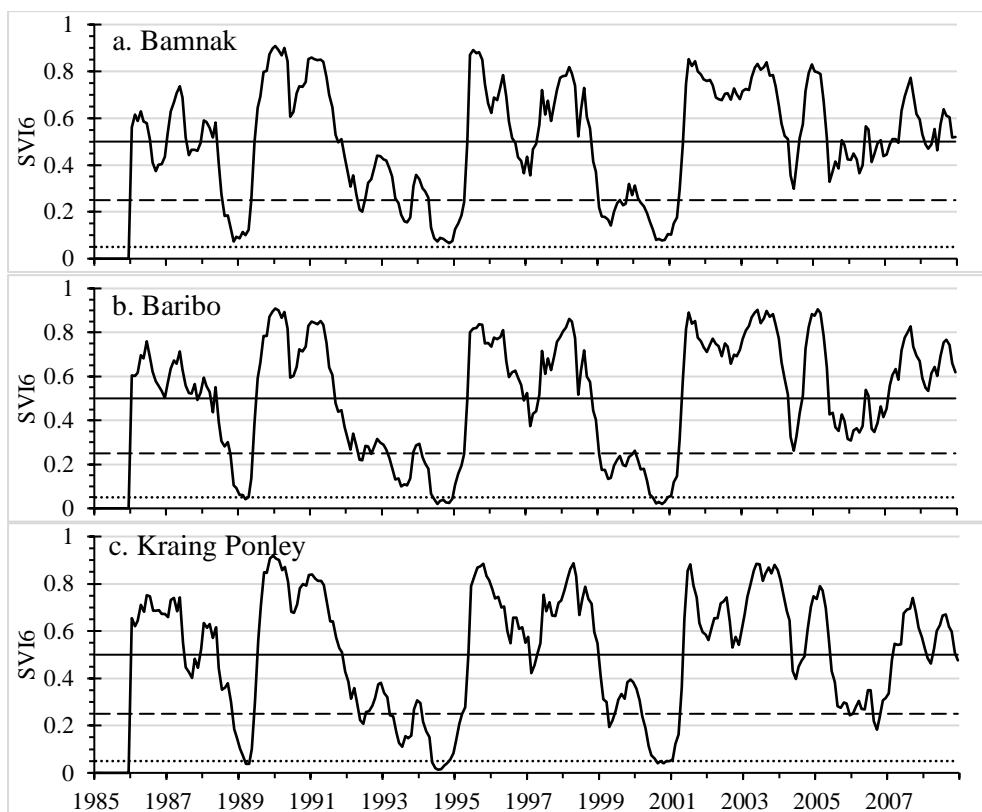


Figure 5.7. SVI6 between 1985 and 2008 of the three sub-basins

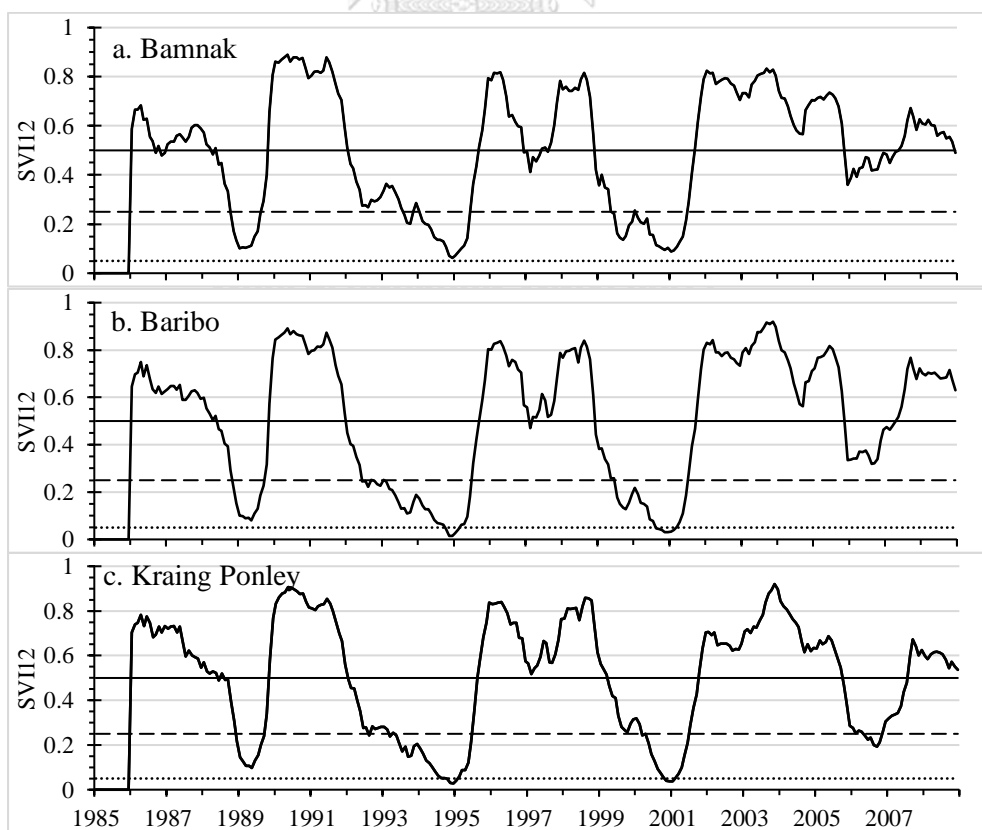


Figure 5.8. SVI12 between 1985 and 2008 of the three sub-basins

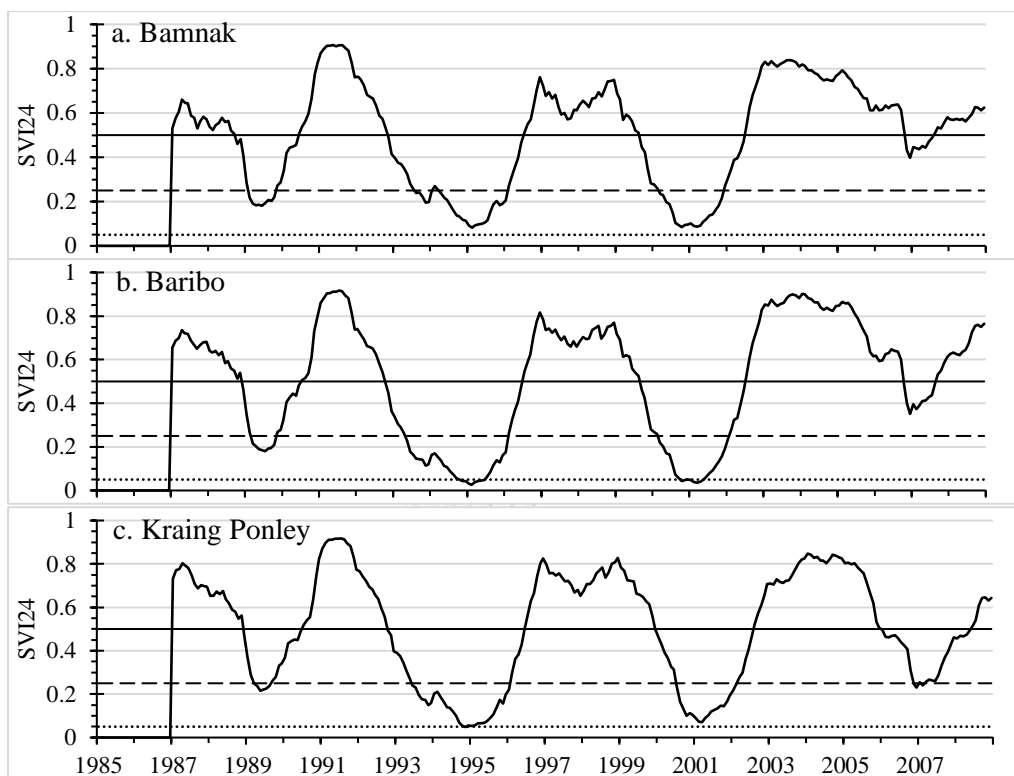


Figure 5.9. SVI24 between 1985 and 2008 of the three sub-basins

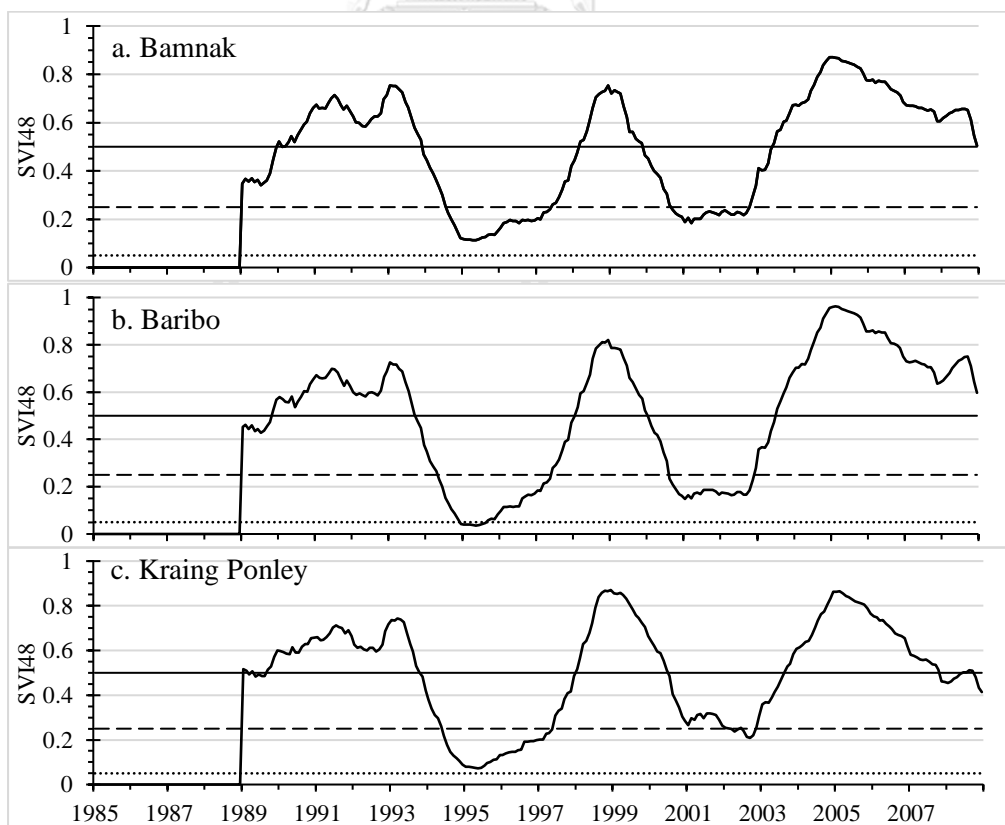


Figure 5.10. SVI48 between 1985 and 2008 of the three sub-basins

5.2.2 Theory of Runs for SVI

Figure 5.6 to Figure 5.10 show the properties of each DE in terms of DD, DS, DI1, and DI2 at the five time-scales in the three sub-basins using ToR method. The result indicated that the number DE of the three sub-basins at all time-scales was comparable to each other. Furthermore, the DE did not strongly change from time-scale to time-scale. For example, SVI3 showed that there were 6, 5 and 5 DEs in the Bamnak, Baribo and Kraing Ponley sub-basins, accordingly. The number of DE in the three sub-basins did not change between SVI6 and SVI24.

In the case of DD, the three sub-basins showed similar duration and it increased slightly from shorter to longer time-scales. The Baribo sub-basin normally experienced longer DD than the other sub-basins. The longest length of DD in the Baribo sub-basin (DD = 42) occurred about two times longer than the Bamnak (DD = 23) and Kraing Ponley (DD = 28) sub-basins at SVI3 while at the rest time-scales, it took about one to three months longer. The short time-scale analysis indicated that the three sub-basins experienced the longest DD between 1991 and 1995. At long time-scale, the longest DD was found between 1992 and 1998.

Regarding the DS, the result indicated that the maximum and minimum of DS occurred in the three sub-basins at different time-scale. The maximum of DS captured in the Bamnak sub-basin at SVI6, SVI12, and SVI48 (DS = 10.85, 10.47, and 11.91, accordingly), Baribo sub-basin at SVI3 (DS = 9.25), and Kraing Ponley sub-basin at SVI24 (DS = 11.06). The minimum of DS occurred in the Baribo sub-basin at SVI3, SVI6, SVI24, and SVI48 (DS = 1.3, 2.46, 5.71, and 9.74, respectively) and the Kraing Ponley sub-basin at SVI12 (DS = 3.55). The low value of DS indicates the poor condition of the vegetation. Thus, the DS suggested that the vegetation in the Baribo sub-basin was the poorest since the minimum DS of SVI occurred in the Baribo sub-basin at most time-scales.

When considering the DI, the result showed that the DI1 value of the three sub-basins were slightly different from each other. The Bamnak sub-basin experienced less severe vegetation condition than the Baribo and Kraing Ponley sub-basins. The very poor ($DI1 \leq 0.05$) condition of the vegetation was not found in the Bamnak sub-basin while it was found in other sub-basins. However, the DI1 in the Bamnak sub-basin also ranged next to the very poor condition of the vegetation. The poor ($0.25 \leq DI1 \leq 0.05$) and very poor condition of vegetation in the three sub-basins occurred at the same period. The poor condition of the vegetation of the three sub-basins between 2004 and 2006 was less

severe than the previous events. Furthermore, the DI2 in the Baribo sub-basin was lower than other sub-basins at the five time-scales. The DI clearly showed that the Baribo sub-basin had the poorest vegetation condition.

Overall, the three sub-basins showed similar characteristics of the vegetation. The poor condition of vegetation based on SVI can be caused either by flood or drought. The poor condition of vegetation from 1988 to 1989, 1992 to 1994, 1998 to 1999 and 2004 to 2006 were believed to be due to drought as the low values of SVI in these periods match with the negative value of the SPI. The poor condition of vegetation in 2000 was possibly impacted by flood as positive value of the SPI was found in this period. For short time-scales, the DE was greater than those of long time-scales but not DS and DD.

Table 5.6. Characteristic of the vegetation in the three sub-basins for SVI3

Sub-basin	DE	DD	DS	DI1	DI2
Bamnak	1. Apr-1988 to Apr-1989	13	2.91	0.08	0.22
	2. Sep-1991 to Jan-1993	23	7.26	0.15	0.32
	3. Jan-1994 to Feb-1995	14	2.15	0.08	0.15
	4. Oct-1998 to Mar-1999	6	1.50	0.12	0.25
	5. May-1999 to Mar-2001	23	5.03	0.06	0.22
	6. Feb-2004 to Jul-2004	6	2.20	0.22	0.37
Baribo	1. Apr-1988 to May-1989	14	3.41	0.04	0.24
	2. Sep-1991 to Feb-1995	42	9.25	0.03	0.22
	3. Nov-1998 to Feb-2001	28	5.04	0.02	0.18
	4. Feb-2004 to Jul-2004	6	1.97	0.20	0.33
	5. Jul-2006 to Oct-2006	4	1.30	0.20	0.33
Kraing Ponley	1. Apr-1988 to May-1989	14	3.57	0.04	0.26
	2. Sep-1991 to Oct-1992	14	4.66	0.23	0.33
	3. Nov-1992 to Feb-1995	27	5.00	0.02	0.19
	4. Nov-1998 to Feb-2001	28	6.70	0.05	0.24
	5. Mar-2005 to Nov-2006	21	6.81	0.13	0.32

Table 5.7. Characteristic of the vegetation in the three sub-basins for SVI12

Sub-basin	DE	DD	DS	DI1	DI2
Bamnak	1. Jun-1988 to Oct-1989	17	3.93	0.10	0.23
	2. Feb-1992 to Aug-1995	43	10.47	0.06	0.24
	3. Dec-1998 to Aug-2001	33	6.78	0.09	0.21
Baribo	1. Jun-1988 to Oct-1989	17	3.81	0.08	0.22
	2. Jan-1992 to Sep-1999	45	8.42	0.02	0.19
	3. Dec-1998 to Sep-2001	34	6.16	0.03	0.18
Kraing Ponley	1. Aug-1988 to Oct-1989	15	3.55	0.10	0.24
	2. Jan-1992 to Jul-1995	43	8.63	0.03	0.20
	3. Apr-1999 to Sep-2001	30	6.65	0.04	0.22
	4. Oct-2005 to Jul-2007	22	6.68	0.19	0.30

Table 5.8. Characteristic of the vegetation in the three sub-basins for SVI24

Sub-basin	DE	DD	DS	DI1	DI2
Bamnak	1. Oct-1988 to May-1990	20	6.08	0.18	0.30
	2. Nov-1992 to Jun-1996	44	10.25	0.08	0.23
	3. Sep-1999 to Jun-2002	34	7.55	0.09	0.22
Baribo	1. Dec-1988 to Jun-1990	19	5.71	0.18	0.30
	2. Dec-1992 to Jun-1996	45	7.87	0.03	0.17
	3. Sep-1999 to Jun-2002	34	6.26	0.04	0.18
Kraing Ponley	1. Dec-1988 to Jun-1990	19	6.35	0.21	0.33
	2. Dec-1992 to Jun-1996	45	9.30	0.05	0.21
	3. Jan-2000 to Jul-2002	31	6.86	0.07	0.22
	4. Jan-2006 to May-2008	29	11.06	0.23	0.38

Table 5.9. Characteristic of the vegetation in the three sub-basins for SVI48

Sub-basin	DE	DD	DS	DI1	DI2
Bamnak	1. Dec-1993 to Feb-1998	51	11.91	0.11	0.23
	2. Dec-1999 to May-2003	42	11.85	0.18	0.28
Baribo	1. Oct-1993 to Jan-1998	52	9.74	0.04	0.19
	2. Jan-2000 to Jun-2003	42	10.49	0.15	0.25
Kraing	1. Nov-1993 to Dec-1997	50	10.33	0.07	0.21
Ponley	2. Jul-2000 to Jul-2003	37	11.53	0.21	0.31

5.3 Hydrological Drought

Streamflow Drought Index (SDI) is a standardized hydrological drought index which uses the time-series streamflow data as the main input. Due to scarcity of the streamflow data, the Prediction in Ungauged Basin (PUB) was applied in the Greater Baribo basin. The six gauged basins (Chikreng, Chinit, Sangker, Sen, Sreng and Staung basins) around the Tonle Sap basin were employed to generate the streamflow data in the Greater Baribo basin. The hydrological drought was assessed using SDI at five different time-scales i.e. 3-, 6-, 12-, 24-, and 48-month. The SDI value was grouped into seven classes with different severities of the drought or wet condition as illustrated in Table 4.5. The SDI value of the three sub-basins were estimated by averaging the ungauged basins which located in the same sub-basin. The ToR was used to analyze the drought characteristics. The drought map was developed using the value of each ungauged basin. The analysis of hydrological drought by SDI is described as in the following sections:

5.3.1 Prediction in Ungauged Basin (PUB)

The Greater Baribo basin can be considered as ungauged basin consisting of nine sub-basins as shown in Figure 4.7. There are 19 parameters of basin properties computed from land use, soil types, basin size, elevation, and rainfall (see Appendix A) and used as independent variables to regress with the IHACRES model parameters. The IHACRES, conceptual-metric rainfall-runoff model, was employed to simulate streamflow in the six gauged basins. The calibration period was from 2001 to 2003 and validation period was from 2004 to 2006. Both automatic and manual calibrations were used. First, the possible range of each parameter was set in the model. Then, the automatic calibration was employed to fit between observed and simulated streamflow. After that, the logical between the model parameters from the calibration and basin characteristics were checked. Finally, the manual calibration was performed to check any error between the observed and simulated streamflow which automatic calibration is not able to address. The simulated streamflow in 2000 was treated as the warm up period. The graph between the observed and simulated streamflow is illustrated in Appendix B. The values of the IHACRES model parameters obtained from the gauged basins were transferred to the ungauged basins.

Figure 5.11 and Figure 5.12 show the scatter plot of six gauged basins comparing the observed and simulated streamflow for the calibration and validation periods, accordingly. For the calibration (Figure 5.11), the scatter plot showed a good

agreement between the observed and simulated streamflow in Chikreng and Chinit basins. For Sangker, Sen, Sreng and basins, the model underestimated at high streamflow while for the Staung basin, the model overestimated at high streamflow. For the validation (Figure 5.12), the scatter plot showed very good agreement between the observed and simulated streamflow in the Chikreng and Sen basins. The model showed some overestimations in the Chinit and Staung basin but underestimation at high streamflow in the Sangker and Sreng and basins.

The coefficient of determine (R^2) and Nash Sutcliffe Efficiency (NSE) were chosen to test the performance of the IHACRES model. Table 5.10 illustrates the performance of the model calibration and validation. The R^2 and NSE of the model calibration and validation of six gauged basins mostly satisfied. For the Sangker basin, the R^2 and NSE of the validation and calibration ranged between 0.46 and 0.47. The R^2 and NSE in the Sangker basin were low. This can be caused by that the number of rainfall stations are only three and not well distributed (see Figure 3.1). For Chikreng basin, the R^2 and NSE value of the validation was 0.62 and 0.42, accordingly. NSE of validation in the Chikreng basin was low which can be caused by the high variation of monthly flow in 2002 which was particularly high. The obtained R^2 and NSE of gauged basins were acceptable for simulating streamflow in the gauged basins.

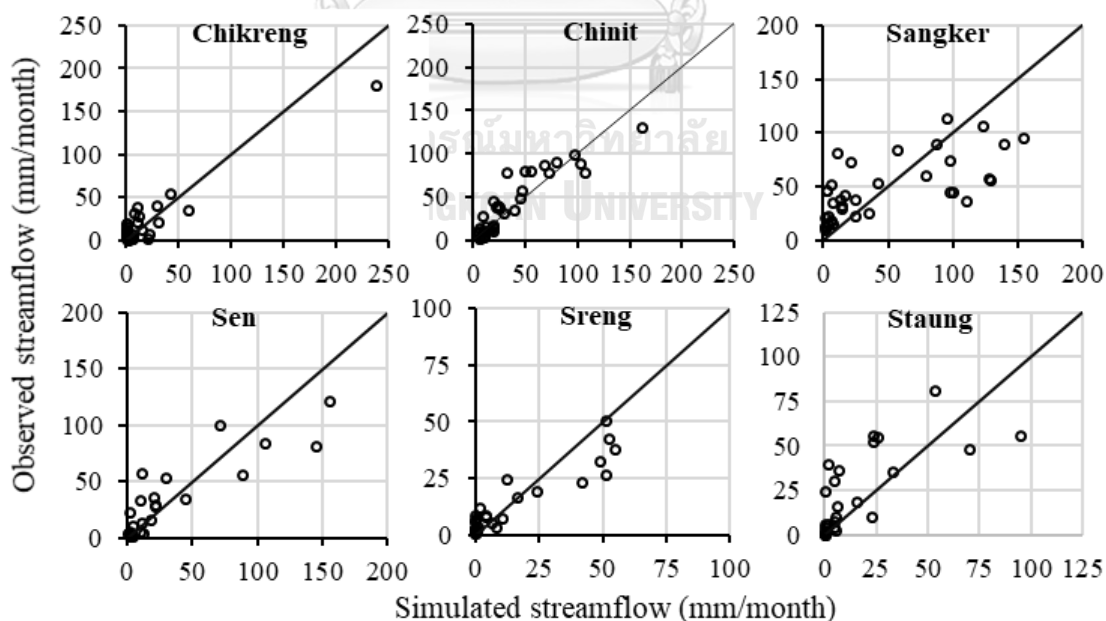


Figure 5.11. Scatter plot of observed and simulated streamflow for calibration

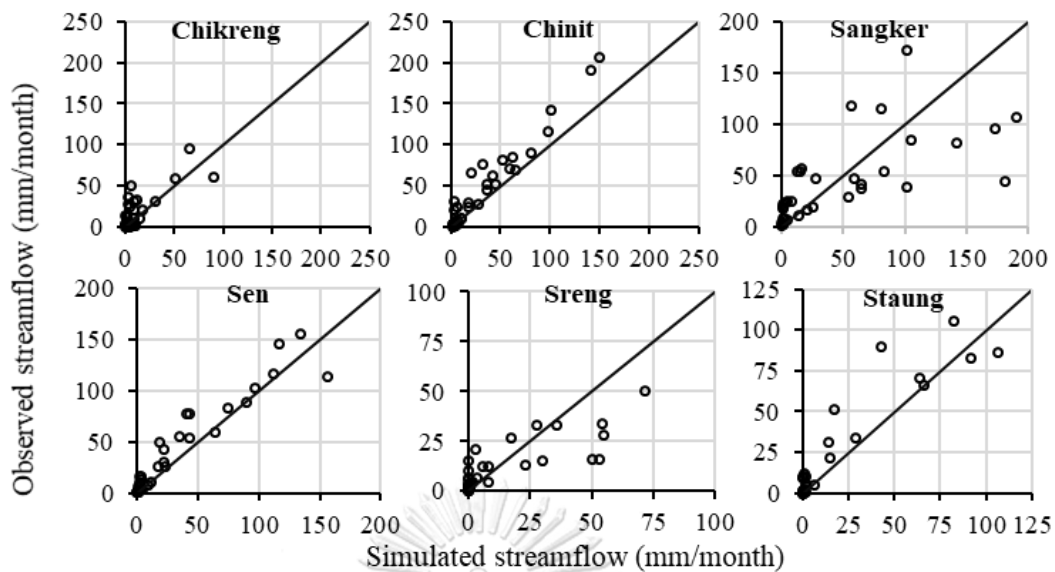


Figure 5.12. Scatter plot of observed and simulated streamflow for validation

Table 5.10. Performance of the model calibration and validation

Basin Name	Calibrated		Validated	
	NSE	R ²	NSE	R ²
Chikreng	0.86	0.89	0.42	0.62
Chinit	0.82	0.83	0.72	0.95
Sangker	0.46	0.47	0.46	0.46
Sen	0.75	0.77	0.88	0.92
Sreng	0.82	0.87	0.63	0.69
Staung	0.75	0.79	0.88	0.90

Six parameters of the model at six gauged basins can be seen in Table 5.11. The model parameters, c , t_w , f , t_q , t_s , and v_s , varied from 0.0004 to 0.0023, 10.33 to 102.43, 3.10 to 13.80, 2.27 to 5.10, 31.90 to 15.61, and 0.26 to 0.79, respectively.

Table 5.11. Six model parameters of six gauged basins from the calibration

Basin Name	c	t_w	f	t_q	t_s	v_s
Chikreng	0.0018	10.33	6.00	3.33	25.00	0.37
Chinit	0.0013	56.63	4.25	4.99	30.00	0.79
Sangker	0.0018	102.34	3.10	2.27	31.90	0.57
Sen	0.0021	30.81	11.22	5.00	27.00	0.76
Sreng	0.0004	70.00	13.80	3.34	23.00	0.78
Staung	0.0023	17.47	3.96	5.10	15.61	0.26

After calibrating and validating the IHACRES model at six gauged basins, the stepwise regression between model parameters and basin properties was developed to generate the streamflow data for assessing the hydrological drought in the Greater Baribo basin. The applicability of the obtained regression was evaluated by considering if the relationships between the model parameters and significant basin properties agree with physical hydrologic processes. For example, in Table 5.12, c is the volumetric storage coefficient which is the loss parameter of the model, and it has a positive and negative correlation with the forest and minimum rainfall in the wet month (Wet Month Rainfall (min)), respectively. The correlation fits with physical process. The basin with high forest coverage can lead to high loss due to high interception, infiltration and evapotranspiration. The six regressive equations of model parameters and basin properties can be found from equation 5.1 to 5.6.

$$c = 0.72 \times \text{Forest} - 0.82 \times \text{Wet Month Rainfall (min)} \quad \text{Eq. 5.1}$$

$$t_w = 0.63 \times \text{Grassland} + 0.46 \times \text{Loamy} \quad \text{Eq. 5.2}$$

$$f = 1.87 \times \text{Basin Size} - 1.21 \times \text{River Length} \quad \text{Eq. 5.3}$$

$$t_q = 1.24 \times \text{Forest} - 0.47 \times \text{Clay} \quad \text{Eq. 5.4}$$

$$t_s = 0.88 \times \text{Grassland} \quad \text{Eq. 5.5}$$

$$v_q = 0.74 \times \text{River Length} + 0.43 \times \text{Wet Month Rainfall (min)} \quad \text{Eq. 5.6}$$

R^2 of basin properties and model parameters: c , t_w , f , t_q , t_s , and v_s are shown in Table 5.12. The value of model parameters of six gauged basins by the stepwise regression are detailed in Table 5.13. The coefficient of R^2 and NSE ranged from 0.45 to 0.94 and 0.40 to 0.89, respectively, as illustrated in Table 5.14. The R^2 and NSE of model parameters from the calibration and regression were comparable to each other. The regressive equations can sufficiently be used to generate the model parameters and streamflow data of the ungauged basin. Furthermore, the hydrograph between the observed and simulated streamflow of model parameters from the stepwise regression of six gauged basins were illustrated in Appendix C.

Table 5.12. Correlation between the model and basin properties parameters

Model Parameters	Basin Parameters	Coefficients	R ² of Regression
c	Forest	0.72	1.00
	Wet Month Rainfall (min)	-0.82	
t_w	Grassland	0.63	0.96
	Loamy	0.46	
f	Basin Size	1.87	0.90
	River Length	-1.21	
t_q	Forest	1.24	0.85
	Clay	-0.47	
t_s	Grassland	0.88	0.78
v_s	River Length	0.74	0.80
	Wet Month Rainfall (min)	0.43	

Table 5.13. Six model parameters of six gauged basins from the regression

Basin Name	c	t_w	f	t_q	t_s	v_s
Chikreng	0.0018	11.04	6.19	3.69	21.72	0.39
Chinit	0.0012	51.18	2.70	4.38	28.60	0.76
Sangker	0.0018	101.84	3.65	2.78	33.00	0.43
Sen	0.0021	43.59	12.48	5.22	24.69	0.85
Sreng	0.0005	67.45	11.93	2.81	26.07	0.69
Staung	0.0023	12.50	5.38	5.15	18.42	0.38

After developing the regressive equations between model parameters and basin properties, model parameters of the ungauged basins were identified as shown in Table 5.15. The result illustrated that model parameters of nine ungauged sub-basins in the Greater Baribo basin were in acceptable range except the *c* parameter of the sub-basin 8 and the *t_q* parameter of the sub-basin 8 and 9, which were out of the possible range. The percentage of the forest of the sub-basin 8 and 9 are 19.7% and 30.0%, respectively, while the forest percentage of other ungauged sub-basins range between 55.0% and 87.5% (see Appendix A). Invalid parameter values were believed to be caused by too low percentage of forest to be represented by the regression. The sub-basin 8 and 9 were then

excluded streamflow prediction for ungauged basins. The sub-basin 1 to 7 are able to use regressive equations to generate model parameters and thus streamflow. The hydrographs of ungauged sub-basins are provided in Appendix D. After generated the streamflow data by PUB technique, the analysis of the hydrological drought using the Streamflow Drought Index (SDI) was performed as detailed in the following sections:

Table 5.14. Performance of model calibration and validation of the model parameters from the regression

Basin name	Calibrated		Validated	
	NSE	R ²	NSE	R ²
Chikreng	0.86	0.89	0.40	0.64
Chinit	0.81	0.81	0.86	0.94
Sangker	0.44	0.45	0.44	0.45
Sen	0.74	0.77	0.58	0.91
Sreng	0.82	0.85	0.65	0.68
Staung	0.62	0.78	0.89	0.89

Table 5.15. Six model parameters of nine ungauged basins of the Greater Baribo basin

Basin Name	c	t _w	f	t _q	t _s	v _s
1	0.0028	59.52	5.18	5.25	25.45	0.19
2	0.0028	59.52	5.18	5.25	25.45	0.19
3	0.0012	138.62	6.15	4.07	50.45	0.32
4	0.0003	165.83	6.31	1.75	57.37	0.34
5	0.0004	71.54	5.45	0.88	31.20	0.34
6	0.0025	53.23	4.73	3.53	25.11	0.15
7	0.0012	29.47	6.24	1.76	25.93	0.21
8	-0.0001	84.21	6.14	-6.67	39.68	0.06
9	0.0004	63.07	6.43	-5.13	35.10	0.03

5.3.2 Analysis of Hydrological Drought

The value of SDI of the three sub-basins at 3-, 6-, 12-, 24-, and 48-month time-scales (SDI₃, SDI₆, SDI₁₂, SDI₂₄, and SDI₄₈, respectively) are shown from Figure 5.13 to Figure 5.17, respectively. The value of SDI normally changed between -3 and 3. There are three graphs in each figure for the Bamnak, Baribo, and Kraing Ponley sub-basins

which locate in the northern, central and southern parts of the Greater Baribo basin, accordingly. There are three different straight lines on each graph which black line (moderate drought), black dashed line (severe drought) and black dotted (extreme drought) refer to SDI value of -1, -1.5, and -2, respectively.

Figure 5.13 to Figure 5.17 show that the characteristic of SPI and SDI were the same to each other. As the result indicated that the variation of the SDI decreased with longer time-scale. The SDI3 and SDI6 varied frequently below and above zero while the value of the SDI12, SDI24 and SDI48 changed slower, last longer, and less frequent. Likewise, the three sub-basins had different pattern since the Baribo sub-basin was less prone to face the drought issue than other sub-basins. An extreme drought event ($SDI \leq -2$) at short time-scale was found in the Bamnak and Kraing Ponley sub-basins. There was no extreme drought in the Baribo sub-basin. For the long time-scale, the extreme drought did not occur in the three sub-basins except in the Kraing Ponley sub-basin at SDI24. According to the analysis above, the Baribo sub-basin was considered the sub-basin with lowest drought hazard in comparing to other sub-basins since it showed less frequent and lower intensity of drought. The Baribo sub-basin did not experienced the drought from 1987 to 1993 while the Bamnak and Kraing Ponley sub-basins was impacted by drought for many times. Later, the three sub-basins experienced the most severe drought between 2002 and 2006.

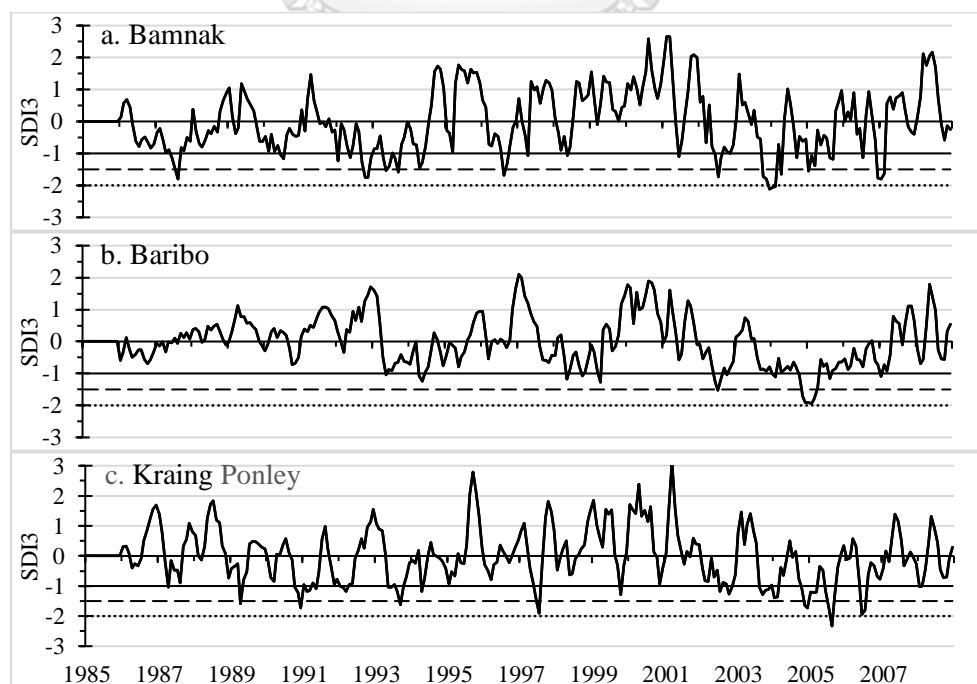


Figure 5.13. SDI6 between 1985 and 2008 of the three sub-basins

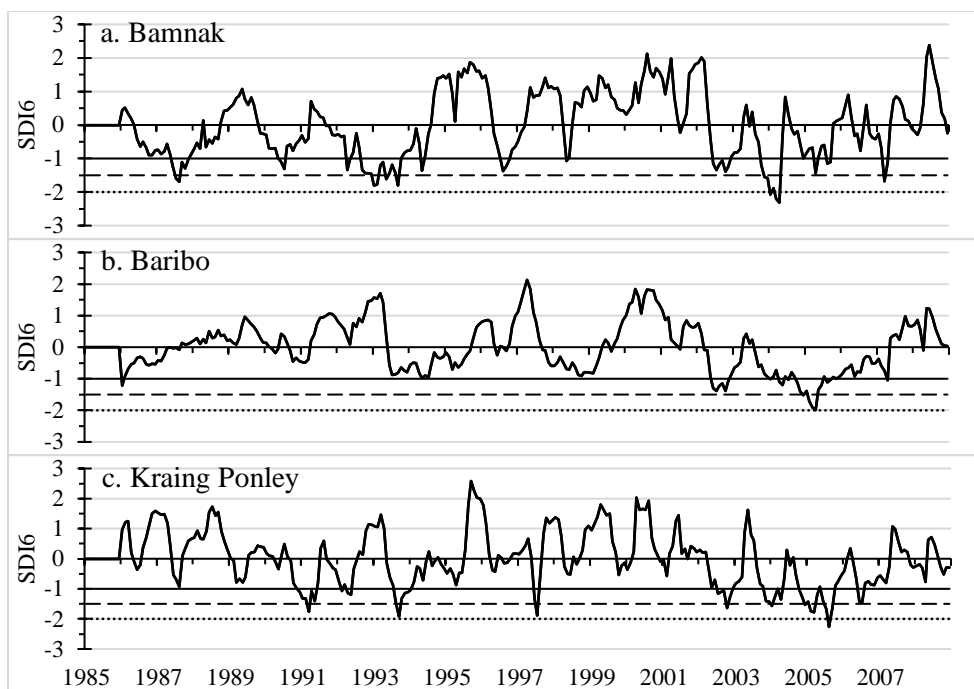


Figure 5.14. SDI3 between 1985 and 2008 of the three sub-basins

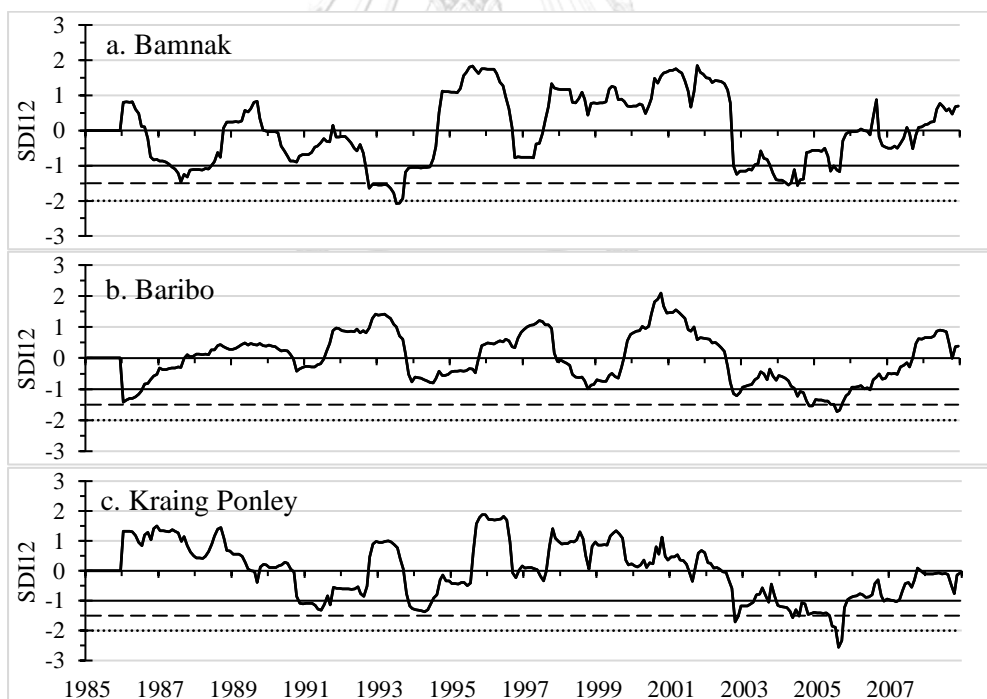


Figure 5.15. SDI12 between 1985 and 2008 of the three sub-basins

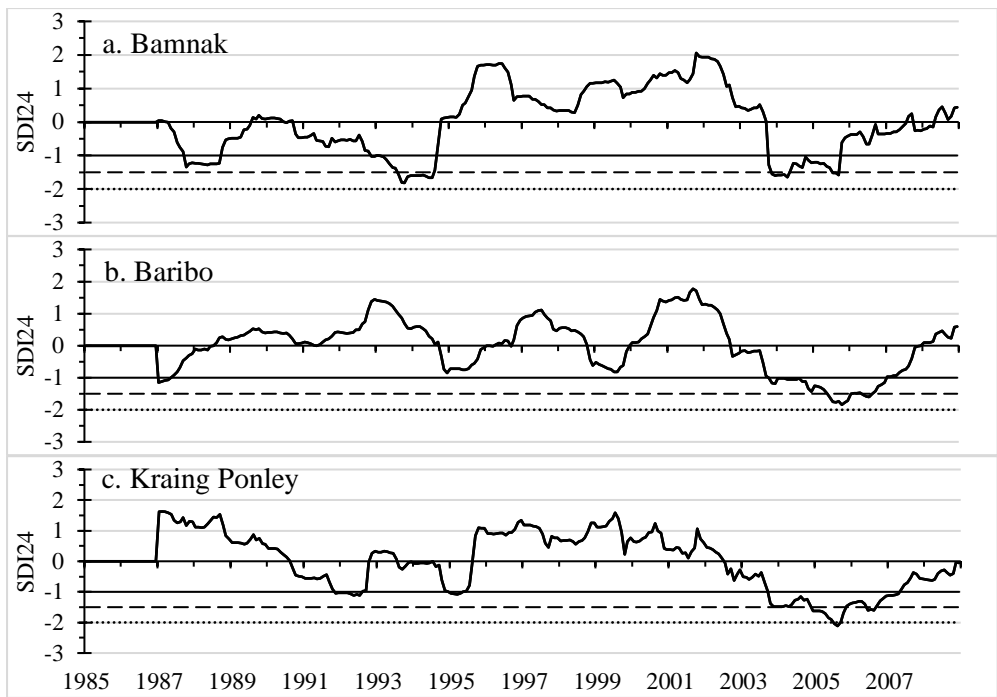


Figure 5.16. SDI24 between 1985 and 2008 of the three sub-basins

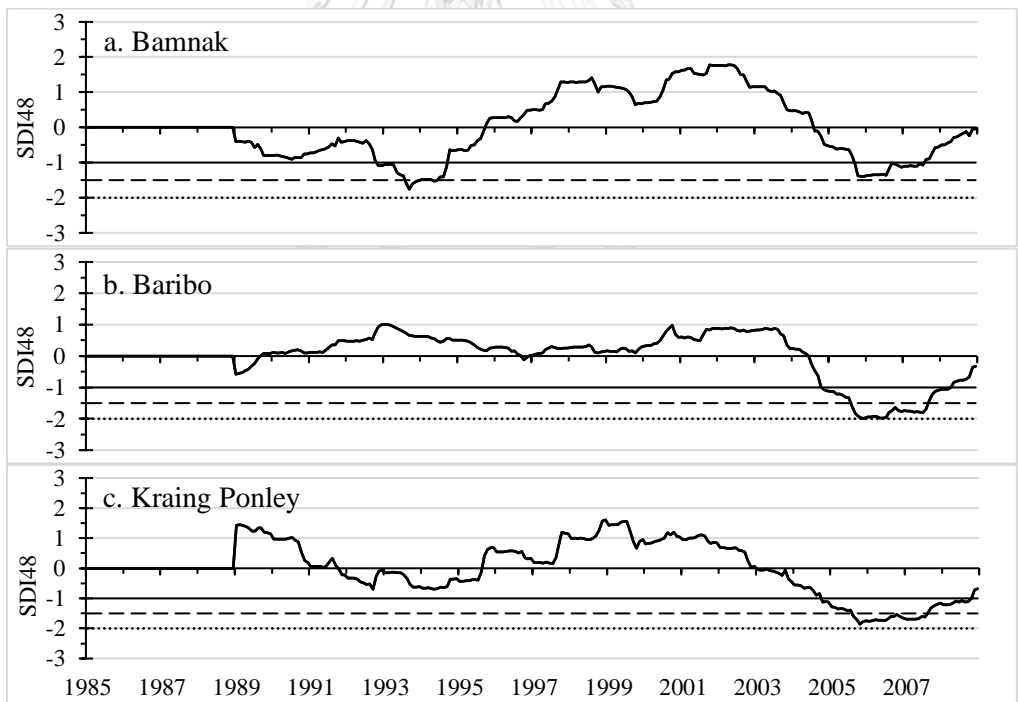


Figure 5.17. SDI48 between 1985 and 2008 of the three sub-basins

5.3.3 Theory of Runs for SDI

Table 5.16 to Table 5.20 illustrate the properties of each DE in terms of DD, DS, DI1, and DI2 at the five time-scales in the three sub-basins using ToR method. When considering the DE, the result indicated that the drought occurred in the Baribo sub-basin less frequent than other sub-basins. The SDI3 and SDI6 indicated that the maximum DE in the Baribo sub-basin (DE = 5 and 3) was about two to three times less than the Bamnak (DE = 12 and 9) and Kraing Ponley (DE = 11 and 8) sub-basins. For SDI12, SDI24, and SDI48, the DE in the three sub-basins were comparable.

The length of DD in the Baribo sub-basin at SDI3 (DD = 38) and SDI6 (DD = 45) were longer than other sub-basins. The SDI12 and SDI24 showed that the length of the DD increased from the north to south of the Greater Baribo basin. The result indicated that the longest length of DD in the Bamnak, Baribo, and Kraing Ponley sub-basin were 42, 61, and 64 at SDI12 and 48, 63 and 78 at SDI24, respectively. In contrast to other time-scales, the longest length of DD of 81 was found in the Bamnak sub-basin at SDI48. The maximum DS of 34.20 and 41.38 in the Baribo sub-basin were the highest at SDI3 and SDI6, respectively. The DS in the Kraing Ponley sub-basin became the highest at SDI12, SDI24, and SDI48 (DS = 66.66, 79.63, and 80.13, accordingly). The three sub-basins were impacted by drought from 1993 to 1994, 1998 to 1999 and 2002 to 2007. The drought in the Bamnak and Kraing Ponley sub-basins were more severe than the Baribo sub-basin between 1985 to 2001; however, it became comparable and more severe than the previous drought events between 2002 and 2006.

The DI showed that the Baribo sub-basin experienced less severe drought compared to other sub-basins. At short time-scale analysis clearly showed that once extreme ($DI1 \geq 2$) and several severe ($1.5 \geq DI1 > 2$) DE impacted in the Bamnak and Kraing Ponley sub-basins while only one severe DE was found in the Baribo sub-basin at each short time-scale. For long time-scale, the three sub-basins showed similar DI1 characteristic, but an extreme drought was found in the Kraing Ponley sub-basin at SDI24 (DI1 = 2.11).

Based on the analysis above, the DE and DI at the short time-scale were greater than those of long time-scale. In contrast to DE and DI, the DS and DD increased with longer time-scale. The DE in the Bamnak and Kraing Ponley sub-basins were about two to three times higher than the Baribo sub-basin at SDI3 and SDI6. Moreover, the Baribo sub-basin did not experience extreme drought while the Bamnak and Kraing Ponley sub-basins did. Thus, the SDI suggested that the Bamnak and Kraing Ponley sub-basins

experienced the drought with higher severity than the Baribo sub-basin. However, the longest DD and highest DS at SDI3 and SDI6 occurred in the Baribo sub-basin. Thus, the Baribo sub-basin is also considered prone to the drought. Thus, the three sub-basins prone to the drought issue but they were different in parameters.

Table 5.16. Characteristics of the drought event in the three sub-basins for SDI3

Sub-basin	DE	DD	DS	DI1	DI2
Bamnak	1. May-1986 to Dec-1987	20	15.03	1.81	0.75
	2. Jan-1989 to Dec-1990	15	9.00	1.16	0.60
	3. Jul-1991 to Jul-1994	33	27.56	1.75	0.84
	4. Mar-1996 to Nov-1996	9	7.21	1.69	0.80
	5. Mar-1997 to Apr-1997	2	1.51	1.07	0.76
	6. Feb-1998 to Jun-1998	5	3.59	1.07	0.72
	7. May-2001 to Jul-2001	3	1.70	1.11	0.57
	8. May-2002 to Dec-2002	8	8.19	1.73	1.02
	9. Aug-2003 to Apr-2004	9	13.16	2.12	1.46
	10. Aug-2004 to Sep-2005	14	11.20	1.56	0.80
	11. May-2006 to Jul-2006	3	1.77	1.14	0.59
	12. Nov-2006 to Feb-2007	4	5.78	1.81	1.45
Baribo	1. Apr-1993 to Aug-1994	17	11.66	1.24	0.69
	2. Apr-1998 to Apr-1999	13	9.24	1.29	0.71
	3. Dec-2001 to Dec-2002	13	9.27	1.54	0.71
	4. Aug-2003 to Sep-2006	38	34.20	1.94	0.90
	5. Nov-2006 to Apr-2007	6	4.51	1.10	0.75
Kraing Ponley	1. Dec-1988 to Jun-1989	7	4.67	1.59	0.67
	2. Sep-1990 to Jun-1991	10	9.92	1.73	0.99
	3. May-1993 to Feb-1994	10	8.16	1.63	0.82
	4. Apr-1994 to Jun-1994	3	2.00	1.18	0.67
	5. Apr-1997 to Aug-1997	5	4.94	1.91	0.99
	6. Sep-1999 to Dec-1999	3	1.90	1.30	0.63
	7. Jan-2002 to Dec-2002	12	9.21	1.27	0.77
	8. Aug-2003 to May-2004	10	9.43	1.39	0.94
	9. Sep-2004 to Oct-2005	14	16.55	2.33	1.18
	10. May-2006 to Jan-2007	9	7.61	1.95	0.85
	11. Nov-2007 to Mar-2008	5	2.79	1.03	0.56

Table 5.17. Characteristics of the drought event in the three sub-basins for SDI6

Sub-basin	DE	DD	DS	DI1	DI2
Bamnak	1. Jul-1986 to Mar-1988	22	19.44	1.70	0.88
	2. Jan-1989 to Mar-1991	17	10.51	1.32	0.62
	3. Sep-1991 to Jun-1994	35	31.86	1.80	0.91
	4. May-1996 to Mar-1997	11	7.68	1.38	0.70
	5. Apr-1998 to Jun-1998	3	2.11	1.07	0.70
	6. May-2002 to Mar-2003	11	11.12	1.34	1.01
	7. Aug-2003 to May-2004	10	13.90	2.32	1.39
	8. Aug-2004 to Sep-2005	14	10.24	1.43	0.73
	9. Oct-2006 to Apr-2007	7	4.75	1.67	0.68
Baribo	1. Jan-1986 to Aug-1987	20	8.33	1.22	0.42
	2. Mar-2002 to Mar-2003	13	11.27	1.39	0.87
	3. Aug-2003 to Apr-2007	45	41.38	1.99	0.92
Kraing Ponley	1. Sep-1990 to Jun-1991	10	10.66	1.76	1.07
	2. Sep-1991 to Jul-1992	11	6.22	1.20	0.57
	3. May-1993 to Jun-1994	14	11.77	1.92	0.84
	4. Jun-1997 to Aug-1997	3	3.70	1.90	1.23
	5. Apr-2002 to Mar-2003	12	11.56	1.65	0.96
	6. Aug-2003 to May-2004	10	10.77	1.56	1.08
	7. Sep-2004 to Feb-2006	18	21.04	2.26	1.17
	8. Apr-2006 to Apr-2007	13	9.90	1.45	0.76

Table 5.18. Characteristics of the drought event in the three sub-basins for SDI12

Sub-basin	DE	DD	DS	DI1	DI2
Bamnak	1. Sep-1986 to Sep-1987	25	24.69	1.46	0.99
	2. Dec-1989 to Aug-1994	34	35.81	2.08	1.05
	3. Oct-2002 to Mar-2006	42	38.20	1.56	0.91
Baribo	1. Jan-1986 to Sep-1987	21	14.91	1.35	0.71
	2. Dec-1997 to Sep-1999	22	11.98	1.00	0.54
	3. Aug-2002 to Aug-2007	61	54.55	1.72	0.89
Kraing Ponley	1. Sep-1990 to Sep-1992	25	20.63	1.32	0.83
	2. Oct-1993 to Jul-1995	22	16.78	1.37	0.76
	3. Jun-2002 to Sep-2007	64	66.66	2.56	1.04

Table 5.19. Characteristics of the drought event in the three sub-basins for SDI24

Sub-basin	Drought Events	DD	DS	DI1	DI2
Bamnak	1. May-1987 to Jul-1989	27	22.02	1.29	0.82
	2. Oct-1990 to Sep-1994	48	45.74	1.82	0.95
	3. Oct-2003 to Jul-2007	46	40.92	1.60	0.89
Baribo	1. Jan-1987 to Jun-1988	18	9.91	1.15	0.55
	2. Oct-2002 to Dec-2007	63	63.58	1.84	1.01
Kraing Ponley	1. Sep-1990 to Oct-1992	26	19.03	1.12	0.73
	2. Aug-1993 to Aug-1995	25	10.99	1.82	0.44
	3. Jul-2002 to Dec-2008	78	79.63	2.11	1.02

Table 5.20. Characteristics of the drought event in the three sub-basins for SDI48

Sub-basin	DE	DD	DS	DI1	DI2
Bamnak	1. Jan-1989 to Sep-1995	81	65.64	1.76	0.81
	2. Aug-2004 to Dec-2008	53	41.07	1.40	0.77
Baribo	1. Jul-2004 to Dec-2008	54	73.08	1.98	1.35
Kraing Ponley	1. Jan-2003 to Dec-2008	72	80.13	1.86	1.11

5.4 Impact of Drought on Cropping Pattern

Table 5.21 to Table 5.29 show the impact of drought on the cropping pattern in the Greater Baribo basin. This section mainly focuses on the rice production since the Greater Baribo basin is mostly used for growing paddy rice (more than 95% of the total agricultural area). There are three main types of rice varieties, i.e. long, medium, and early duration rice (LD, MD, and ED, respectively) which are widely grown in this basin. The LD, MD, and ED rice normally take 6, 3 to 4, and 3 months, accordingly for cropping period. The LD rice is utilized in the rainfed area and seeding is transplanted between May and July and harvested between late of November to December. The MD rice is grown in the wet season between mid-August and early-December. The ED rice is recently introduced to Cambodia farming system because it takes shorter of cropping period, needs less water, and gives higher revenue. Besides, it can be harvested just about three months after seeding and can be grown at any time of the year. Cambodian farmers prefer to plant ED three time per year, for example, during December to March (ED1), farmer uses standing water and residual soil moisture which can be supplemented by irrigation; during May to August (ED2), farmer uses

early wet season rains before harvesting during the long absence of rainfall in the wet season (ITCZ); during September to November (ED3), farmer heavily relies on rainfall during wet season and the harvest period coincides with LD and MD rice varieties. Based on the cropping pattern explained, only 3- and 6- month time-scales of SPI, SVI, and SDI were employed for the analysis in this section. The proportions of the LD, MD and ED rice by area planted are approximately 20, 40, and 33 percent respectively (Chhinh and Millington, 2015). The detail of the cropping calendar of the three rice varieties are illustrated in Figure 5.18.

The assessment of the impact of drought on rice production can be drawn based on the cropping calendars shown in Figure 5.18. Table 5.21 to Table 5.29 present the drought intensity using different colors and cropping calendars using different bar legends. The white bar is for post harvesting period. The bar with dotted point is for vegetation period. The vertical line is for reproductive period and horizontal line is for ripening period.

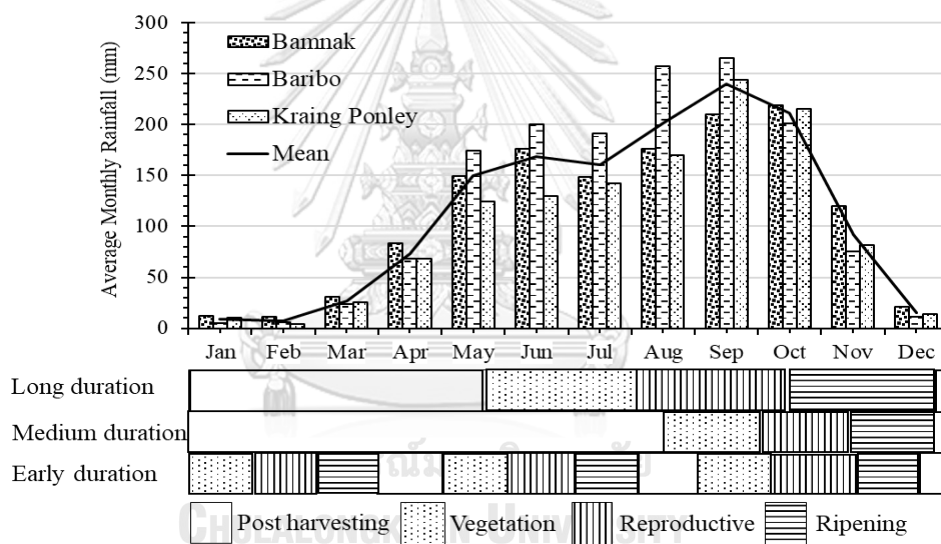


Figure 5.18. Rice development phases for long, medium, and early rice varieties

Table 5.21 to Table 5.23 show the drought severity with cropping pattern of the three sub-basins in terms of SPI. Based on the cropping pattern of the three types of rice, the Bamnak and Kraing Ponley sub-basins were more severely affected than the Baribo sub-basin. As illustrated from Table 5.21 to Table 5.23, the Bamnak and Kraing Ponley sub-basins frequently experienced the drought from 1987 to 1998 while the drought occurred in the Baribo sub-basin only between 1994 and 1998. Later between 2001 and 2006, the three sub-basins faced drought issue with similar intensity and frequency. The rice which ripened in November and December (LD, MD, and ED3) experienced the drought more often than other periods. The ED1 rice was less prone to drought issue since only near normal condition was

found during the reproductive and ripening periods. For ED2 rice, the drought occurred high frequency with low intensity since many near normal conditions were found during the cropping period. For ED3, MD (Table 5.22) and LD rice (Table 5.23), the result indicated that the drought occurred more frequently with higher intensity on cropping period.

Table 5.24 to Table 5.26 represent the vegetation condition assessed by SVI and cropping pattern over the Greater Baribo basin. What presented in the tables were the cropping patterns in the three sub-basins experienced the poor condition of the greenness density at the same period but slightly different in the intensity. The period and duration of drought occurrence in the three sub-basins were similar to each other. However, the Bamnak sub-basin did not experience the very poor greenness density while the Baribo and Kraing Ponley sub-basins did. Based on the cropping pattern, the ED1, ED2, and LD rice were affected more severely than the ED3 and MD rice. As illustrated from Table 5.24 to Table 5.26, many very poor conditions of greenness density were found for the ED1, ED2, and LD rice while there were less for the ED3 and MD rice. When considering the frequency, ED3 and MD rice experienced poor vegetation condition more frequent. The poorest condition of the three types of rice were captured in 1989, 1994 and 2000 while it seemed less severe between 2001 and 2008.

Table 5.27 to Table 5.29 illustrate the drought severity on cropping pattern of the three sub-basins assessed by SDI of each month between the study period. The result suggested that the cropping pattern in the Baribo sub-basin was not as severely damaged by drought as other sub-basins. The most interesting result is that the extreme low streamflow ($SDI < -2$) in the river did not occur in the Baribo sub-basin but it did in the Bamnak and Kraing Ponley sub-basins. The three types of rice were impacted by drought in Bamnak and Kraing Ponley sub-basins but not in the Baribo sub-basin between 1987 and 1997. Later, the drought severely affected the cropping period of the three types of rice over the Greater Baribo basin between 2001 and 2006. The analysis of SDI on the cropping pattern was focused on the ED1 since only ED1 relies on the standing water and residual soil moisture which can be supplemented by irrigation. The ED1 of the three sub-basins were slightly impacted between 1993 and 1994 and severely damaged between 2004 and 2007.

Overall, the result from the three indices indicated that the ED1 was not severely damaged by drought assessed based on the SPI but it was affected by the SVI and SDI. It can be caused by that the ED1 does not rely on rainfall, but it relies on the streamflow. Furthermore, the drought occurred the most frequent with the highest intensity in the late season (November and December). The drought occurred in the late season causing serious damage on the rice production because the three types of rice varieties are harvested at the

same time during that period. The SPI and SDI indicated that the drought occurred more severe, or the rainfall and streamflow quantities were less between 2002 and 2005. On the other hand, the SVI was defined that the vegetation condition was better than the previous events. It can be caused by the agricultural management and adaptation of the “Rectangular Strategies” of the RGC’s policy. The SPI is good for assessing the impact of drought on agriculture during the wet season since the SPI was calculated using rainfall while rice varieties (LD, MD, ED2, and ED3) which cropped during the wet season, heavily depends on the rainfall. The SDI is good for evaluating the impacted of drought on agriculture during dry season because SDI was calculated based on streamflow. The SDI is good for assess the impact of drought for ED1 since it mainly relies on the irrigated water. The SVI is good to assess all rice varieties since it was assessed based on the greenness density of the vegetation. Moreover, it could evaluate the impact on agriculture by not only drought but also flood, crop rotation, and unseasonal coolness. Thus, the SVI is better in assessing the impact on the agriculture.

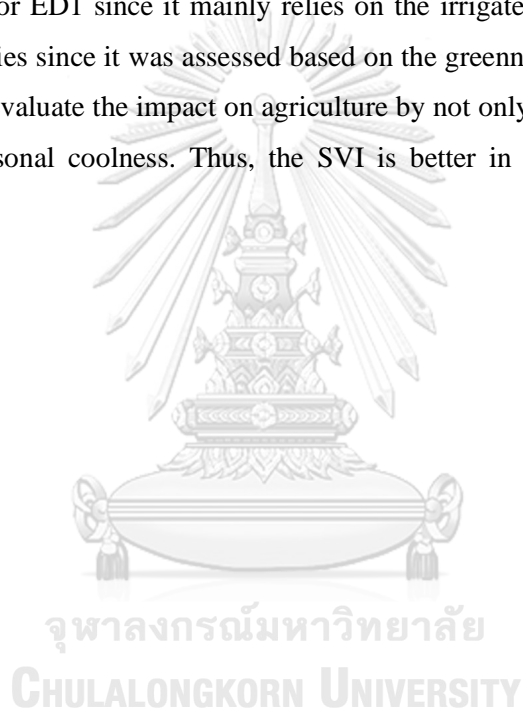


Table 5.21. SPI3 for early duration rice

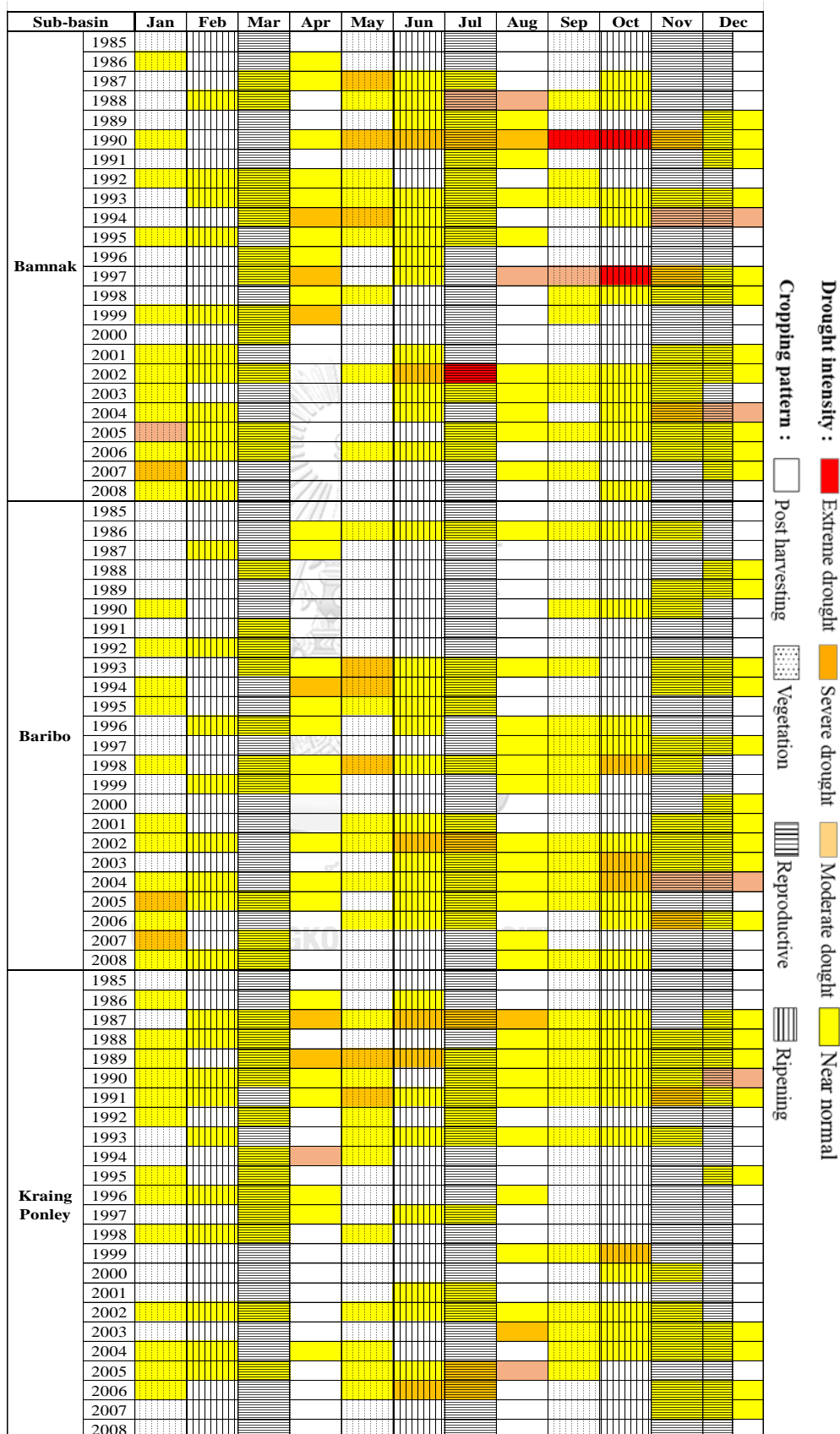


Table 5.23. SPI6 for long duration rice

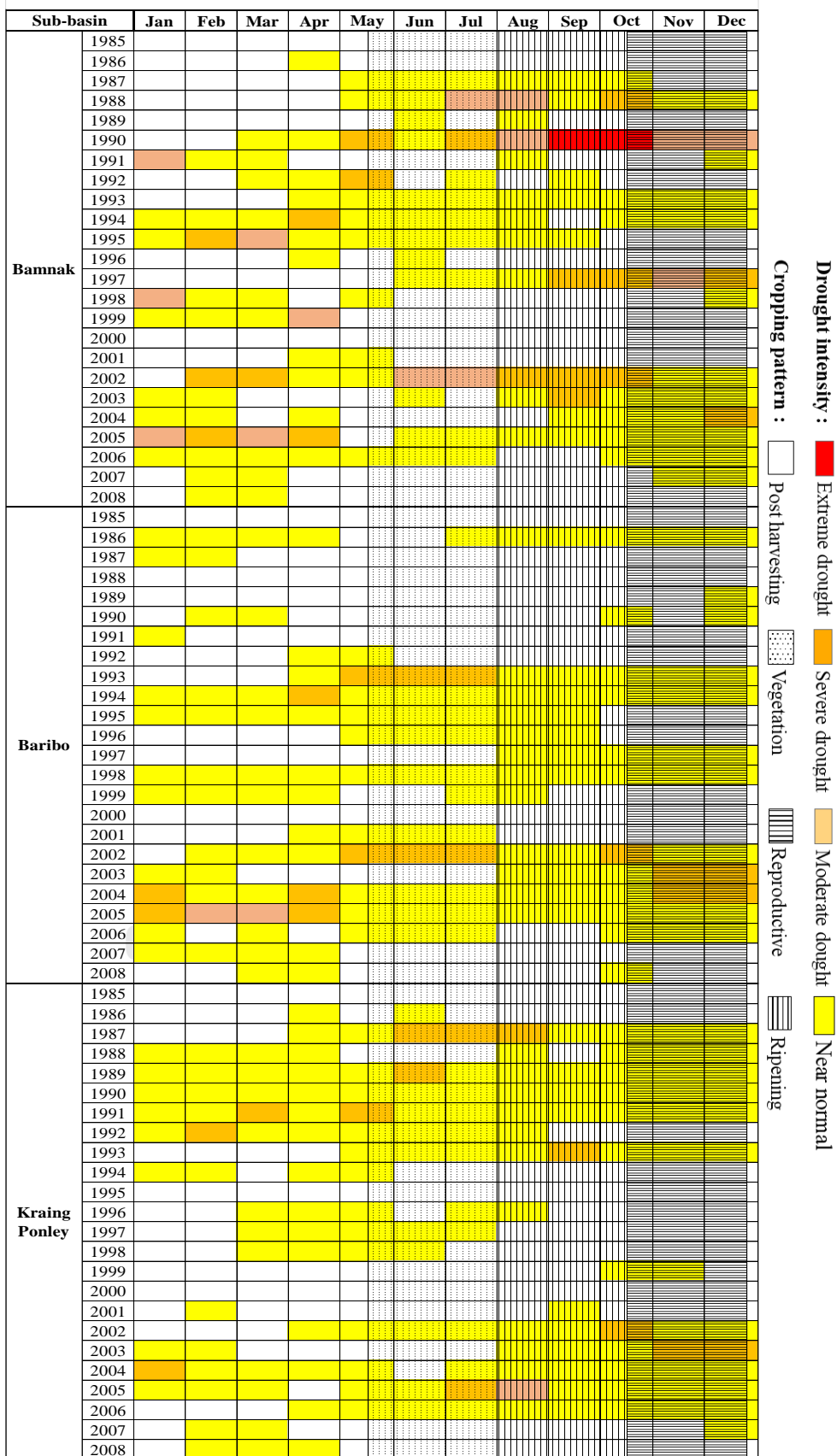


Table 5.25. SVI3 for medium duration rice

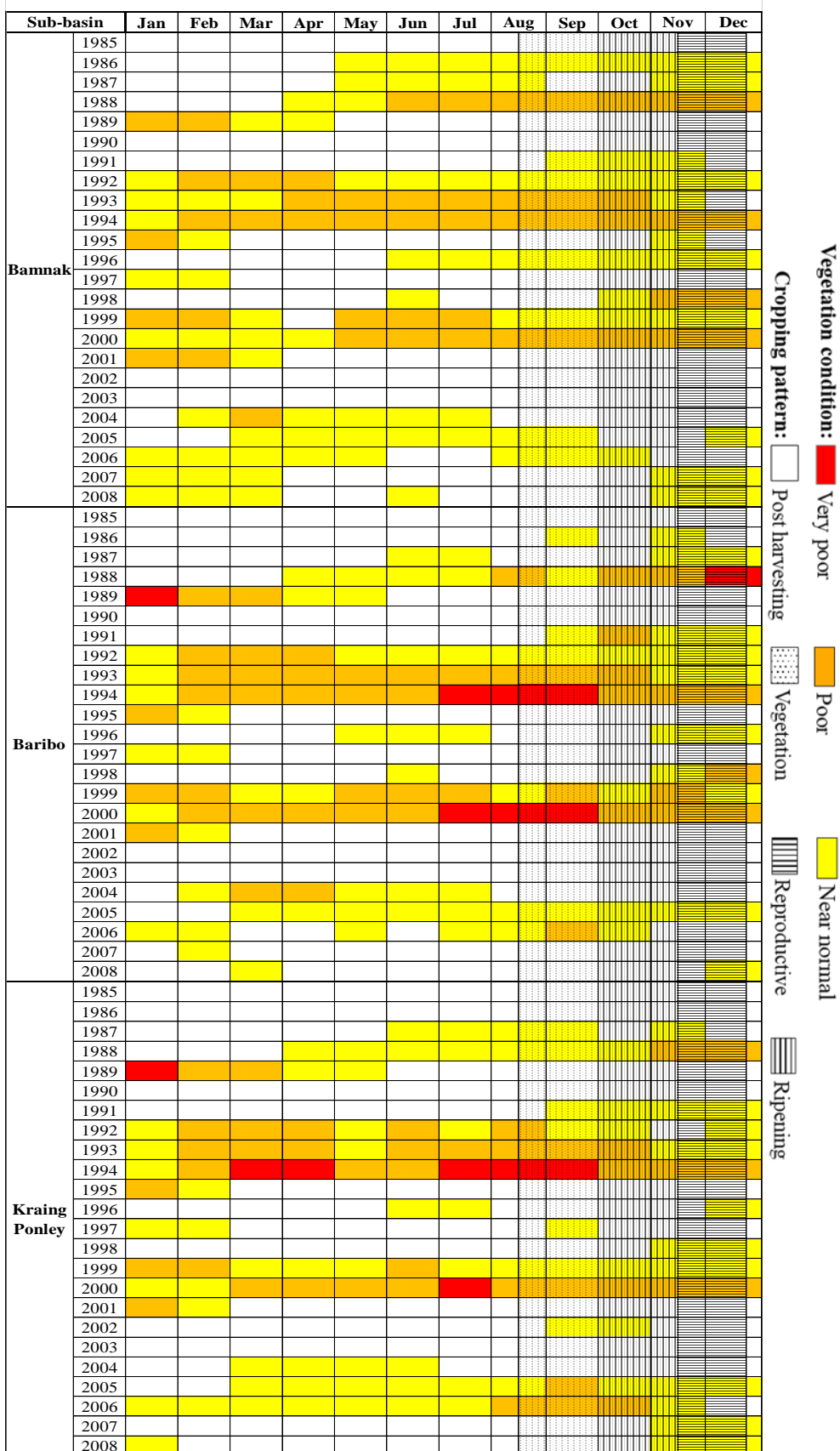


Table 5.26. SVI6 for long duration rice

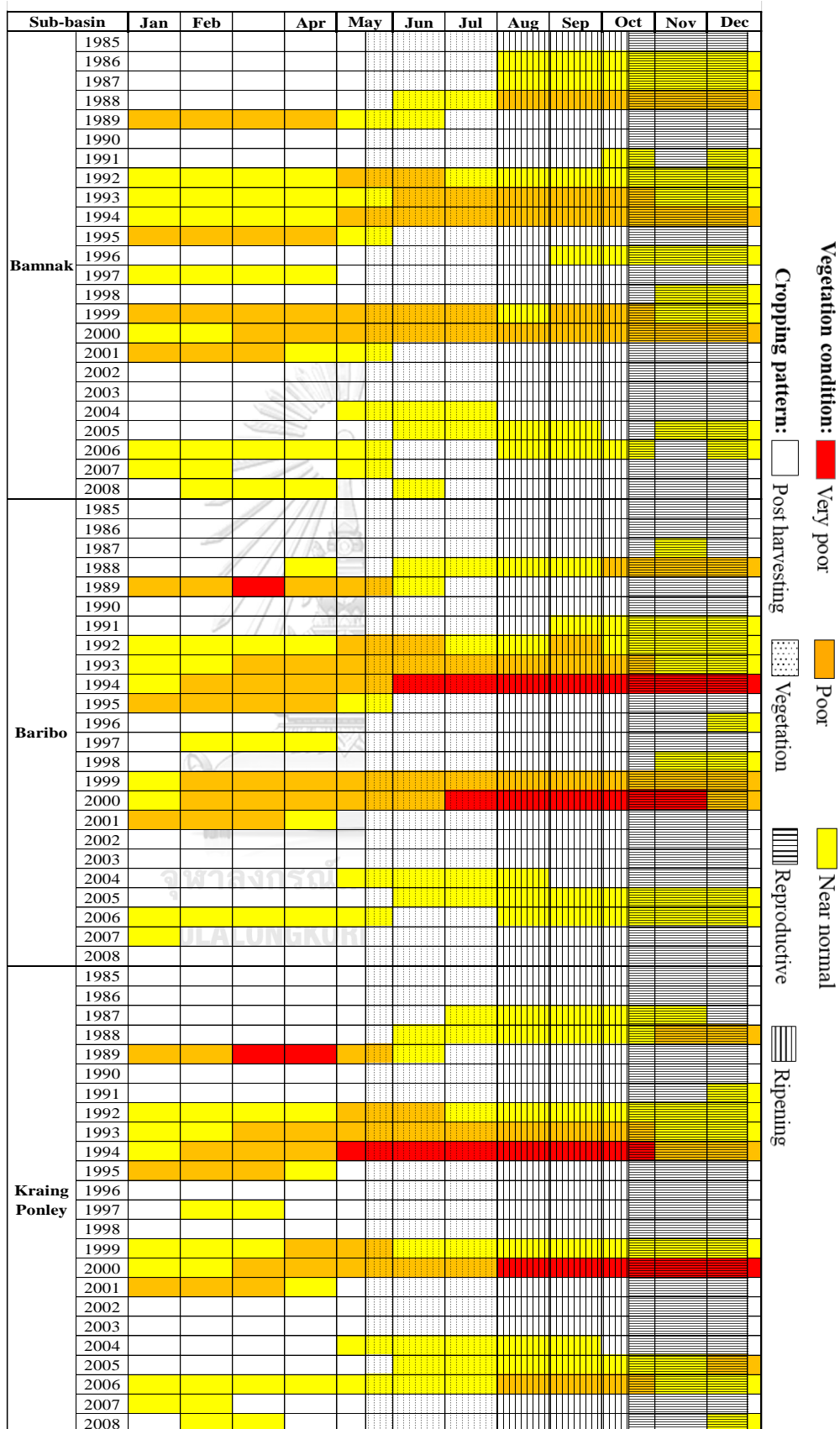


Table 5.27. SDI3 for early duration rice

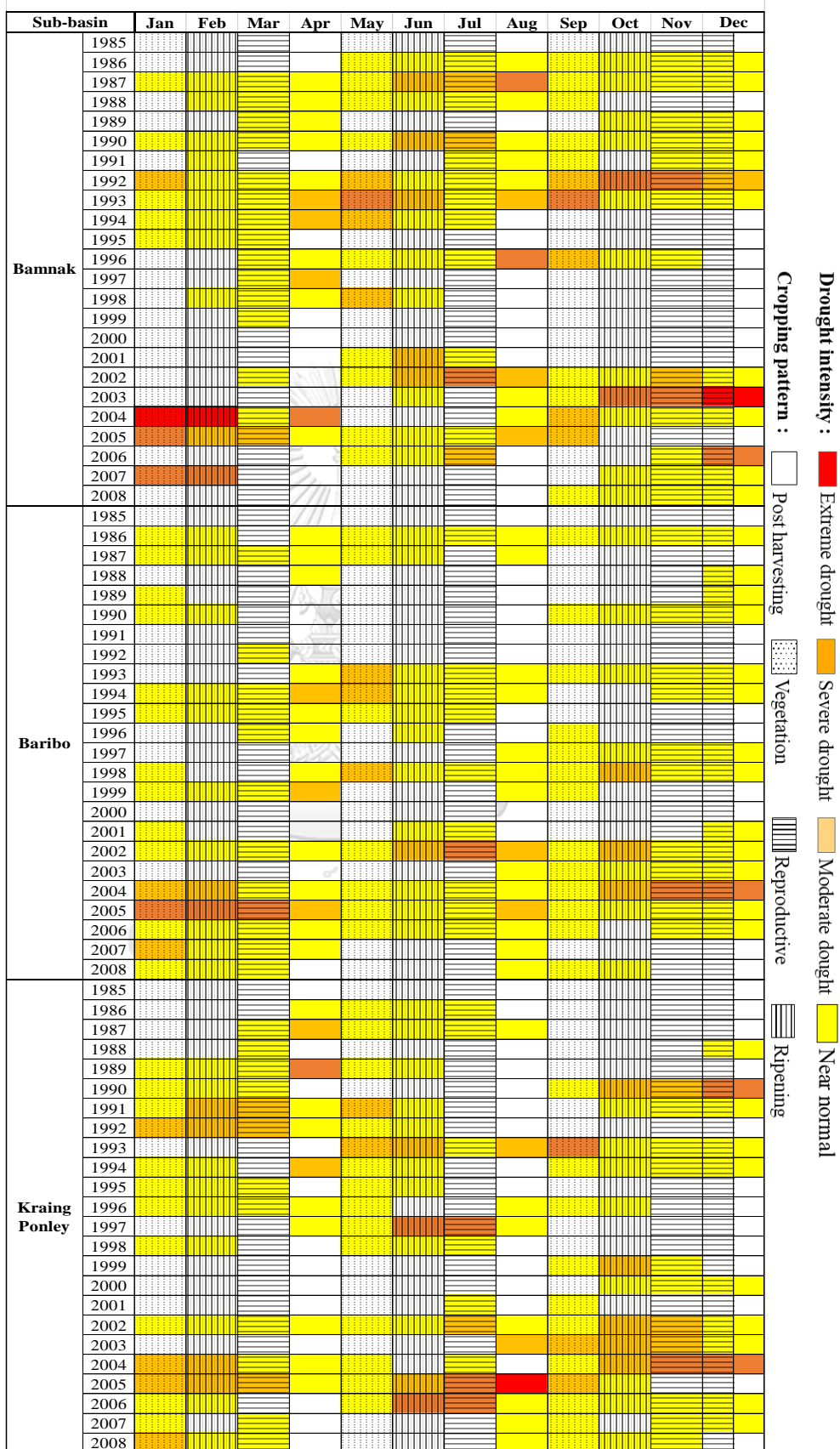
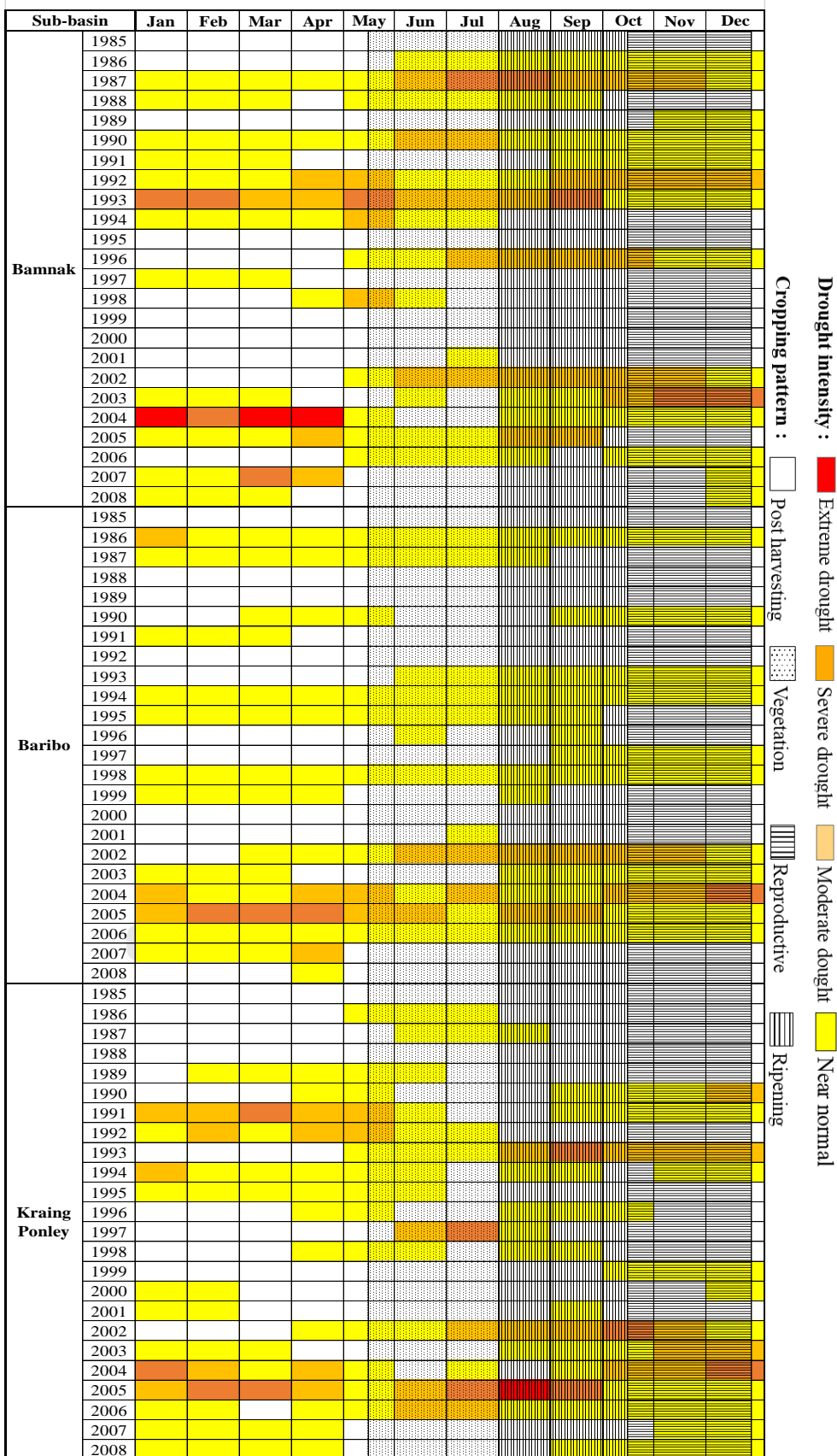


Table 5.29. SDI6 for long duration rice



5.5 Spatial Distribution of Drought

The distribution of the drought and agricultural area over the entire Greater Baribo basin is shown from Figure 5.19 to Figure 5.21. The agricultural area particularly distributes in the eastern part of the Bamnak and Baribo sub-basins and almost the entire Kraing Ponley sub-basin. Six DEs were selected to develop drought maps of SPI, SVI and SDI at 3-, 6-, 12-, 24-, and 48-month time-scales. The selected DEs were in the month which at least two indices either SPI or SDI captured a severe or an extreme intensity of drought (SPI or $SDI \leq -1.5$) or SVI captured a very poor condition of vegetation ($SVI \leq 0.05$). Six selected DEs were July 1987, October 1990, November 1993, April 1994, August 2000, and March 2005. It is noted that the drought map for the 48-month time-scale in July 1987 cannot be developed owing to the unavailability of the calculated three indices.

The drought distribution map of SPI over the Greater Baribo basin is illustrated in Figure 5.19. When considering the short time-scale, the drought in July 1987 was found in the southern part of the Kraing Ponley sub-basin. In October 1990, the drought did not occur in only in the southern part of the Kraing Ponley sub-basin but also in the entire Bamnak sub-basin. The drought intensity in the Bamnak sub-basin was higher than that of the Kraing Ponley sub-basin; however, the impact of drought on agriculture in the Kraing Ponley sub-basin was the most severe since the agricultural covers over wide area. In November 1993 and April 1994, the drought was found in large area of the Bamnak and Baribo sub-basins and in the northern part of the Kraing Ponley sub-basin. Later in August 2000, the entire Bamnak, Kraing Ponley, and western part of the Baribo sub-basins were found to have high rainfall. In March 2005, the SPI3 showed that the Greater Baribo basin was generally in near normal condition while SPI6 and SPI12 showed that the basin was severely affected by drought. For longer time-scales of six selected DEs, the drought mostly found in the southern part of the Kraing Ponley sub-basin except in March 2005, the moderate drought distributed almost the entire Bamnak and Baribo sub-basins and partly in the Kraing Ponley sub-basin. According to six selected DEs, the drought distributed in the Baribo sub-basin became more severe from year to year since the drought did not occur in the Baribo sub-basin in July 1987 and October 1990, but drought distributed severely at the Baribo sun-basin in November 1993, April 1994, and March 2005.

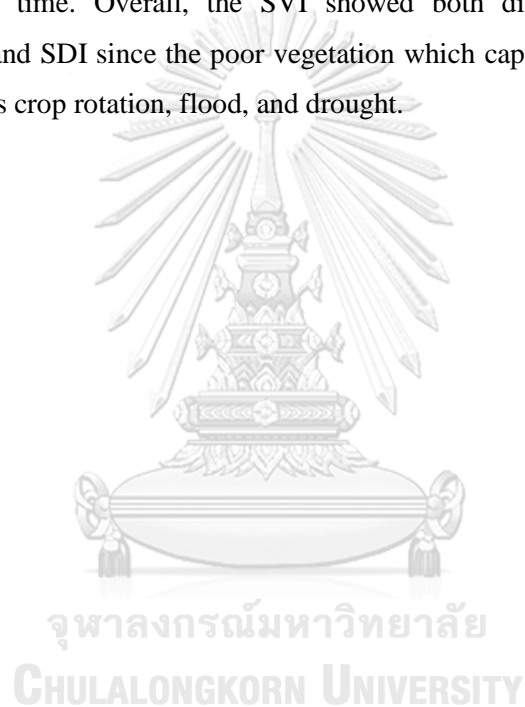
In Figure 5.20, the map shows the distribution of the vegetation condition over the Greater Baribo basin which produced by the SVI at five time-scales of interest. In July 1987, the SVI3 showed that the Greater Baribo basin mostly distributed by normal vegetation condition and partly distributed by poor vegetation. For SVI6 to SVI24, the normal and good

conditions of vegetation found in the Greater Baribo basin while the good vegetation condition was found only in the eastern part of the Greater Baribo basin. In October 1990, the Greater Baribo basin was found to have normal, good, and very good condition of the vegetation. At five time-scales of interest, the good and very good condition of the vegetation distributed particularly at the eastern part of the basin while the short time-scales (SVI3 to SVI12) showed better vegetation condition than the long time-scale (SVI24 and SVI48). Later, the poor and very poor condition of the vegetation were found over the entire basin in November 1993, April 1994, and August 2000. The intensity of the poor vegetation of SVI6 to SVI 24 were more severe than other time-scales except SVI3 in April 1994 which the intensity was comparable to SVI6 to SVI24. The intensity of the poor vegetation which occurred in August 2000, was the most severe and the highest intensity was mostly found in the Baribo sub-basin. In March 2005, the Greater Baribo basin was distributed by the good and very good condition of the vegetation at all time-scales except at the SVI3 which it was partly distributed by the poor vegetation condition. Generally, the condition of vegetation in the eastern part of the Greater Baribo basin was better than other parts of the basin since it is located next to the Tonle Sap Great lake.

The drought distribution map over the Greater Baribo basin produced based on the SDI at five time-scales is illustrated in Figure 5.21. The result showed that the drought intensity from the first to fourth selected DEs was less severe than in March 2005. From the first to fourth selected DEs, the drought distributed partly of the basin with difference intensities. When considering at short time-scales, the drought was found in the Bamnak sub-basin in July 1987 and the Baribo and Kraing Ponley sub-basins in October 1990. In November 1993 and April 1994, the drought occurred in the three sub-basins but more often in the Baribo sub-basin at short time-scales and in the Bamnak sub-basin at longer time-scales. In August 2000, the Greater Baribo basin was also severely affected by the extreme flood at short time-scales but they were less severe at long time-scales. Furthermore, the Baribo sub-basin was the most severely impacted by flood. In March 2005, the entire basin was severely impacted by drought while the highest intensity was found in the Baribo sub-basin and the lowest intensity was found in the Bamnak sub-basin. Overall, the SDI suggested that the Baribo sub-basin was the most severely impacted by both flood and drought.

The comparison of the drought distribution over the Greater Baribo sub-basins of three indices at six selected DEs are shown from Figure 5.22 to Figure 5.27. The result showed that the SPI and SDI did not agree with SVI in July 1987, October 1990, August 2000, and March 2005. In July 1987 and the SPI and SDI captured the drought partly in the three sub-basins but the SVI showed normal, good, and very good condition of the vegetation

over the basin in October 1990. Furthermore, the good to very good condition particularly occurred in the eastern part of the basin. In contrast to July 1987 and October 1990, the SVI indicated that very poor and poor vegetation distributed over the entire basin in August 2000 while SPI and SDI showed that the extreme rainfall and streamflow occurred. Thus, it clearly shown that poor and very poor condition of the vegetation in the basin was impacted by flood in August 2000. For March 2005, the SPI and SDI showed that the rainfall and streamflow were severely low than the previous DEs but the SVI captured the good to very good vegetation over the basin. On the other hand, three indices showed a good agreement in November 1993 and April 1994 since the low rainfall, streamflow, and poor vegetation were found at the same time. Overall, the SVI showed both different and similar drought distribution to SPI and SDI since the poor vegetation which captured by SVI, was caused by many factors such as crop rotation, flood, and drought.



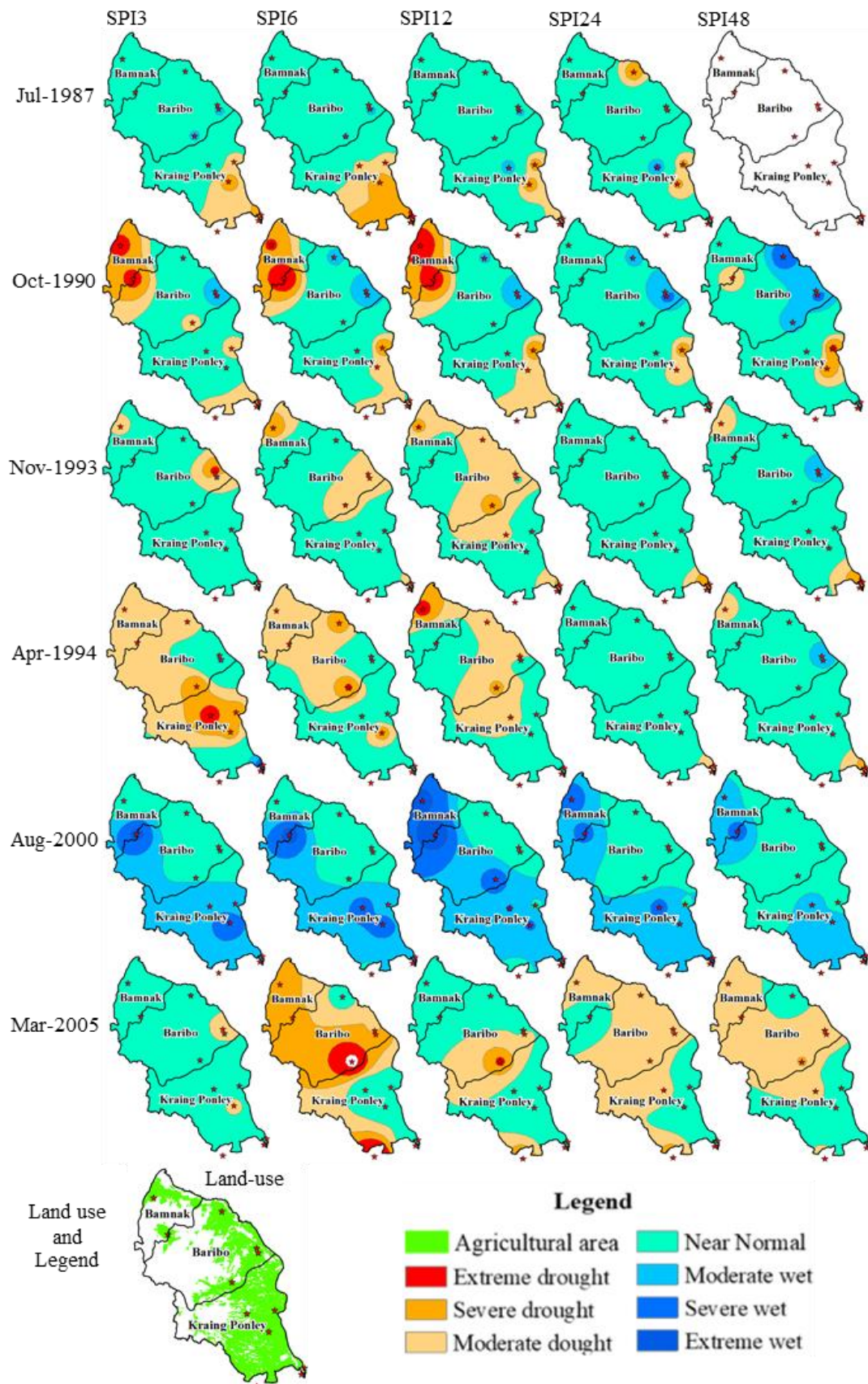


Figure 5.19. Drought map of SPI

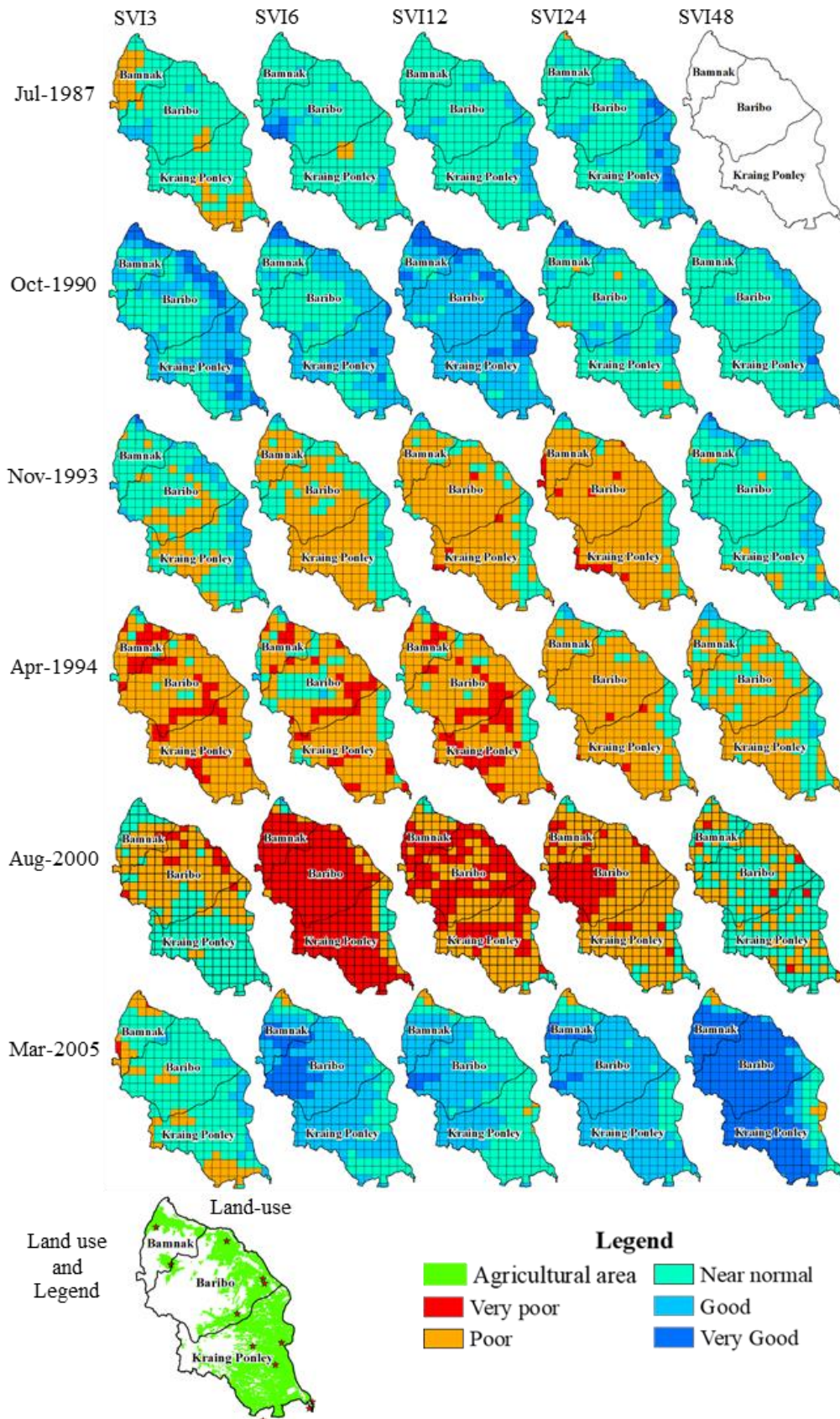


Figure 5.20. Vegetation condition map of SVI

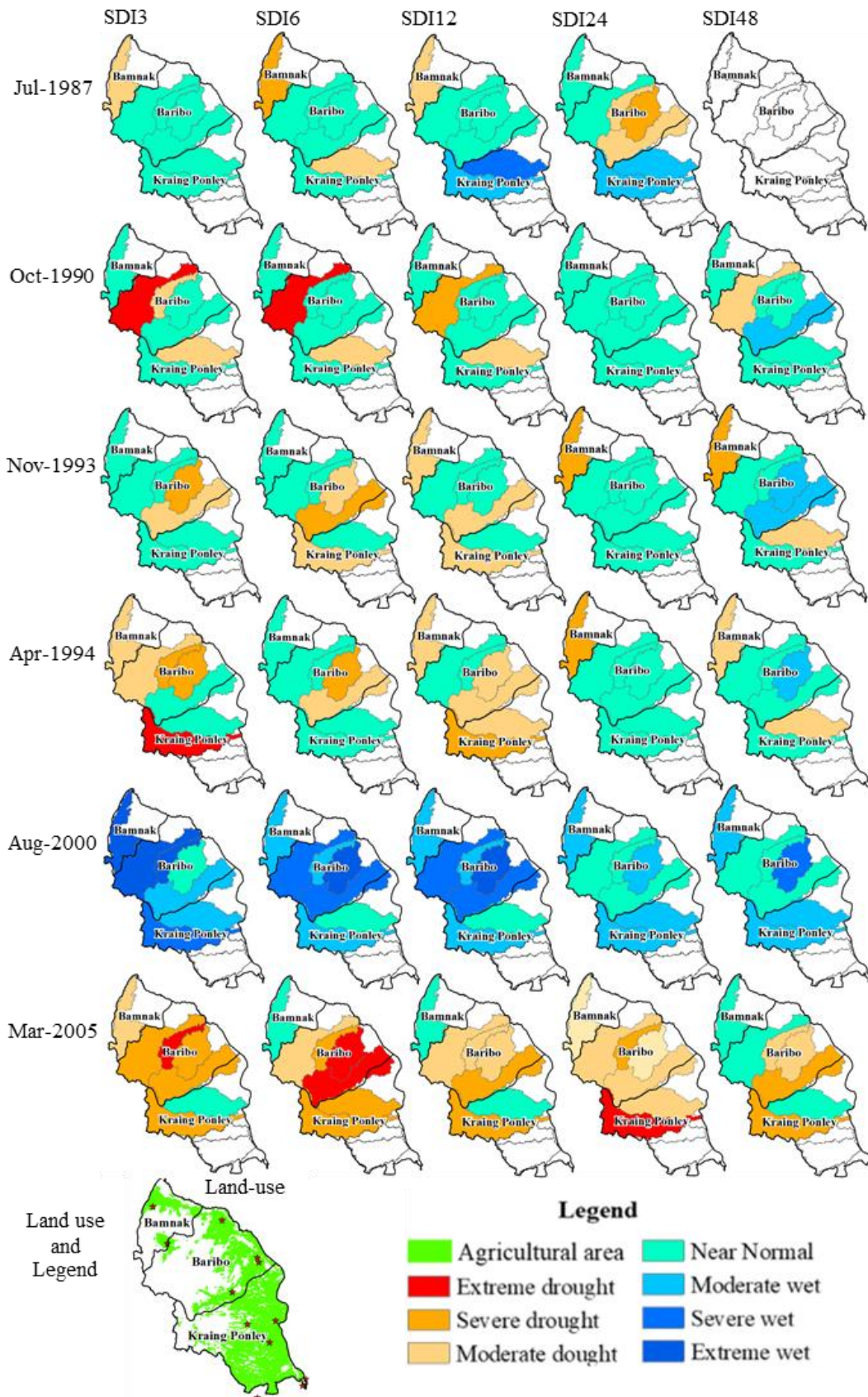


Figure 5.21. Drought map of SDI

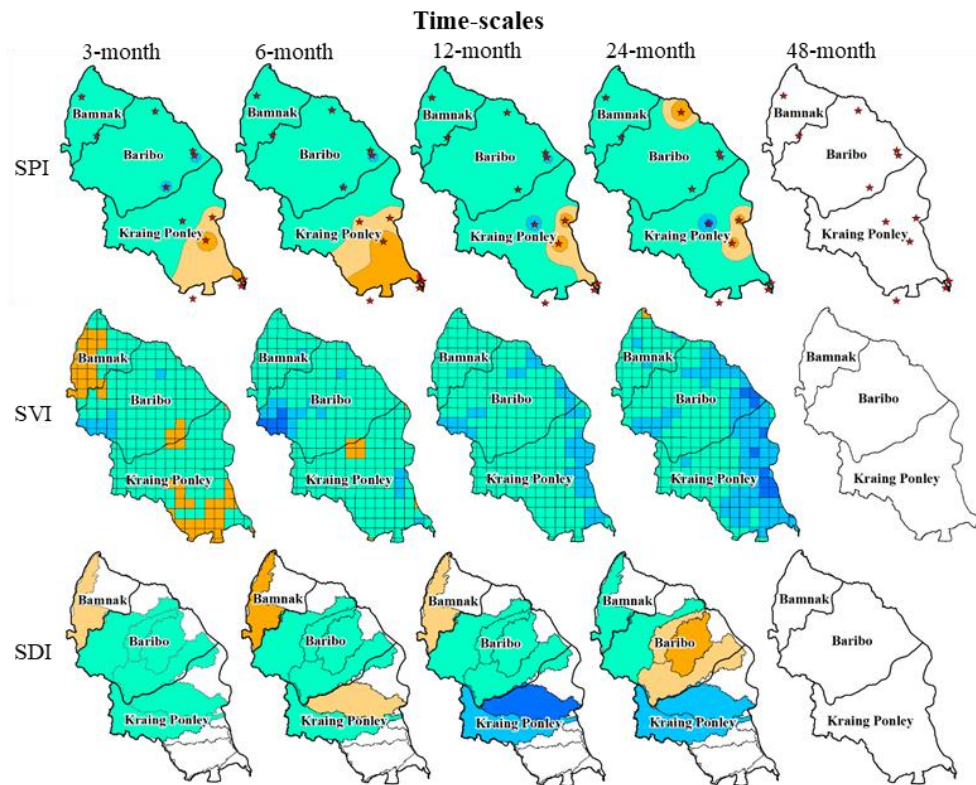


Figure 5.22. Drought map of the three indices in July 1987

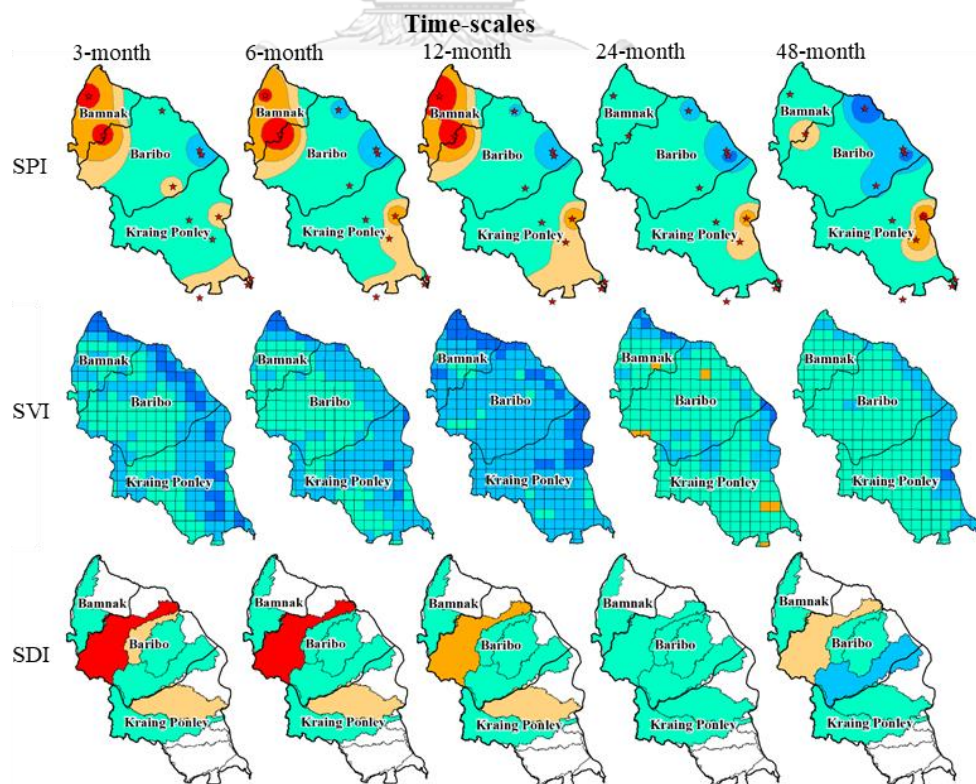


Figure 5.23. Drought map of the three indices in October 1990.

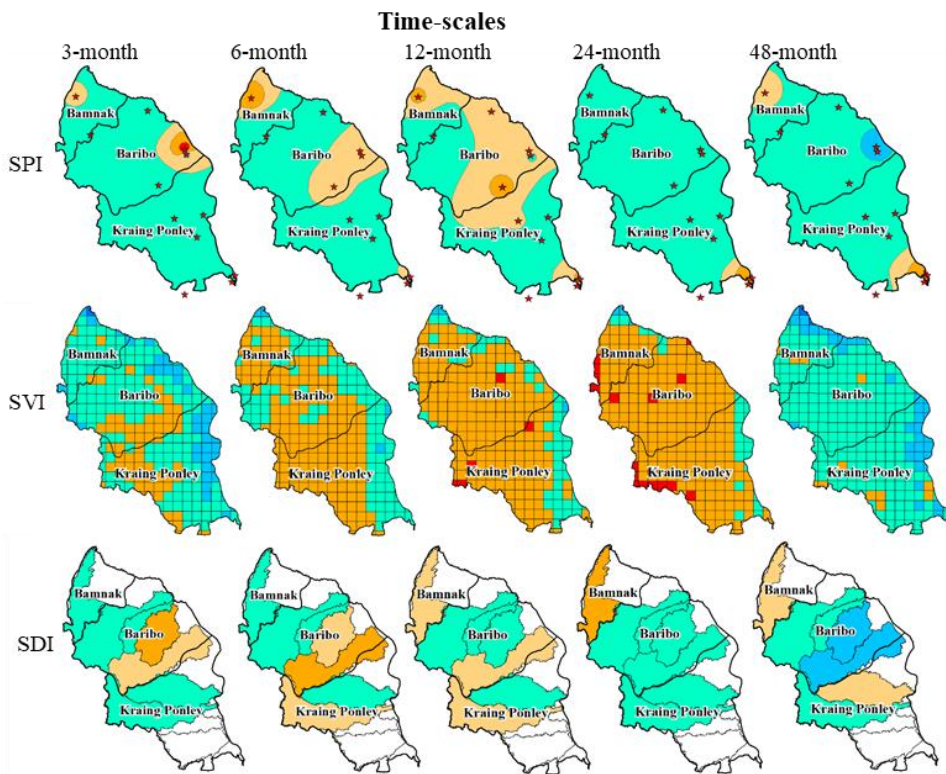


Figure 5.24. Drought map of the three indices in November 1993

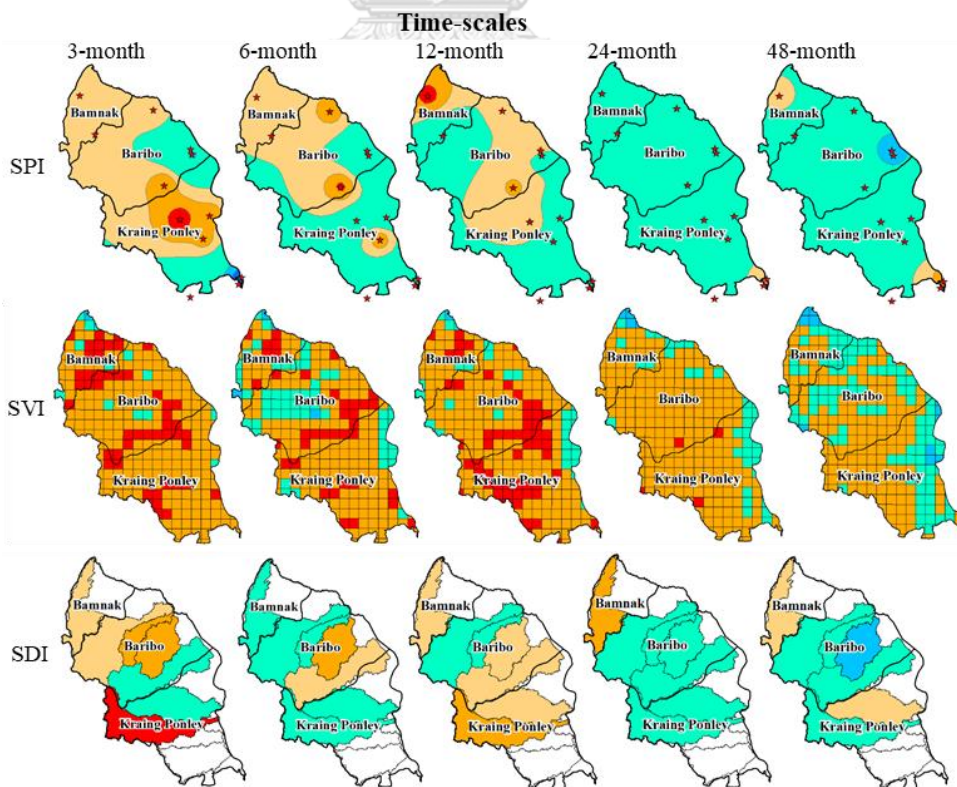


Figure 5.25. Drought map of the three indices in April 1994

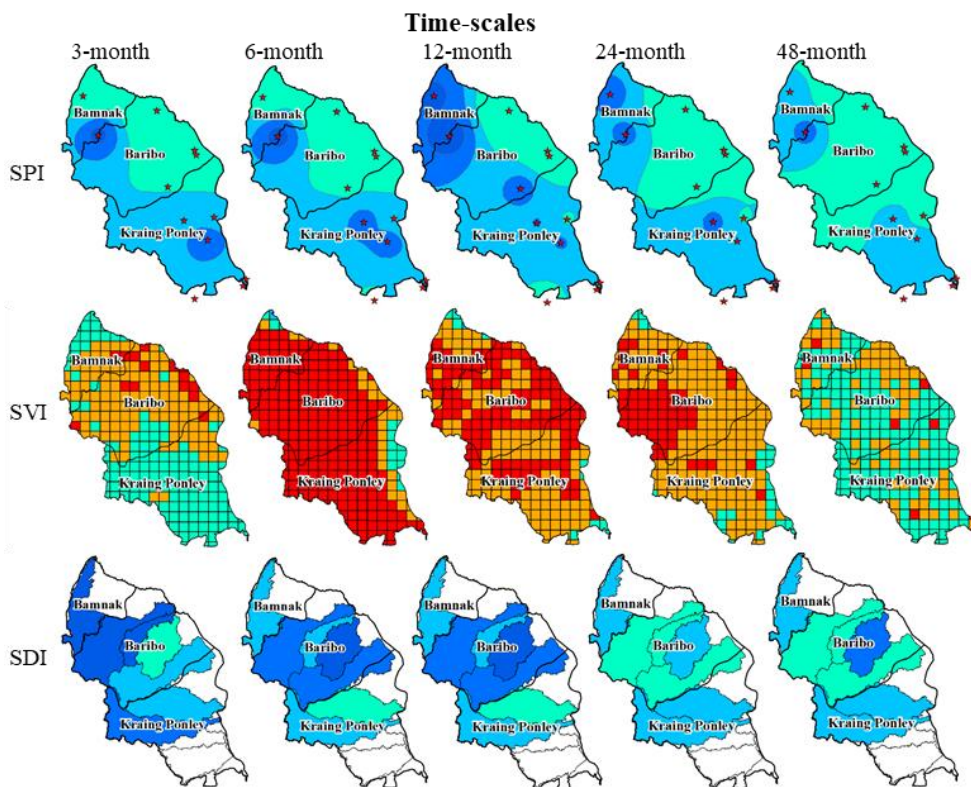


Figure 5.26. Drought map of the three indices in August 2000

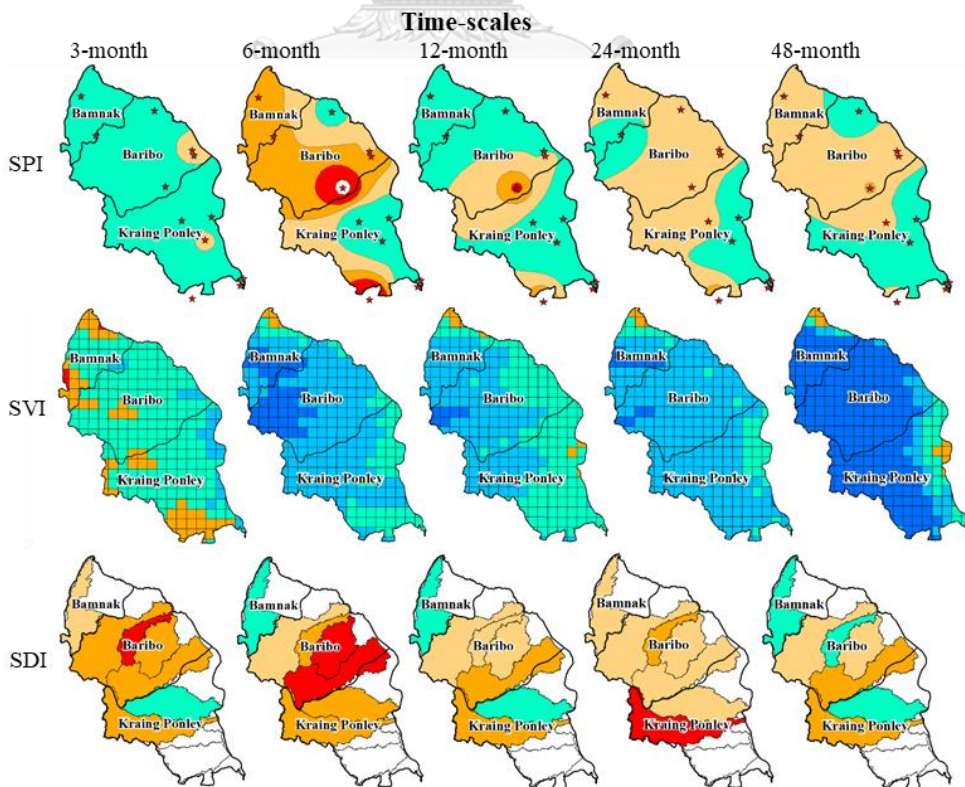


Figure 5.27. Drought map of the three indices in March 2005

5.6 Discussion

According to the analysis above, the SPI and SDI showed similar results of drought characteristics, but they were different from the results of the SVI. The SPI used rainfall and the SDI used streamflow as the key input. Due to relatively high correlation between rainfall and streamflow, it was expected that the SPI and SDI would be similar, but it was not always the case. For example, the SPI3 captured the drought in the Kraing Ponley sub-basin from February 1987 to October 1987 while the SDI3 did not (Table 5.1 and Table 5.16). This difference is probably caused by uncertainty in streamflow predictions. The streamflow in this study was generated using regressive equations between model parameters and basin properties. The calculation of three indices involved with fitting the distribution. Mathematically, both SPI and SDI are based on the same procedure of the calculation by identifying the distribution of the monthly rainfall and streamflow and then transform them to the standard Normal distribution. For the SVI, it directly transforms the monthly NDVI to the standard Normal distribution and it relies on the data from satellite image to detect the vegetation condition on the ground surface. The vegetation does not depend on only rainfall and streamflow but also the development on the agricultural management and adaptation (irrigation system, reservoir operation, type of crop etc.). Thus, the improvement of the agricultural management and adaptation policy of the RGC can be the main cause which leads to different results of the SVI in comparison with the SPI and SDI.

The SPI, SVI, and SDI showed that the drought and poor condition of the vegetation occurred in both wet and dry months. It is believed to be caused by the input of the three indices at each time-scale which were classified into 12 groups of each month. Mathematically, the calculation of each 12 month (January, February, ..., and December) of the three indices was computed independently. For SPI and SDI, the drought considers to be occurred if the rainfall or streamflow of each month are found lower than its mean with once time of variance. For SVI, poor condition of the vegetation can be found when the CDF of greenness density in each month is lower than 0.25.

On the other hand, the poor and very poor greenness density of the vegetation was found in the western part of the Greater Baribo basin where covers by the forest. Generally, the forest should be green at most of the time; however, the poor and very poor greenness density was found in the western part of the basin. Due to the limitation of the SVI, the calculation was computed based on the probability distribution of the greenness density of each single grid. Therefore, the poor and very poor of greenness density can be found in each grid whereas the CDF of greenness density (SVI) is low than 0.25.

It is noted that the Bannak sub-basin has never experienced very poor condition of vegetation from the temporal analysis; however, it was found in the spatial analysis. The difference between the temporal and spatial analysis of the vegetation in the Bannak sub-basin may be caused by the high variation of the SVI value in each grid in the Bannak sub-basin. For example, a few grids next to the Tonle Sap Great lake in the Bannak sub-basin were found in the near normal condition with high value of the SVI while other grids were found in the poor and very poor condition in April 1994 and August 2000 (Figure 5.20). It is the main reason which contributes to the spatial and temporal analysis of the drought in the Bannak sub-basin indicating different results.

Three indices are capable to evaluate the impact of drought on the agriculture since they are able to calculate at 3- and 6-month time-scales which comply with the cropping period of the three types of rice varieties. Either SPI or SDI shows the availability of the rainfall or streamflow, accordingly for LD, MD, and ED rice varieties during the cropping period. In case either SPI or SDI at 3- and 6- month time-scales captured the drought during a cropping period, it means that the rainfall or streamflow is insufficient to fulfil the crop water requirement. The SVI at 3- and 6- month time-scales showed the greenness density of the crop during the growing period. If the SVI captured a poor greenness density in a cropping period, it refers to an unhealthy condition of the crop during the cropping period. As the result, three indices at 3- and 6-month time-scales indicated that three rice varieties (LD, MD, and ED3) experienced the drought more often than other rice varieties.

The drought during the late wet season (November and December) should be taken into account for improving and increasing the agricultural production. The analysis showed that the drought occurred frequently, and the variation of the rainfall and streamflow were very high during that period. Furthermore, more than 60 percent of the total annual rice production cropped during the wet season and harvested during late wet season. Thus, the drought which occurs in the wet season would cause severe damage on the annual rice production.

CHAPTER 6

CONCLUSIONS AND RECOMMENDATIONS

6.1 Conclusions

This research aims to assess the meteorological, agricultural, and hydrological droughts from 1985 to 2008 using the SPI, SVI, and SDI, accordingly. However, the Greater Baribo basin is considered an ungauged basin lacking the streamflow data. Therefore, the PUB technique was used to generate the streamflow for assessing the hydrological drought in this study. The stepwise regression is employed to predict the regressive equation for estimating the model parameters and streamflow of ungauged basins.

The meteorological drought assessment using the SPI indicated that Bannak and Kraing Ponley sub-basins were the drought prone area. The drought characteristics used in this study are DE, DD, DS, and DI which refer to the drought event, drought duration, drought severity, and drought intensity, accordingly. The drought was found heavily impacted in the Bannak sub-basin as the highest DE, DI, and the most severe DS were found in the Bannak sub-basin at most time-scale while the Kraing Ponley experiences the longest length of DD. Between 2001 and 2006, the drought characteristics became higher than the previous DEs and the drought characteristics in three sub-basins became comparable to each other.

The assessment of the vegetation condition using the SVI showed that characteristics of the vegetation in the Bannak, Baribo, and Kraing Ponley sub-basins had high correlation to each other. The poor condition of vegetation from 1988 to 1989, 1992 to 1994, 1998 to 1999, and 2004 to 2006 were believed to be due to drought as the low values of SVI in these periods matched with the negative value of the SPI and SDI. Furthermore, the poor condition of the vegetation between 2004 and 2006 was better than the previous DEs which is believed owing to the improved management and adaptation strategies of the farmer and government. The poor condition of vegetation in 2000 was possibly impacted by flood as positive value of the SPI and SDI were found in this period.

The result of PUB indicated that the regressive equations of six model parameters for ungauged sub-basins have significant correlation with basin properties i.e. forest, wet month rainfall (min), grassland, loamy, basin size, river length, and clay (see equation 6.1 to 6.6). The regressive equations perform well in predicting the model parameters of ungauged sub-basins since the R^2 and NSE mostly range from 0.45 to 0.89 and 0.44 to 0.86 for calibration and 0.4 to 0.89 and 0.45 to 0.94 for validation, accordingly. The regressive equations are able to predict the streamflow in 7 out of 9 sub-basins since they are not applicable to the basins

with the percentage of forest is less than 55%. The prediction of streamflow using PUB technique are employed to generate streamflow time series which is used as an input to calculate the hydrological drought, SDI.

$$c = 0.72 \times \text{Forest} - 0.82 \times \text{Wet Month Rainfall (min)} \quad \text{Eq. 6.1}$$

$$t_w = 0.63 \times \text{Grassland} + 0.46 \times \text{Loamy} \quad \text{Eq. 6.2}$$

$$f = 1.87 \times \text{Basin Size} - 1.21 \times \text{River Length} \quad \text{Eq. 6.3}$$

$$t_q = 1.24 \times \text{Forest} - 0.47 \times \text{Clay} \quad \text{Eq. 6.4}$$

$$t_s = 0.88 \times \text{Grassland} \quad \text{Eq. 6.5}$$

$$v_q = 0.74 \times \text{River Length} + 0.43 \times \text{Wet Month Rainfall (min)} \quad \text{Eq. 6.6}$$

The evaluation of the hydrological drought by the SDI indicated that three sub-basins prone to the drought issue with difference drought characteristics and time-scales. The most frequent (DE) and severe intensity (DI) of drought were found in the Bamnak and Kraing Ponley sub-basins and the longest DD and highest DS occurred in the Baribo sub-basin at SDI3 and SDI6. For other time-scales, the frequency the drought in three sub-basins are comparable to each other but the most severe drought characteristics i.e. DD, DS, and DI are found in the Kraing Ponley sub-basin. Moreover, the drought between 2002 and 2006 became more severe than the previous DEs since the longest DD, the most severe DS, and the highest DI were found.

According to the result presented above, the SPI and SDI provided a high agreement in drought assessment while they showed less agreement with SVI. They suggested that the agriculture was severely impacted by drought in 1993 and 1994 while by flood in 2000. The reduction of the rainfall and streamflow in the Greater Baribo basin became more severe between 2001 and 2006 while the SVI showed that the vegetation was better than the previous DEs. The Baribo sub-basin was less severe impacted by drought between 1985 and 1992 than that of other two sub-basins; nevertheless, it showed comparable drought characteristics to other two sub-basins between 2001 and 2006.

The impact of drought on the cropping pattern is assessed using three indices at 3- and 6-month time-scales. The SPI and SDI showed that the drought does not frequently impact the crop during the dry season while the SVI did. Both SPI and SDI indicated that the longest duration and the most severe drought occurred between 2001 and 2006; however, this had slight impacts on the agriculture. This could probably be caused by the improvement of agricultural management and adaptation strategies of the government. The drought occurring

in November at 3- and 6-month time-scales lead to severe damages on agriculture since more than 60 percent of annual rice production is cropped during wet season and ripening during November.

The spatial distribution of the drought over the Greater Baribo sub-basin indicated that the SPI and SDI had high agreement to each other but less with SVI. These three indices indicated that the distribution of drought and poor vegetation condition in the Baribo sub-basin become more severe from year to year. The drought was found partly in the Kraing Ponley sub-basin but caused higher damage on the agriculture because the Kraing Ponley sub-basin was mostly covered by agricultural area. The poor condition of the vegetation in November 1993 and April 1994 was by drought and by flood in August 2000.

The finding in this study suggests that the, SPI is the most suitable index for assessing drought in the Greater Baribo basin because it uses the observed rainfall which is directly measured as the input. The SVI and SDI used indirect measurement data as the input which might cause higher error in the assessment of drought compared to the SPI. The SVI uses the satellite products as the input and it is measured from the space which is easy to cause error or bias. For the SDI, the streamflow is the main input. In this research, the streamflow is predicted from the regressive equations between model parameters and basin properties which tends to produce high uncertainty in streamflow prediction.

This study is important to the new researcher on drought assessment to understand clearly about the development and computation of drought indices. Moreover, it is also crucial to the new research of drought assessment in Cambodia to select a suitable drought index for their study area. This study helps to figure out that drought is a major natural hazard which is harmful to the agriculture in Cambodia and government should develop measures to increase awareness of the impacts of drought on the national development

6.2 Recommendations

Further research should extend the study area to the entire Tonle Sap basin because it is the major agricultural region of Cambodia. Moreover, they should focus more on the impact of drought on the agriculture since it is a crucial sector to support the development and economic of the country.

The government should consider on installing new rainfall and streamflow gauges because there are few stations in most of the basins especially at the mountainous area. Furthermore, the network of existing gauges is not well distributed.

Future study should consider extending the period of the study to most recent year. Moreover, further research should use other new drought index which use the ground observation data. It also recommended that future study should attempt to combine ground gauged data with satellite products for assessing the drought. In data-scarce basins, the satellite products are recommended for assessing the drought.



REFERENCES

- Alexander, M. E. 1990. Computer calculation of the Keetch-Byram Drought Index (KBDI)-programmers beware. *Fire Management Notes (FMN)*, 51, 23-35.
- Bansok, R., Chhun, C. & Phirun, N. 2011. Agricultural development and climate change: the case of Cambodia, CDRI.
- Bates, B. 2009. Climate change and water: IPCC technical paper VI, World Health Organization.
- Bert, C. & Elga, S. 2016. Drought analysis 2016: Cambodia. UNESCO-IHE, Water Accounting Analyst Institute for Water Education.
- Bhalme, H. N. & Mooley, D. A. 1980. Large-scale droughts/floods and monsoon circulation. *Monthly Weather Review*, 108, 1197-1211.
- Bryant, S., Arnell, N. & Law, F. The long-term context for the current hydrological drought. *Proceedings of the IWEM Conference on the Management of Scarce Water Resources*, 1992.
- Byun, H.-R. & Wilhite, D. A. 1999. Objective quantification of drought severity and duration. *Journal of Climate*, 12, 2747-2756.
- Cai, G., Du, M. & Liu, Y. 2011. Regional drought monitoring and analyzing using MODIS data—A case study in Yunnan Province. *Computer and Computing Technologies in Agriculture IV*, 243-251.
- Chang, T. J. 1991. Investigation of precipitation droughts by use of kriging method. *Journal of Irrigation and Drainage Engineering*, 117, 935-943.
- Chang, T. J. & Kleopa, X. A. 1991. A proposed method for drought monitoring¹. *Wiley Online Library*.
- Chang, T. J. & Teoh, C. B. 1995. Use of the kriging method for studying characteristics of ground water droughts. *JAWRA Journal of the American Water Resources Association*, 31, 1001-1007.
- Chen, T., Ren, L., Yuan, F., Yang, X., Jiang, S., Tang, T., Liu, Y., Zhao, C. & Zhang, L. 2017. Comparison of spatial interpolation schemes for rainfall data and application in hydrological modeling. *Water*, 9, 342.
- Chhin, N. & Millington, A. 2015. Drought monitoring for rice production in Cambodia. *Climate*, 3, 792-811.
- Council, A. 2004. AMS statement on meteorological drought. *Bull Amer Meteor Soc*, 85, 771-773.
- Croke, B., Merritt, W. & Jakeman, A. 2004. A dynamic model for predicting hydrologic

- response to land cover changes in gauged and ungauged catchments. *Journal of Hydrology*, 291, 115-131.
- David, G. & Claudia, W. S. 2006. *Water for growth and development*. Mexico City.
- David, S. 2003. *Water resources management*, University of the Witwatersrand
- Ding, Y., Liu, Y., Song, Y. & Zhang, J. 2015. From MONEX to the global monsoon: A review of monsoon system research. *Advances in Atmospheric Sciences*, 32, 10-31.
- Dracup, J. A., Lee, K. S. & Paulson, E. G. 1980. On the definition of droughts. *Water resources research*, 16, 297-302.
- Edwards, D. C. 1997. Characteristics of 20th century drought in the United States at multiple time scales. Air force inst of tech wright-patterson AFB OH.
- Eltahir, E. A. 1992. Drought frequency analysis of annual rainfall series in central and western Sudan. *Hydrological sciences journal*, 37, 185-199.
- Eltahir, E. A. & Yeh, P. J. F. 1999. On the asymmetric response of aquifer water level to floods and droughts in Illinois. *Water Resources Research*, 35, 1199-1217.
- Estrela, M., Peñarrocha, D. & Millán, M. 2000. Multi-annual drought episodes in the Mediterranean (Valencia region) from 1950–1996. A spatio-temporal analysis. *International Journal of Climatology*, 20, 1599-1618.
- Food and Agriculture Organization (FOA) of United Nations & Land and Water Development Division (LWDD) 1983. *Guidelines : land evaluation for rainfed agriculture/soil resources management and conservation services*, land and water development division., Rome : Food and Agriculture Organization of the United Nations, 1983., Food and Agriculture Organization of the United Nations (FAO) and Land and Water Development Division (LWDD).
- General UN Secretariat 1994. United Nations (UN) convention to combat drought and desertification in countries experiencing serious droughts and/or desertification, particularly in Africa. Particularly in Africa.
- Ghulam, A., Li, Z.-L., Qin, Q. & Tong, Q. 2007a. Exploration of the spectral space based on vegetation index and albedo for surface drought estimation. *Journal of Applied Remote Sensing*, 1, 013529-013529-12.
- Ghulam, A., Qin, Q. & Zhan, Z. 2007b. Designing of the perpendicular drought index. *Environmental Geology*, 52, 1045-1052.
- Ghulam, A., Qin, Q., Teyip, T. & Li, Z.-L. 2007c. Modified perpendicular drought index (MPDI): a real-time drought monitoring method. *ISPRS Journal of Photogrammetry and Remote Sensing*, 62, 150-164.

- Gibbs, W. 1975. Drought: its definition, delineation and effects. WMO Drought p 11-39(SEE N 76-12595 03-47).
- Gommes, R. & Petrassi, F. 1996. Rainfall variability and drought in Sub-Saharan Africa since 1960. Agro-meteorology series working paper, 9. Food and Agriculture Organization (FAO), Rome, Italy.
- Gumbel, E. 1963. Statistical forecast of droughts. *Hydrological Sciences Journal*, 8, 5-23.
- Guo, H., Bao, A., Liu, T., Ndayisaba, F., He, D., Kurban, A. & De Maeyer, P. 2017. Meteorological drought analysis in the Lower Mekong Basin (LMB) using satellite-based long-term CHIRPS product. *Sustainability*, 9, 901.
- Guttman, N. B. 1999. Accepting the standardized precipitation index: a calculation algorithm. *JAWRA Journal of the American Water Resources Association*, 35, 311-322.
- Hardisky, M., Klemas, V. & Smart, R. M. 1983. The influence of soil salinity, growth form, and leaf moisture on the spectral radiance of *Spartina alterniflora* canopies. *Photogrammetric Engineering and Remote Sensing*, 49, 77-83.
- Hayes, M. J. 2006. Drought indices, National Drought Mitigation Center, Wiley Online Library.
- Hong, X., Guo, S., Zhou, Y. & Xiong, L. 2015. Uncertainties in assessing hydrological drought using streamflow drought index for the upper Yangtze River basin. *Stochastic environmental research and risk assessment*, 29, 1235-1247.
- Huete, A., Didan, K., Miura, T., Rodriguez, E. P., Gao, X. & Ferreira, L. G. 2002. Overview of the radiometric and biophysical performance of the MODIS vegetation indices. *Remote sensing of environment*, 83, 195-213.
- Huete, A. R. 1988. A Soil-Adjusted Vegetation Index (SAVI). *Remote sensing of environment*, 25, 295-309.
- Hundecha, Y., Zehe, E. & Bárdossy, A. 2002. Regional parameter estimation from catchment properties prediction in ungauged basins.
- Idso, S., Jackson, R., Pinter, P., Reginato, R. & Hatfield, J. 1981. Normalizing the stress-degree-day parameter for environmental variability. *Agricultural Meteorology*, 24, 45-55.
- Jackson, R. D., Idso, S., Reginato, R. & Pinter, P. 1981. Canopy temperature as a crop water stress indicator. *Water resources research*, 17, 1133-1138.
- Katz, R. W. & Glantz, M. H. 1986. Anatomy of a rainfall index. *Monthly Weather Review*, 114, 764-771.
- Keskinen, M., Matti, K., Aura, S., Someth, P. & Hannu, L. 2011. Exploring Tonle Sap futures study. Aalto University and 100Gen with Hatfield Consultants Partnership, VU University Amsterdam, EIA and Institute of Technology of Cambodia.

- Keyantash, J. & Dracup, J. A. 2002. The quantification of drought: an evaluation of drought indices. *Bulletin of the American Meteorological Society*, 83, 1167-1180.
- Kifer, R. & Stewart, H. 1938. Farming hazards in the drought area," works progress administration research monograph XVI, Washington DC: Government Printing Office.
- Kogan, F. 1990. Remote sensing of weather impacts on vegetation in non-homogeneous areas. *International Journal of Remote Sensing*, 11, 1405-1419.
- Kogan, F. N. 1995. Droughts of the late 1980s in the United States as derived from NOAA polar-orbiting satellite data. *Bulletin of the American Meteorological Society*, 76, 655-668.
- Le Comte, D. 1994. Highlights around the world. *Weatherwise*, 47, 23-26.
- Lester, R. & Gurenko, E. 2003. Financing rapid onset natural disaster losses in India: a risk management approach. Technical Paper. Washington, DC: The World Bank.
- Liu, L., Xiang, D., Dong, X. & Zhou, Z. Improvement of the drought monitoring model based on the cloud parameters method and remote sensing data. *Knowledge Discovery and Data Mining*, 2008. WKDD 2008. First International Workshop on, 2008. IEEE, 293-296.
- Lloyd-Hughes, B. & Saunders, M. A. 2002. A drought climatology for Europe. *International journal of climatology*, 22, 1571-1592.
- Loukas, A., Mylopoulos, N. & Vasiliades, L. 2007. A modeling system for the evaluation of water resources management strategies in Thessaly, Greece. *Water Resources Management*, 21, 1673-1702.
- Madsen, H., Mikkelsen, P. S., Rosbjerg, D. & Harremoes, P. 1998. Estimation of regional intensity-duration-frequency curves for extreme precipitation. *Water Science and Technology*, 37, 29-36.
- Matera, A., Fontana, G., Marletto, V., Zinoni, F., Botarelli, L. & Tomei, F. 2007. Use of a new agricultural drought index within a regional drought observatory. *Methods and tools for drought analysis and management*, 103-124.
- McKee, T. B., Doesken, N. J. & Kleist, J. The relationship of drought frequency and duration to time scales. *Proceedings of the 8th Conference on Applied Climatology*, 1993. American Meteorological Society Boston, MA, 179-183.
- Meshcherskaya, A. V. & Blazhevich, V. 1997. The drought and excessive moisture indices in a historical perspective in the principal grain-producing regions of the former Soviet Union. *Journal of Climate*, 10, 2670-2682.
- Mestre, A. Drought monitoring in Spain. *Agricultural drought indices proceedings of an expert*

- meeting, 2011. 95.
- Meyer, S. & Hubbard, K. Extending the crop-specific drought index to soybean. Preprints, ninth conf. on applied climatology, Dallas, TX, Amer. Meteor. Soc, 1995. 258-259.
- Meyer, S. J., Hubbard, K. G. & Wilhite, D. A. 1993. A crop-specific drought index for corn: I. Model development and validation. *Agronomy Journal*, 85, 388-395.
- Mishra, A., Singh, V. & Desai, V. 2009. Drought characterization: a probabilistic approach. *Stochastic Environmental Research and Risk Assessment*, 23, 41-55.
- Mishra, A. K. & Singh, V. P. 2010. A review of drought concepts. *Journal of Hydrology*, 391, 202-216.
- MoE 2005. Vulnerability and adaption of climate hazards and to climate change: a survey of rural Cambodian households. Ministry of Environment (MoE): Phnom Penh, Cambodia.
- Moran, M., Clarke, T., Inoue, Y. & Vidal, A. 1994. Estimating crop water deficit using the relation between surface-air temperature and spectral vegetation index. *Remote sensing of environment*, 49, 246-263.
- Motha, R. P. Use of crop models for drought analysis. In: Sivakumar, M. V. K., Motha, R. P., Wilhite, D. A. & Wood, D. A., eds. *Agricultural Drought Indices Proceedings of an Expert Meeting, 2011 Murcia, Spain*. World Meteorological Organization, 138-148.
- MOWRAM. 2008. GMS flood and drought risk managemet and mitigation project [Online]. Phnom Penh, Cambodia.: Ministry of Water Resources and Meteorology (MOWRAM), Department of Hydrology and River Works (DHRW). Available: <http://www.dhrw-cam.org/> [Accessed 17/Dec/2018].
- MRC 2011. Planning atlas of the lower Mekong River basin. Mekong River Commission (MRC), Vientiane, Laos.[online] URL: <http://www.mrcmekong.org/assets/Publications/basin-reports/BDP-Atlas-Final-2011.pdf>.
- Nalbantis, I. & Tsakiris, G. 2009. Assessment of hydrological drought revisited. *Water Resources Management*, 23, 881-897.
- Narasimhan, B. & Srinivasan, R. 2005. Development and evaluation of Soil Moisture Deficit Index (SMDI) and Evapotranspiration Deficit Index (ETDI) for agricultural drought monitoring. *Agricultural and Forest Meteorology*, 133, 69-88.
- Niemeyer, S. 2008. New drought indices. *Options Méditerranéennes. Série A: Séminaires Méditerranéens*, 80, 267-274.
- Omondi, P. Agricultural drought indices in the Greater Horn of Africa (GHA) countries. In:

- Sivakumar, M. V. K., Motha, R. P., Wilhite, D. A. & Wood, D. A., eds. Agricultural Drought Indices Proceedings of an Expert Meeting, 2011 Murcia, Spain World Meteorological Organization 128-136.
- Palmer, W. C. 1965. Meteorological drought, US Department of Commerce, Weather Bureau Washington, DC.
- Palmer, W. C. 1968. Keeping track of crop moisture conditions, nationwide: The new crop moisture index. *Weatherwise*, 22, 156-161.
- Peters, A. J., Walter-Shea, E. A., Ji, L., Vina, A., Hayes, M. & Svoboda, M. D. 2002. Drought monitoring with NDVI-based standardized vegetation index. *Photogrammetric engineering and remote sensing*, 68, 71-75.
- Post, D. A. & Jakeman, A. J. 1999. Predicting the daily streamflow of ungauged catchments in SE Australia by regionalising the parameters of a lumped conceptual rainfall-runoff model. *Ecological Modelling*, 123, 91-104.
- Potgieter, A., Hammer, G., Doherty, A. & De Voil, P. 2005. A simple regional-scale model for forecasting sorghum yield across North-Eastern Australia. *Agricultural and Forest Meteorology*, 132, 143-153.
- Rahmat, S., Jayasuriya, N. a. & Muhammed, B. 2014. Assessing droughts using meteorological drought indices in Victoria, Australia. *Hydrology Research*, 46, 463-476.
- Saburo, M., Marko, K., Pech, S. & Masahisa, N. 2006. Tonle Sap experience and lesson learned brief. Kyoto, Japan: University of Kyoto, Helsinki University of Technology, Mekong River Commission, Shiga University.
- Sam, S. & Pech, S. 2015. Climate change and water governance in Cambodia: challenges and perspectives for water security and climate change in selected catchments. Cambodia. Phnom Penh: CDRI.
- Sarkar, J. Monitoring drought risks in India with emphasis on agricultural drought. *Agricultural Drought Indices Proceeding of an expert meeting*, 2011. 59.
- Shafer, B. & Dezman, L. Development of a Surface Water Supply Index (SWSI) to assess the severity of drought conditions in snowpack runoff areas. *Proceedings of the western snow conference*, 1982. Colorado State University Fort Collins, CO, 164-175.
- Sok, K., Visessri, S. & Heng, S. 2017. Meteorological Drought Assessment for the Baribo Basin in Cambodia. *Internet Journal of Society for Social Management Systems*, 11, 146-157.
- Son, N., Chen, C., Chen, C., Chang, L. & Minh, V. 2012. Monitoring agricultural drought in the Lower Mekong Basin using MODIS NDVI and land surface temperature data. *International Journal of Applied Earth Observation and Geoinformation*, 18, 417-427.

- Stahl, K. 2001. Hydrological drought: a study across Europe. Institut für Hydrologie der Universität.
- Suwanwerakamtorn, R., Mongkolsawat, C., Srisuk, K. & Ratanasermping, S. 2006. Matrix overlay for drought assessment in the Nam Choen watershed, NE Thailand.
- Thornthwaite, C. W. 1948. An approach toward a rational classification of climate. *Geographical review*, 38, 55-94.
- Thornthwaite, C. W. 1955. The water balance. Drexel Institute of Technology, Centerton, NJ (EUA). Laboratory of Climatology.
- Todorovic, P. & Woolhiser, D. 1976. Stochastic structure of the local pattern of precipitation [Water resources].
- Tsakiris, G. & Vangelis, H. 2005. Establishing a drought index incorporating evapotranspiration. *European Water*, 9, 3-11.
- Tucker, C. J. 1979. Red and photographic infrared linear combinations for monitoring vegetation. *Remote sensing of Environment*, 8, 127-150.
- Tucker, C. J. & Choudhury, B. J. 1987. Satellite remote sensing of drought conditions. *Remote sensing of Environment*, 23, 243-251.
- Van Lanen, H. & Peters, E. 2000. Definition, effects and assessment of groundwater droughts. *Drought and drought mitigation in Europe*. Springer.
- Van Rooy, M. 1965. A rainfall anomaly index independent of time and space. *Notos*, 14, 6.
- Vicente-Serrano, S. M., Beguería, S. & López-Moreno, J. I. 2010. A multiscalar drought index sensitive to global warming: the standardized precipitation evapotranspiration index. *Journal of climate*, 23, 1696-1718.
- Visessri, S. & McIntyre, N. 2016. Uncertainty in Flow Time-Series Predictions in a Tropical Monsoon-Dominated Catchment in Northern Thailand. *Journal of Hydrologic Engineering*, 21, 04016036.
- Vlachos, E. & James, L. D. 1983. Drought impacts: Coping with droughts. *water resources publications*, Littleton, CO. 44-73.
- Wattanakij, N., Thavorntam, W. & and Mongkolsawat, C. 2006. Analyzing spatial pattern of drought in the northeast of Thailand using multi-temporal Standardized Precipitation Index (SPI).
- Weghorst, K. The reclamation drought index: Guidelines and practical applications. *North American Water and Environment Congress & Destructive Water*., 1996. ASCE, 637-642.
- Welford, M. R., Hollinger, S. E. & Isard, S. A. 1993. A new soil moisture drought index for

predicting crop yields.

- Wilhite, D. A. & Glantz, M. H. 1985. Understanding: the drought phenomenon: the role of definitions. *Water international*, 10, 111-120.
- Wilhite, D. A. 2011. Quantification of agricultural drought for effective drought mitigation and preparedness: Key issues and challenges.
- WMO & GWP 2016. Handbook of drought indicators and indices, World Meteorological Organization (WMO) and Global Water Partnership (GWP).
- World Meteorological Organization (WMO) 1986. Report on drought and countries affected by drought during 1974–1985. Geneva, Switzerland: WMO.
- Wu, H., Svoboda, M. D., Hayes, M. J., Wilhite, D. A. & Wen, F. 2007. Appropriate application of the standardized precipitation index in arid locations and dry seasons. *International Journal of Climatology*, 27, 65-79.
- WWAP 2003. Water for people, water for life: executive summary Paris: UNESCO and World Meteorological Organization (WMO).
- Yang, X., Xie, X., Liu, D. L., Ji, F. & Wang, L. 2015. Spatial interpolation of daily rainfall data for local climate impact assessment over greater Sydney region. *Advances in Meteorology*, 2015.
- Yevjevich, V. M. 1967. An objective approach to definitions and investigations of continental hydrologic droughts. *Hydrology papers (Colorado State University)*; no. 23.
- Yihui, D. 2007. The variability of the Asian summer monsoon. *Journal of the Meteorological Society of Japan*. Ser. II, 85, 21-54.
- Zargar, A., Sadiq, R., Naser, B. & Khan, F. I. 2011. A review of drought indices. *Environmental Reviews*, 19, 333-349.
- Zou, X., Zhai, P. & Zhang, Q. 2005. Variations in droughts over China: 1951–2003. *Geophysical Research Letters*, 32.

APPENDICES

Appendix A: 19 basin properties parameters of six gauged and nine ungauged basins are showed in the Table A1. These parameters were computed from land use, soil types, catchment characteristics, and rainfall characteristics.

Table. A1. 19 basin properties of the gauged and ungauged basins

Properties	Types	Gauged basins						Ungauged basin								
		Chikreng	Chinit	Sangker	Sen	Streng	Staung	1	2	3	4	5	6	7	8	9
Landuse	Agriculture	15.9	11	20.4	9.2	25.7	11.8	23	14	14.2	25.4	34.5	25.6	35.1	65.7	61.4
	Flooded forest	0.2	0.2	4.6	0.4	1.4	0.3	4.1	0.5	0.2	0.4	1.3	0.1	0.6	3	0.2
	Forest	82.2	84.3	68.1	87.2	68.9	87.5	71.5	82.2	71.8	57.2	55	71.1	60.1	19.7	30
	Grassland	1.5	4.5	6.3	2.8	3.4	0.1	1.4	3.1	13.7	16.7	5.6	3	3.3	9.2	7.2
	Impervious area	0.2	0.1	0.7	0.4	0.5	0.3	0	0.2	0	0.3	3.7	0.2	1	2.4	1.1
Soil tyes	Clay	87.9	74.9	35.5	61.4	39.5	66.1	75.1	30.8	10.8	7.5	25.8	26.2	24.5	89	94.5
	Loamy	12.1	25.1	64.5	36.6	58.7	31.4	24.9	52.2	17.1	14	36.5	46.3	12.5	7.1	5.2
	Sandy	0	0	0	1.9	1.8	0	0	17	72.1	78.5	37.8	27.6	63	3.9	0.2
Catchment characteristic	Mean elevation (m)	251	332	698	383	324	288	425	886	284	372	798	795	324	111	44
	Catchment size (Km2)	1740	4183	3721	14138	8716	1876	523	916	284	545	780	803	712	536	225
	Annual rainfall (mm)	1435	1406	1008	1332	1284	1415	1356	1373	1445	1539	1503	1240	1360	1222	1222
	Mean temp. (oC)	28.3	27.6	28.3	28	28	27.6	28.5	28.5	28.5	28.5	28.5	28.5	29.1	29.1	29.1
	River length (Km)	104.1	275.3	236.4	436.5	241.7	127.4	81.7	95.3	49.3	55.8	83.9	101.1	63.6	59.2	41
Rainfall characteristic	W.Rainfall (min)	128.6	152.1	100.2	125.7	148.4	120.2	94.4	92.4	129.2	132.3	123.8	83	104.9	77.4	76.6
	D.Rainfall (min)	7.5	0.6	8.7	2.5	1.7	3	0.6	0.2	0.6	0.2	0.4	1.6	0.9	0.7	0.1
	W.Rainfall (mean)	200.2	201.4	132.4	190.1	186.5	209.2	179.2	183.8	203.4	222.9	216.1	173	197.6	167.3	169
	D.Rainfall (mean)	25.3	18.6	28.2	20.9	15	19.9	46.8	45	37.5	33.5	34.4	33.7	29.1	36.3	34.7
	W.Rainfall (max)	285.6	251.1	185.5	244.5	270.7	317	294.9	310.4	290.2	322.5	329.3	282	314.8	264.2	265.9
	D.Rainfall (max)	50.5	45.8	61.2	42.8	29.3	42.1	141.7	137.2	113	113.6	116.7	103.5	96	105.2	97.8

Remark*: Mean Temp. = Mean Temperature, W.Rainfall = Wet Month Rainfall, D.Rainfall = Dry Month Rainfall

Appendix B: Figure. B1 is illustrated about the warm up (2000), calibration (2001-2003) and validation (2004-2006) periods between observed and simulated streamflow of gauged basins. For Sen basin, the warm up period was from 2000-2001 and calibration period from was from 2002-2003 since the rainfall in Sen basin was missing in 2001.

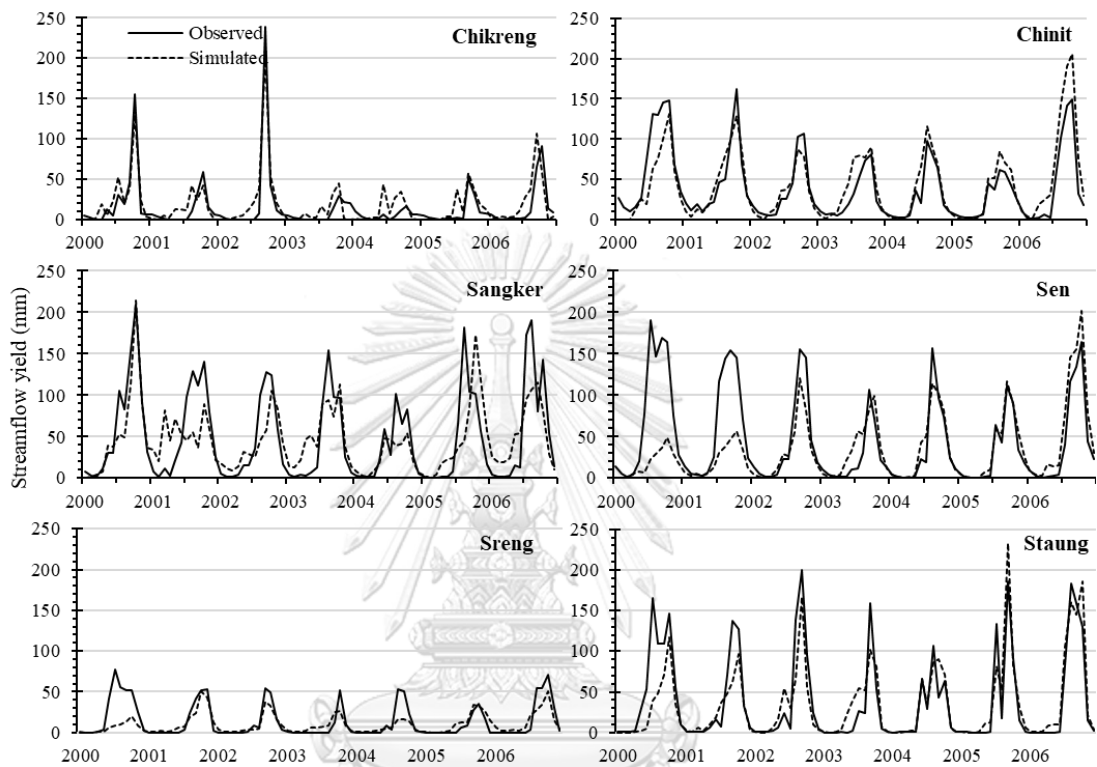


Figure. B1. Observed and simulated flow of the six gauged basins in the Tonle Sap Basin with the model parameters from the calibration

Appendix C: Figure. C1 showed the warm up, calibration, validation periods of gauged basins using model parameters which generated from regressive equations between the model parameters and basin characteristics. It indicated that the simulated streamflow using the parameters from the model calibration and regressive equation showed similar result. Thus, regressive equations are usable to estimate the model parameters of the ungauged basins.

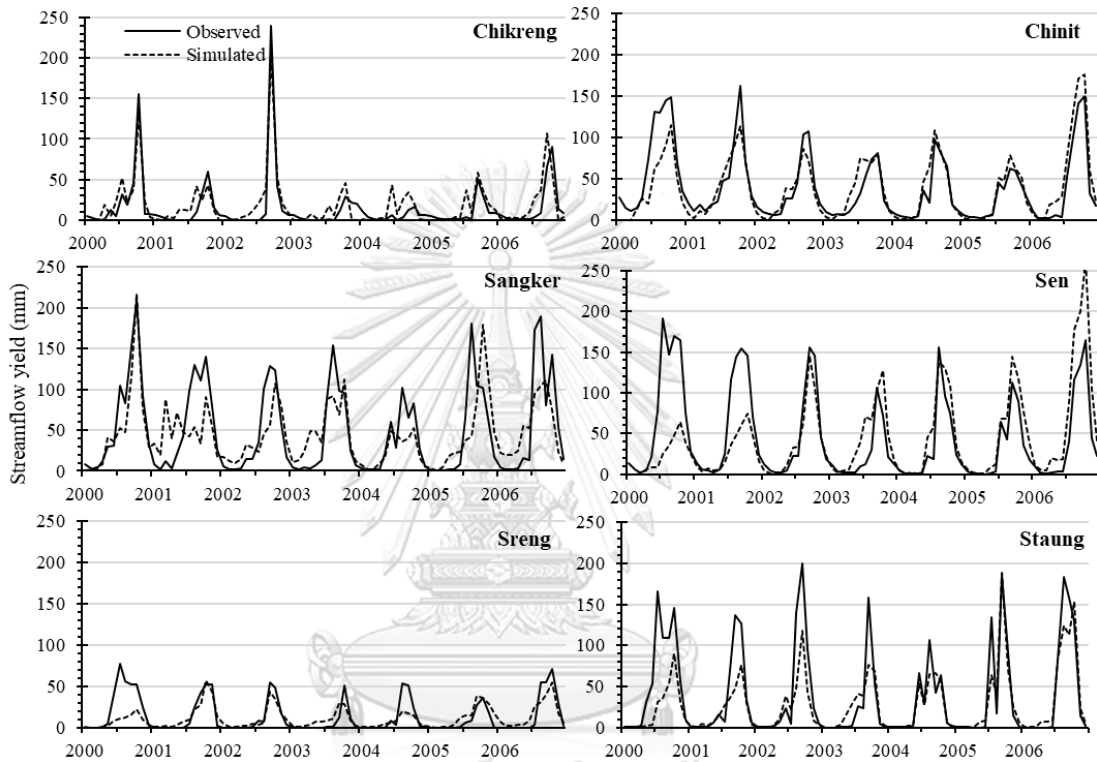


Figure. C1. Observed and simulated flow of the six gauged basins in the Tonle Sap Basin with the model parameters from the stepwise regression

Appendix D: Figure D1. illustrated the streamflow of the seven ungauged basins in the Greater Baribo basin which generated from the regressive equations. These streamflow data were used to assess the hydrological drought using SDI.

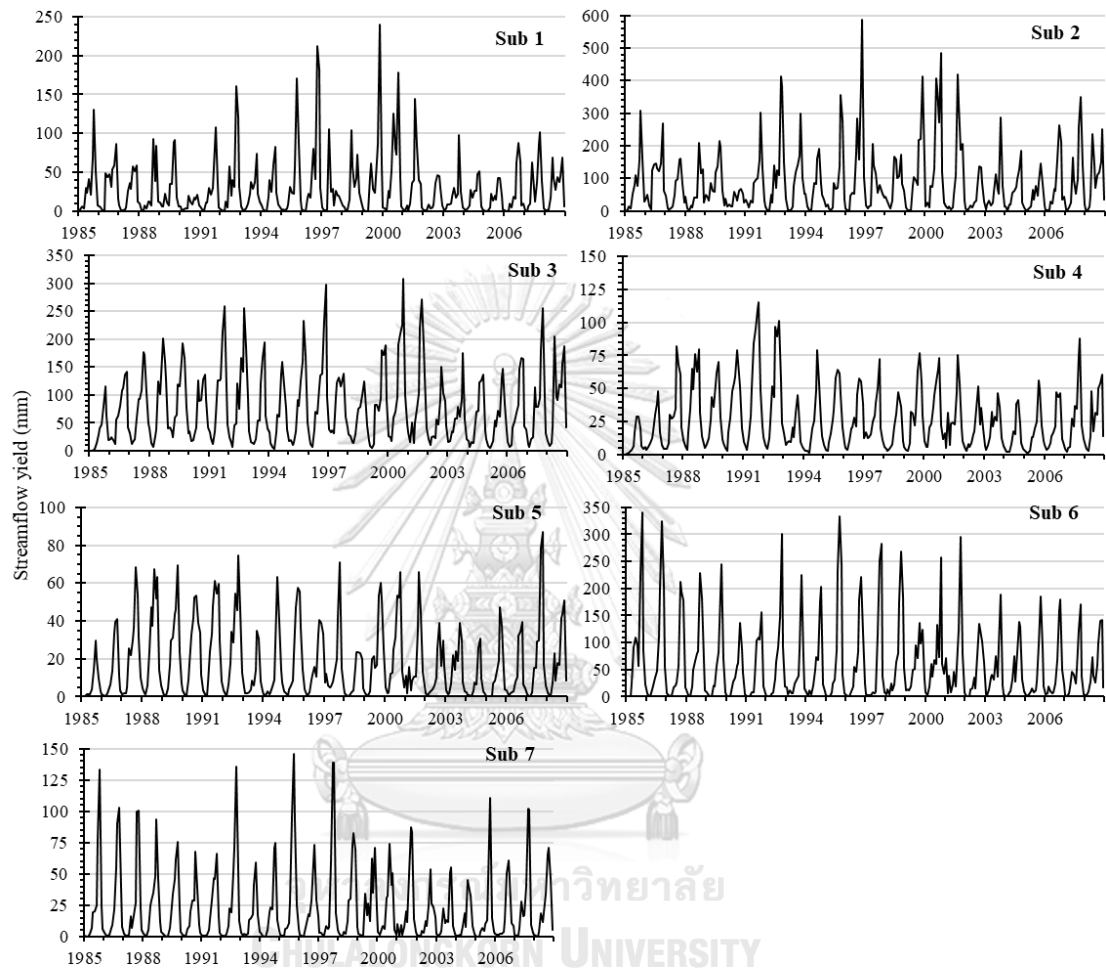


Figure D1. Hydrograph of the ungauged basins

Appendix E : The site visiting to the Greater Baribo basin in the Kompong Chhnang province, Cambodia, was arranged between 27 and 28 June 2017 for purposes of the basic field survey, data collection, and data verification through an interview with local government agencies and residents regarding water-related issues. The first day of the visit focused on interviewing local residents about their experiences on the flood and drought. The second day was mainly about the data collection and discussion with local government agencies regarding water management issues in the Greater Baribo basin. The summary of the first day of the interview and second day of the discussion is detailed below.

On the first day, the team were assisted by Ms. Ket Pinnara, a researcher at Institute of Technology of Cambodia (ITC), to conduct interviews three farmers, namely Ms. Sarith, Mr. Khout Not, and Ms. Chan Sareun in a village in the Kompong Chhnang province. Ms. Sarith is a farmer who has grown the paddy rice in which the setting of her farm is shown in the attached photo. The main water supply to her farm is a small reservoir which is managed by the local committee. This reservoir has insufficient capacity to provide water to the large farm land, especially during the dry season when the reservoir can only supply water to the upstream farm land. The year 2015 was told to be the driest year when the reservoir was totally empty due to several months delay in rainfall influencing to no water for drinking and agriculture. The variation in the climate is significantly strong in recent years. The driest year 2015 was followed by the flood in the early 2016 and 2017. The evidence of the crop failure owing to the heavy rainfall remained detectable during our visit. In her case, drought is more challenging to deal with than the flood as it is less predictable. She has totally relied on water from this reservoir and does not have her own pond. Ms. Sarith also shared her opinion that installing more meteorological stations to allow reliable rainfall forecasting could better help her to plan her crop and prevent the loss of the revenue. The second interview was with Mr. Khout Not who has applied the integrated farming system to his farm which helps reducing impacts of floods and droughts on the crop production. His main crop is the paddy rice, but a variety of crops has been also grown depending on the market price and environmental conditions of the farm. Having multiple crops reduces the difficulty in controlling weeds, diseases, and insect pests. While having a better management than other farms, floods and droughts have been considered critical situations for Mr. Khout. As he has two ponds to store water during the wet season to use during the dry season, the water shortage is less problematic compared to the excessive water caused by the flood. Higher impacts associated with drought is from the increased temperature that leads to the crop loss and low revenue. According to his interview, 2015 and 2016 were the worst years because he has experienced

both drought and flood. He stated that having access to information such as flood or drought maps could be potentially beneficial for his farm management.



a. Interview atmosphere

b. The farm behind her house



c. The small reservoir

d. The main canal to supply water to the farm

Figure E1. Interview with Ms. Sarith.



a. Interview atmosphere

b. The pond for irrigating his farm



c. The paddy rice field

d. The plantation of his vegetation

Figure E2. Interview with Mr. Khout Not.

For the second day, we went to meet Mr. Sok Phun, the Head of Department of Agricultural, Forestry and Fisheries and Department of Water Resources and Meteorology of Kompong Chhnang province as shown in the photo. The eastern part of the Kompong Chhnang province is connected to the Tonle Sap great lake where is the floodplain area while the western part is mostly the mountainous area. There are several rivers in this province but only Baribo and Kraing Ponley rivers have reservoirs. The reservoir at Kraing Ponley was built by Korean while the reservoir at Baribo river is still under construction by the Chinese company. Cassava and sugar cane were grown by the Chinese company next to the reservoir of the Baribo river. These two types of the crop consume abundant water; thus, farmers at the downstream have always experienced the water shortage during the dry season. The Kraing Ponley reservoir shares some water to the Kompong Speu province and supplies water for irrigating rice in the dry season and mixed crops, rice and vegetable during the dry season in the Kompong Chhnang province. In the Kompong Chhnang province, major problem is the shortage and the variation of rainfall, especially in 2017 the rainfall came very early with the high intensity thus the crop was damaged. He identified that five out of eight districts in the Kompong Chhnang province are mostly and partially considered as the drought prone area. The Caribbean Agricultural Research and Development Institute (CARDI) which helps to provide the good seed and the technique to farmers to adapt with the occurrence of either drought or flood, which forty agricultural committees have been organized and assigned to further assist in keeping the provided seed.

Mr. Douk Bunthun, who is the Head Department of Water Resources and Meteorological in the Kompong Chhnang province, has come to work since 2004 reported that 2004 was the dry year; however, he cannot do any to such natural hazard because to address and partially manage such hazard may require not only the equipment but also the reservoir. Beside the drought, the flood then happened in 2011. The water elevation in 2011 increased very high, and most agriculture area for the entire of country was damaged, but hundreds of small reservoirs which are situated in the Tonle Sap floodplain area partially helped to consume the flood water and minimize the damage from the flood. Moreover, there are. The people built the dike to form the reservoir. When the water elevation in Tonle Sap increases, the water fills into the reservoir and when the water elevation starts to decrease, people close the gate of the reservoir to store the water. According to the record, he found that 2015 and 2016 were driest years, but he could manage and provide the water to some important parts of the province because he has 20 pumping machines and 2 reservoirs.

Mr. Sat Song is a staff in the Department of Water Resources and Meteorological in the Kompong Chhnang province. He has collected the meteorological, soil moisture, and discharge data. There are 28 meteorological stations that have been recorded. Among those 28 stations, 17, 6, 4, and 1 station(s) belong to Department of Water Resources and Meteorological of Kompong Chhnang, Japan International Cooperation Agency (JICA), Institute of Technology of Cambodia (ITC), and Asian Development Bank, respectively. There are 8 stations for recording the water elevation which 5 stations were installed in the Tonle Sap and other 3 were installed in the Baribo, Kraing Ponley, and Chrey Bak River. There is only one temperature station which is located in Department of Water Resources and Meteorological of Kompong Chhnang province.



a. The office of Mr. Sok Phun

b. The photo after the interviewing

Figure E3. Interviewing Mr. Sok Phun.



a. The system on irrigation schemes

b. Interviewing atmosphere

c. Department of Water Resources and Meteorological

Figure E4. Interviewing Mr. Douk Bunthun.



a. The manual data recording sheet

b. Explanation of the collection of data

Figure E5. Interviewing Mr. Sat Song.

VITA

NAME Mr. Kimhuy Sok

DATE OF BIRTH 20 October 1993

PLACE OF BIRTH Battambang province, Cambodia

INSTITUTIONS ATTENDED
HOME ADDRESS

1. Faculty of Hydrology and Water Resources, Institute of Technology of Cambodia (ITC)
2. Faculty of Engineering, Chulalongkorn University (CU) Battambang province, Cambodia

PUBLICATION

1. Meteorological Drought Assessment for the Baribo Basin in Cambodia
2. A Comparative Assessment of Meteorological Drought Indices for the Baribo Basin, Cambodia

AWARD RECEIVED

1. Scholarship of the Asian Development Bank (ADB) for Bachelor degree of Engineering
2. Scholarship of ASEAN University Network Southeast Asia Engineering Education Development Network Program (AUN/SEED-Net) of Japan International Cooperation Agency (JICA) for Master degree of Engineering